2016-11-22

# Fluvial archives, a valuable record of vertical crustal deformation

Demoulin, A

http://hdl.handle.net/10026.1/8533

10.1016/j.quascirev.2016.11.011
Quaternary Science Reviews
Elsevier BV

# Fluvial archives, a valuable record of vertical crustal deformation

A. Demoulin, University of Liege, Dept. of Physical Geography and Quaternary, Belgium
A. Mather, School of Geography, Earth and environmental Sciences, UK
A. Whittaker, Dept. of Earth Science and Engineering, Imperial College, London, UK

Acceptance Date 10th Nov 2016
Embargo Release Date 10th Nov 2017

# Fluvial archives, a valuable record of vertical crustal deformation

*A. Demoulin, A. Mather, A. Whittaker*

**Abstract.** The study of drainage network response to uplift is important not only for understanding river system dynamics and associated channel properties and fluvial landforms, but also for identifying the nature of crustal deformation and its history. In recent decades, geomorphic analysis of rivers has proved powerful in elucidating the tectonic evolution of actively uplifting and eroding orogens. Here, we review the main recent developments that have improved and expanded qualitative and quantitative information about vertical tectonic motions (the effects of horizontal deformation are not addressed). Channel long profiles have received considerable attention in the literature, and we briefly introduce basic aspects of the behaviour of bedrock rivers from field and numerical modelling perspectives, before describing the various metrics that have been proposed to identify the information on crustal deformation contained within their steady state characteristics. Then, we review the literature dealing with the transient response of rivers to tectonic perturbation, through the production of knickpoints propagating through the drainage network. Inverse modelling of river profiles for uplift in time and space is also shown to be very effective in reconstructing regional tectonic histories. Finally, we present a synthetic morphometric approach for deducing the tectonic record of fluvial landscapes.

As well as the erosional imprint of tectonic forcing, sedimentary deposits, such as fluvial terrace staircases, are also considered as a classical component of tectonic geomorphology. We show that these studies have recently benefited from rapid advances in dating techniques, allowing more reliable reconstruction of incision histories and estimation of incision rates. The combination of progress in the understanding of transient river profiles and larger, more rigorous data sets of terrace ages has led to improved understanding of river erosion and the implications for terrace profile correlation, i.e., extrapolation of local data to entire profiles. Finally, planform changes in fluvial systems are considered at the channel scale in alluvial rivers and regional level in terms of drainage reorganisation. Examples are given of how numerical modelling can efficiently combine with topographic data to shed new light on the (dis)equilibrium state of drainage systems across regional drainage divides.

**Keywords.** Drainage system; fluvial archives; mountain uplift; active tectonics; river profile; fluvial erosion modelling

## 1 Introduction

Alongside climate, uplift, and associated crustal deformation, exerts a strong control on the behaviour and evolution of fluvial systems. This is mainly through its impact on local or regional relative base-level changes and slope variations. Whilst it has long been acknowledged that fluvial landscapes hold a detailed record of past crustal deformation (e.g., Davis, 1899), isolating the causative component within this record is often complicated because of the interplay with many other controls (for example climate, lithology) and feedback mechanisms (e.g., isostatic rebound of erosional origin). Therefore, although understanding and modelling of multiple controls on fluvial evolution have rapidly improved in recent years (e.g., Roe et al., 2002; Lague et al., 2005; Stark, 2006; Turowski et al., 2007, 2008; Lague, 2010), inferences about tectonic forcing often rely on an extensive set of simplifications regarding boundary conditions (uniform rainfall depth and bedrock erodibility, constant and uniform uplift rate, sediment load) and free variables (such as channel geometry). Typical hydraulic scaling of channel width is for instance implicitly accepted in the wide use of the simplest form of the stream power incision model (e.g., Berlin and Anderson, 2007; Beckers et al., 2015). The fact that inferences about crustal deformation are nevertheless generally consistent with independent information underlines its significance in shaping fluvial landscapes and demonstrates how powerful the geomorphological approach can be (e.g., Kirby and Whipple, 2001, 2012; Anthony and Granger, 2007; Cook et al., 2009).

The rapidly growing body of data of increasing quality and resolution published from Quaternary fluvial archives, in which the interdisciplinary group FLAG has played a significant role (see Cordier et al. this volume), combined with worldwide research on modern analogues (e.g., Lane et al., 2003; Wohl, 2010, 2014; Church et al., 2012) has enhanced our understanding of how fluvial systems respond to environmental perturbations. Combined with recent developments in numerical modelling of river evolution (e.g., Veldkamp et al., this volume), it has also shed much light on the sedimentary, hydrologic, and geomorphic responses of fluvial systems to crustal deformation (e.g., Schumm et al., 2000; Whipple, 2004; Crosby et al., 2007; Kirby and Whipple, 2012; Whittaker and Boulton, 2012). Meanwhile, the inverse use of the response characteristics recorded in these archives has enabled the tracing back of deformation events in a variety of active settings (e.g., Westaway et al., 2002; Westaway, 2007; Cook et al., 2009; Schildgen et al., 2009; Roberts and White, 2010; Kirby and Ouimet, 2011). Fluvial archives can basically be considered as being made of two main types, namely the morphology of fluvial landforms and landscapes and the sedimentary deposits produced in response to a tectonic or climatic driver. Uplift information is both embedded within erosional fluvial features such as river profiles or reconstructed terrace staircases, and recorded in the characteristics of fluvial depositional sequences (e.g., texture, thickness, architecture, provenance). However, as mountainous landscapes typically associated with tectonically active regions are often dominated by incision, most geomorphic studies of active tectonics have been overwhelmingly focussed on erosional topography and the forms sculpted by the incising rivers. Importantly, however, these studies are not limited to active mountain belts and the study of river incision and terrace sequences is also powerful in unravelling the history and modalities of more moderate tectonic activity (e.g., Krzyszkowski et al., 2000; Abou Romieh et al., 2009) and epeirogenic deformation driven by far-field stresses (e.g., Cloetingh et al., 2002, 2005; Bourgeois et al., 2007), deep crustal processes (e.g., Ritter et al., 2001) or isostasy (e.g., Westaway, 2001) in intraplate areas.

Investigating the relationships between crustal deformation and drainage system evolution may be envisioned as a means to gain understanding of the river processes in response to the deformation (e.g., Ouchi, 1985; Holbrook and Schumm, 1999; Bianchi et al., 2015 in alluvial systems; Whipple and Tucker, 1999; Whittaker et al., 2007a; Finnegan, 2013; Cook et al. 2013, 2014 for bedrock rivers). However, since the pioneering work of Hack (1957, 1973), a large proportion of studies have conversely focussed on using fluvial archives and landscapes (catchment morphometry, terrace staircases, river profiles, knickpoints) as tools to gain insight into the spatial and temporal variations of uplift and crustal deformation patterns (e.g., Snyder et al., 2000; Berlin and Anderson, 2007; Bridgland and Westaway, 2008, 2014; Pérez-Peña et al., 2009, 2010; Roberts et al., 2012; Demoulin et al., 2013, 2015; Boulton et al., 2014; Goren et al., 2014; Viveen et al., 2014; Geach et al., 2015a). These studies cover a wide range of time scales, from very short term ($10^0$-$10^1$ years) coseismic knickpoint propagation along modern river profiles (Yanites et al., 2010; Cook et al., 2013; Huang et al., 2013) to very long term ($10^7$ years) mantle upwelling and dynamic uplift effects (Roberts and White, 2010; Barnett-Moore et al., 2014; Czarnota et al., 2014). There is also a corresponding variety of spatial scale (from individual faults to continental-scale river or terrace profile inversion) and contrasting structural settings, from rapidly uplifting mountain ranges (e.g., Lavé and Avouac, 2001; Fuchs et al., 2014) through moderately active intraplate areas (e.g., Demoulin and Hallot, 2009; Larue, 2011) to cratonic areas with long histories of extremely low deformation rates (e.g., Westaway et al., 2003; Roberts and White, 2010).

This renewed interest in the use of fluvial archives and river morphometry in tectonic studies has been strongly fostered by major recent advances in geochronological techniques, including continuous improvements in established dating methods such as luminescence dating and exponential developments in the exploitation of terrestrial cosmogenic nuclides (Brocard et al., 2003; Cordier et al., 2010, 2014; Rixhon et al., 2011, 2016). Age estimates have added much value to the huge quantity of field data carefully collected in river valleys over the last century, enabling the calibration and validation of models that simulate the drainage system response to crustal deformation. This revival was invigorated by the availability of digital elevation models (DEM) of ever-increasing resolution and accuracy and the parallel explosion in computing power and capabilities of spatial analysis softwares. Our goal in this paper is to embrace the interdisciplinary nature of FLAG by bringing together research on fluvial archives spanning the Quaternary fluvial terrace literature together with sedimentological and river profile studies to provide an overview of the wide spectrum of mainly post-2000 advances in fluvial geomorphology that shed light over Quaternary histories of vertical crustal deformation. We will use these examples to highlight the main challenges ahead for the fluvial archives community with a focus mainly on the evolution of drainage systems in erosional terrains responding to vertical crustal deformation.

## 2 Decoding river long profiles

We first describe the shape a river longitudinal profile evolves towards with time under constant boundary conditions and briefly review how this shape has been expressed mathematically and how it can similarly be derived from the relation between river incision and stream power. Then, we examine various metrics used to characterize river profiles and discuss the indications they provide about the crustal deformation underlying the drainage system evolution.

### 2.1 The graded profile: observation and theory

Topography and river long profiles in particular are a potentially rich archive of the time-variable factors that governed their evolution. In a general way, rivers adjusting to constant controls tend to establish a graded profile that, according to Mackin (1948), corresponds to a dynamic equilibrium between channel slope and geometry, discharge, and sediment load (**Fig. 1**). As underlined by Mackin, this shouldn't be misunderstood as a situation in which, transport capacity and sediment load being equal, the river has no energy left for incision. Rather, this subtle equilibrium considers the energy used for channel bottom erosion as part of that energy expended in the transport of sediments acting as a tool for erosion. In the case of uplift, for instance, increased slopes will essentially be equilibrated by increased sediment transport, which is itself allowed in the first instance by channel erosion. Therefore, the steady state to which the graded profile refers may be viewed as a topographic steady state *sensu* Willett and Brandon (2002) in which removal of material by river erosion balances influx of rock by uplift, so that the topography of the valley network does not change with time. Conversely, as long as the response of the fluvial system to a perturbation resulting (in this article) from crustal deformation is ongoing, the river is said to be in a transient state.

Several authors have proposed a variety of empirical mathematical formulations to describe the concave upward graded profile of a river. Hack's (1957) seminal paper contributed to the spread of the idea that the graded profile is best expressed by elevation z decreasing logarithmically with distance x from the source

$$z = C - k_l \ln(x) \qquad (1)$$

(with $k_l$ = constant), a function that he derived from the observed linear relationship between channel slope and distance. However, as also argued recently by Goldrick and Bishop (2007), Hack noted that the graded profile could also follow a power law in the form

$$z = C - k_p x^{\alpha} \qquad (2)$$

with $0<\alpha<1$ and $k_p$ = constant. Considering the usual values of the involved exponents (Whipple and Tucker, 1999, their dimensionless equation 21a), the widely used equilibrium long profile formulation derived from the stream power model of river incision (see below)

$$z = z_{out} + \mathcal{K}(1 - x^{\alpha}) \tag{3}$$

(with $z_{out}$ = catchment outlet elevation and $\mathcal{K}$ = constant) implicitly acknowledges this power law relationship. Anecdotally, exponential (Snow and Slingerland, 1987; Morris and Williams, 1997; Rice and Church, 2001) and quadratic expressions of the graded profile (Rice and Church, 2001) have also been mentioned in specific circumstances such as simple alluvial systems without significant water or sediment inputs by tributaries, in which the effect of downstream comminution of bed load particles dominates (Rice and Church, 2001).

Another way to describe how rivers achieve their graded profile is numerical modelling of river incision. A review of the huge literature that deals with this field of research is beyond the scope of this paper. We therefore summarize briefly the basics of such models in order to highlight the relationships they allow us to explore between the respective characteristics of river long profiles and tectonic history. Models are differently expressed in detachment-limited conditions, where channel erosion is first controlled by the river's ability to detach particles from its bed, and transport-limited conditions, where the channel's evolution depends primarily on the transport capacity of the river. While alluvial rivers are obviously transport-limited, detachment-limited conditions are typical of bedrock rivers in steeper areas. Noting that stream power can be thought of as energy dissipation per unit channel area, many variants among the widely acclaimed family of stream power incision models (SPIM) postulate that channel incision (E) of bedrock rivers is a function of unit stream power ($\omega$), yielding the fundamental equation

$$E = k_a \rho_w g Q S / W \tag{4}$$

where $k_a$ = constant, $\rho_w$ = water density, g = gravitational acceleration, Q = water discharge, S and W = channel slope and width, respectively. Empirical static relationships expressing Q and W as powers of drainage area (A) and Q, respectively, allow the rewriting of equation (4) as (Whipple and Tucker, 1999)

$$E = KA^m S^n \tag{5}$$

(K = erosivity coefficient), i.e., in a form easily accessed with the use of digital elevation models. If we allow the dependence of E on $\omega$ to be linear, the slope exponent n = 1 in equation (5). Moreover, based on the observed values of 0.8-1 and 0.4-0.5 for the exponents of the Q = f(A) and W = f(Q) power law functions (e.g., Bravard and Petit, 1997), we obtain $m \approx 0.5$. Relating E to stream power $\Omega$ or to bed shear stress $\tau$ instead of $\omega$ simply changes the values of m and n in the operational equation (5). In the first case, m = n = 1, in the second, $m \approx 1/3$ and $n \approx 2/3$. It should however be noted that these equations include no direct consideration of the actual erosion processes at the channel bottom. Whipple et al. (2000) provided field and theoretical evidence showing for example that, while n conforms with the above values if plucking is the dominant process, it rises to values around 5/3 when abrasion prevails. Although field studies have shown that observed bedrock river erosion is broadly consistent with $n \sim 1$ in many cases (e.g., Berlin and Anderson, 2007; Whittaker et al., 2007a; Whittaker and Boulton, 2012), this assumption has been challenged by theoretical and field work emphasizing a non-linear relation between E and S, implying $n > 1$ when other controls on erosion are included in the modelling, such as an erosion threshold and a stochastic distribution of erosive flood events (Snyder et al., 2003; Lague et al., 2005; DiBiase et al., 2010; Lague, 2014), the scaling of channel width as a function of slope (Finnegan et al., 2005), or temporal variations in precipitations (Braun et al., 2015).

The decision on the most appropriate n value illustrates how many controls on incision are difficult to apprehend in the most basic SPIM expression provided by equation (5). One further major control hidden in the erosivity coefficient K is that of sediment load. Much theoretical and experimental work has been devoted to it, highlighting the role of sediment flux, grain size, relative rock strength of load particles and channel bottom and grain protrusion (Sklar and Dietrich, 1998, 2001; Stark et al., 2009; Yager et al., 2012), and underlining how the sediment load control results from the balance between the antagonistic tool and cover effects of the sediments (Sklar and Dietrich, 2004, 2006; Turowski et al., 2007; Lague, 2010). Other important controls embedded in K include rock resistance, climate, erosion process, hydraulic geometry and the return period of the effective discharge (Anderson and Anderson, 2010). Although the assumption of constant K is often made in case studies, the interpretation of river profiles focused on surface deformation should thus always keep in mind not to underestimate the potential role of these hidden controls.

The principle of conservation of mass implies that, at any point, profile elevation change with time must be the result of a difference between uplift rate U and river incision rate E. As steady state is attained when erosion and uplift balance, unchanging elevations of the equilibrium profile are expressed by

$$U = KA^{m}S^{n} \tag{6}$$

from which we derive the equation of profile equilibrium slope

$$S = (U/K)^{1/n}A^{-m/n} \tag{7}$$

Using Hack's (1957) law, which states that A is a power of x, to substitute drainage area A with along-stream distance x, equation (7) may in turn be integrated to yield equation (3) as the mathematical expression of the graded profile, where

$$\alpha = 1 - hm/n \tag{8}$$

h being the exponent on x in Hack's law and taking values in the order of 5/3.

To summarize, observation and numerical modelling agree on the power law representation of the graded profile of most bedrock rivers that incise uplifting areas and equation (7) implies that uplift rate U contributes to determining this profile. Profile characteristics thus record vertical crustal deformation in some way. However, limitations arise because of the excessive use of the steady state assumption and its easily manageable profile equations, although steady state is probably much less often achieved than generally thought (Willett et al., 2001; Phillips, 2011). However, the above equations are strongly affected by transient conditions. To take only one example, the static relationship between channel width and discharge becomes invalid under such conditions and should be substituted with a dynamic expression of width entailing a slope-width dependence (Whittaker et al., 2007b; Attal et al., 2008; Turowski et al., 2009) that effectively makes n > 1, highlighting the transient strongly non-linear dependence of erosion rate on channel gradient.

## 2.2 River profile analysis

### *2.2.1 Characterizing a profile*

The analysis of real long profiles, either graded or in transient state, requires the definition of metrics that capture their tectonic content in an identifiable way. Several such metrics have been devised over time with various purposes. One, the stream-gradient index SL, was first applied to profile analysis by Hack (1957, 1973). By differentiating equation (1) as the best approximation of long profile curves at the local scale (Hack, 1957), he obtained the channel slope equation

$$|S| = k_1 x^{-1} \text{ or } k_1 = |S|x \tag{9}$$

and renamed the $k_1$ coefficient stream-gradient index SL. This index may be calculated for any point or reach of the profile as the product of local gradient and distance from the source to the reach's midpoint and, as such, should be constant over the length of a perfectly graded (logarithmic) profile (**Fig. 2**). Basically, Hack (1973) was more interested in tracking along-stream variations of SL indicative of local perturbations of any origin (tectonic, but also lithologic or hydrologic) than comparing river average index values, and all studies dealing with the still much used SL index continue to follow Hack's logic, measuring SL for a specified reach length over entire drainage systems and analysing its along-stream changes (e.g., Seeber and Gornitz, 1983; Brookfield, 1998; Mather and Hartley, 2006) or interpolating SL maps (e.g., Keller, 1986; Troiani and Della Seta, 2008; Troiani et al., 2014). Recent advances in this domain revolved around purpose-oriented scales of reach length over which SL is optimally calculated (Pérez-Peña et al., 2009; Troiani et al., 2014) and normalization of SL in an SLk index weighted by the $SL_g$ value calculated as

$$SL_g = (z_{source} - z_{outlet})/\ln(x_{tot}) \quad (10)$$

over the entire length $x_{tot}$ of the stream under consideration (Seeber and Gornitz, 1983; Chen et al., 2003; Pérez-Peña et al., 2004, 2009; Azañón et al., 2012). Moreover, Goldrick and Bishop (2007) proposed a generalized form $SL_{equiv}$ of the stream gradient index by extracting it from the power law expression of long profiles in equation (2), thus getting

$$|S| = \alpha k_p x^{\alpha-1} \text{ or } \alpha k_p = SL_{equiv} = |S| x^{1-\alpha} \quad (11)$$

Interestingly, beyond this new metric for stream gradient, Goldrick and Bishop (2007) also introduce the notion of profile concavity (in the geometric sense, based on the distance-elevation relation), corresponding to the exponent $\alpha$ (which they note as $\lambda$ in their paper). Instead of this mathematical expression of concavity, Demoulin (1998) used a pragmatic and more readable (especially in the case of disequilibrium profiles) way to measure profile concavity through two complementary metrics $E_r$ and $E_q$ measured on normalized long profiles (**Fig. 3**).

The concept of profile concavity brings us to the second major family of profile metrics which are closely related to stream gradient index and concavity $\alpha$. Arguing that channel gradient is related to discharge more readily through drainage area than distance from the source, this second approach also takes advantage of the widespread availability of DEMs for spatial analysis to exploit the slope-drainage area relation that emerges from the stream power equations (e.g., Wobus et al., 2006). This relation, first stated by Flint (1974) and given by equation (7) for a river profile at steady state is more simply written as

$$S = k_s A^{-\theta} \quad (12)$$

where $\theta = m/n$ is the concavity index and the coefficient $k_s = (U/K)^{1/n}$ is called the profile steepness. The log-log representation of the slope-drainage area relation is known as a S-A plot, where a graded profile plots as a straight line whose slope is $-\theta$ and *y* intercept (A being expressed in $m^2$) is $\log_{10}(k_s)$ (**Fig. 1**). While the similarity between concavity measures $\alpha$ and $\theta$ is obvious, the similar affinity between stream gradient SL and steepness $k_s$ has received much less notice. Essentially, however, the only difference between these related metrics lies in the relation of S with either x or A and is in fact easily erased by Hack's law (**Fig. 4**).

The S-A plots of **figure 1** evidence the high degree of correlation between steepness and concavity, which has led to the need for a normalized form of $k_s$. Based on the observation that $\theta$ varies within a narrow range centred on 0.5, the normalization method most widely used defines a reference concavity $\theta_{ref}$ (often taken as the regional average concavity or 0.5, although other fixed values are acceptable) to calculate normalized steepness $k_{sn}$ through

$$S = k_{sn} A^{-\theta_{ref}} \text{ or } k_{sn} = k_s A_c^{-(\theta-\theta_{ref})} \quad (13)$$

with $A_c$ being the geometric mean of the drainage area values at both ends of an investigated reach (Wobus et al., 2006). Another approach was suggested by Sklar and Dietrich (1998), who normalized steepness through drainage area normalization, thus describing the relative steepness by the gradient $S_r$ associated to the reference drainage area $A_r$

$$S_r = k_s A_r^{-\theta} \quad (14)$$

Finally, a third way to dispose of the dependence of steepness on concavity, proposed by Demoulin et al. (2013), simply consists of taking the residuals of the regression of steepness on concavity as an expression of relative steepness. This approach has proved to be slightly more efficient than others in separating areas of distinct steepness (Demoulin et al., 2013).

Two additional comments on the use of S-A plots should be made. First, although they are related to the stream power equations of detachment-limited settings and their use should thus be restricted to bedrock rivers (Snyder et al., 2000), the steady state equations derived for transport-limited conditions yield a similar power dependence of channel slope on drainage area (Whipple and Tucker, 2002). Therefore, as far as equilibrium profiles are concerned, no change in steady state profile form is expected at the transition from the bedrock to the alluvial part of a river and S-A analysis may be safely performed over entire rivers, at least as far as other controls (uplift rate, rock type) are uniform over their whole length. Second, while the original use of S-A plots was more dedicated to the analysis of whole profile steepness (Snyder et al., 2000; Wobus et al., 2006), the calculation of local $k_{sn}$ values per reaches of specified length or separated by prominent profile discontinuities allows the production of $k_{sn}$ maps (Harkins et al., 2007; Ouimet et al., 2009; DiBiase et al 2010) very similar to SL(k) maps (**Fig. 4**). In such maps, differences in $k_{sn}$ reflect deviations from what a SPIM would predict for a river with concavity $\theta_{ref}$, uniform bedrock lithology, and under uniform uplift rate conditions. These maps should be interpreted with due care in terms of rock type variations, differential uplift, abrupt changes in sediment load, e.g., at confluences, or, only in the case in which steady state cannot be safely assumed, transient indicators of temporal change in U.

The quality of concavity and steepness estimates from S-A plots also suffers from the significant noise affecting slope data obtained by differentiation of DEM elevation data, and the question of how to bin effectively slope data in drainage area space. Moreover, beyond the resulting vertical scatter of data points in the plot, the statistical meaning of the regression may also be perturbed by their horizontal clustering due to large jumps in A at tributary confluences. To overcome this limitation, Perron and Royden (2013) developed a new approach allowing estimation of the profile metrics based on elevation rather than slope data. They simply integrate equation (7) rewritten as

$$dz = (U/K)^{1/n} A^{-m/n} dx \qquad (15)$$

to obtain, under assumption of constant U and K,

$$z(x) = z(x_0) + (U/(KA^{m}_{ref}))^{1/n} \chi \qquad (16)$$

where $x_0$ = river outlet, $A_{ref}$ = reference drainage area, introduced to give a dimension of length to $\chi$, and

$$\chi = \int_{x_0}^{x} \left(\frac{A_{ref}}{A(x)}\right)^{\frac{m}{n}} dx \qquad (17)$$

The new variable $\chi$, after which the new profile graph is called a chi plot (**Fig. 5A**), is such that elevation depends linearly on it and a perfectly graded profile appears as a straight line. Profile concavity, corresponding to the exponent of the integrand in equation (17), will now be obtained as the m/n value that yields either the best linear fit of a single z = f($\chi$) profile or the best collinearity between profiles of a main stem and its tributaries. Once the best m/n and thus the $\chi$ scale have been determined, steepness, which appears as the coefficient of $\chi$ in equation (16), simply corresponds to the slope of the linear fit.

Chi plots not only reduce uncertainties on concavity and steepness but they also facilitate the separation of successive profile segments with distinct parameters. For instance, Mudd et al. (2014) developed a method to identify the statistically most meaningful partition of a chi profile into segments of different steepness but same concavity. Demoulin et al. (2015) relied on visual inspection of entire chi profiles to identify their segmentation and recalculate individual concavity and steepness values (even though normalized steepness still refers to a single reference concavity). They noted that producing a single plot of the successive segments of a river profile with their different concavities, and thus also different $\chi$ scales, makes z offsets appear between successive segments, which provide valuable information about the type and the magnitude of the profile discontinuities (**Fig. 5B**). The versatility of chi plots is further demonstrated by Willett et al. (2014) who used them to highlight zones of disequilibrium between competing river basins and analyse the dynamic reorganization of drainage systems. In this example they mapped $\chi$ along the actual river courses and examined contrasts in its values across divides.

*2.2.2 Meaning of the metrics*

The above review of the various metrics available to analyse river profiles underlines their relatedness, with two emerging profile characteristics, namely concavity ($\alpha$, $\theta$, chi plot best fit m/n) and steepness (SL, SLk, $E_r$-$E_q$, $k_s$, $k_{sn}$, chi plot slope). We now examine how much these metrics respond to perturbations from crustal deformation, which properties of the deformation they may record, and how much other controls interfere to determine their variations.

Identification of concavity with the m/n exponent on drainage area in the SPIM-derived slope equation (7) provides clues about factors affecting its variations. At steady state and for uniform uplift rate U, it has been repeatedly stated and verified that it is independent of direct tectonic control (e.g., Whipple and Tucker, 1999; Snyder et al., 2000; Duvall et al., 2004; Wobus et al., 2006; DiBiase et al., 2010; Lague, 2014), whereas lithology (Duvall et al., 2004; Boulton et al., 2014) or the transition from bedrock to alluvial channel may occasionally be responsible for concavity changes. However, this no longer holds as soon as U systematically varies downstream, and as Kirby and Whipple (2001) showed, a power law dependence of U on along-stream distance results in concavity varying with the river orientation with respect to tilt direction. Moreover, variations of a normalized index of channel width compiled by Lague (2014) from several studies suggest a possible dependence of m (through the b exponent of the Q – W relation), and thus of concavity, on incision rate E. One should nevertheless remain cautious not to over-interpret regional variations in concavity in terms of uplift gradient because similar variations may also be caused by systematic downstream change in any parameter included in K, such as lithology or sediment load (Sklar and Dietrich, 1998, 2004), or altering m, such as the orographic effect on rainfall depths and runoff (Roe et al., 2002). The steady state assumption should also be considered with general suspicion when analysing real profiles. An easy test of this assumption, which gives at the same time a qualitative hint of the relative youth of the tectonic perturbation, is provided by regressing concavity values against catchment size (or river order) (Demoulin et al., 2013). In the same vein, it is sometimes meaningful to search for tectonic memory especially in the lowest-order streams of a system, which are the most sensitive to external change. In the Mendocino triple junction area of northern California, while $2^{nd}$- and $3^{rd}$-order stream concavity shows no correlation with drainage area (as estimated from data in Snyder et al., 2000), suggesting quasi steady state profiles that are confirmed by their smoothed shape and the strongly damped control of uplift rate on their mean channel gradient (Merritt and Vincent, 1989), the mean gradient of $1^{st}$-order streams still faithfully follows the uplift rate variations, but with an estimated time lag in the order of $10^5$ years (Merritt and Vincent, 1989). Finally, as noted by Whipple (2004), concavity may vary between successive segments of a single transient river profile. Demoulin et al. (2015) proposed that the decrease in profile concavity observed downstream of tectonic knickpoints in rivers of the northern Peloponnese might be partly related to the incompleteness of profile regrading.

As shown by equation (7), steady state profile steepness should be directly related to uplift rate, of which it is in fact a main indicator. In the case of non steady state profiles, one readily sees from equation (5) that steepness can still be related to erosion rate E. The fact that spatial variations in U or E may also impact profile concavity (Kirby and Whipple, 2001) emphasizes the need for steepness normalization to a reference concavity in order to analyse the U - $k_{sn}$ relation (e.g., Miller et al., 2007). Theoretically, accepting the usual assumption of n = 1, and all else equal (i.e., K constant), the normalized steepness $k_{sn}$ should increase linearly with U. Although field evidence seems to support such a relationship for tributary rivers in the Siwalik Hills (Nepal), in an area undergoing uplift rates in the range 6-15 mm/yr (Wobus et al., 2006), many case studies (Snyder et al., 2003; Gioia et al., 2014; Lague, 2014; Harel et al., 2016) point to a non-linear dependence, modelled by including in the SPIM an erosion threshold (critical bed shear stress) and stochastic effective discharges (Tucker and Bras, 2000). In this case of $k_{sn} \propto U^p$, with $0<p<1$, i.e., $n > 1$, steepness increases very rapidly for low uplift rates (<1 mm/yr) before the curve flattens for higher rates (Snyder et al., 2003) (**Fig. 6**). This would explain the lower than expected contrast in $k_{sn}$ generally observed between regions of intermediate and high uplift rates (e.g., Snyder et al., 2000; Troiani and Della Seta, 2011; Molin et al., 2012; Demoulin et al., 2013; Cyr et al., 2014; see also compilations of worldwide data in Gioia et al., 2014 and Lague, 2014). However, despite the limited influence of large K variations on steepness also suggested by the limited $k_{sn}$ range, data compiled by Lague (2014) show considerable noise in the $k_{sn}$ – U relations, especially in the low uplift rate domain (<0.1 mm/yr), and still more significant differences between the relations calculated for different regions, possibly in part related to differences in K. Noteworthy is also the observation that, though more limited by the constraining reference to logarithmic long profiles, SL and SLk indices show barely larger variations than $k_{sn}$ with U (e.g., Giaconia et al., 2012).

The examination of steepness maps produced from local steepness measurements over river reaches generally a few 100 metres in length (e.g., DiBiase et al., 2010; Troiani et al., 2014) offers a quite different view on the incision-triggering tectonic activity. As noted by Wobus et al. (2006), these maps may suit the identification of tectonic boundaries such as a discrete break in uplift rate, e.g., at a fault, where higher steepness values will characterize the uplifting wall of the fault. However, similar spatial patterns often arise from the transient propagation of an erosion wave within the drainage system as a response to regional uplift. In this case, in which steepness essentially reflects erosion rate variations, a sharp change in $k_{sn}$ does not necessarily identify a local tectonic feature or local uplift rate gradient but instead echoes the remote uplift gradient. In a general sense, interpretation of $k_{sn}$ or SL(k) maps is not straightforward because regional patterns may be obscured by scattered patches of anomalously high index values that require a careful individual analysis, being alternatively indicative of permanent "lithologic" knickpoints, landslide dams (Troiani et al., 2014), places of hydrologic changes such as confluence of large tributaries, the migrating front of a wave of incision (DiBiase et al., 2010), or fixed tectonic structures such as faults and growing anticlines (Pérez-Peña et al., 2009) (**Fig. 2B**).

### 2.3 Transience and knickpoints in river profiles

The existence, timescales and expression of drainage system steady state are often intricate and unclear. While graded profiles may actually not be in a topographic steady state if $E \neq U$, e.g., in post-orogenic landscapes (continued relief decay despite zero uplift), river profiles that do not follow regular power law curves and display convexities, known as knickpoints or knickzones and easily identified on S-A plots (**Fig. 1**), may in fact be in equilibrium if local rates of rock uplift are balanced by fluvial incision at that point (Whittaker et al., 2007b). Indeed, permanent (immobile) convexities may appear in such profiles as a local compensation for lithological contrasts, non-uniform uplift rate or durable change in water discharge – sediment load balance at tributary junctions (e.g., Brocard and Van der Beek, 2006; Beckers et al., 2015). In intermediate cases, profile discontinuities can also show some mobility when they cut through valley damming caused by, e.g., landslides or lava flows, re-establishing equilibrium in locally perturbed profiles (e.g., Korup, 2006). However, many sets of mobile knickpoints and knickzones may represent large-scale upstream propagation of an erosion wave through entire drainage systems which are transiently responding to a relative base level lowering. This lowering may relate to a relatively sudden drop in base level bought about by river capture (discussed in 5.2) or reflect the margin of uplifting regions or the crossing of active dip-slip faults. The notion of response to a specific tectonic signal is important: Whittaker et al. (2008) showed for rivers in the Apennines that only profiles crossing normal faults that underwent an increase in slip rate within the last ~1 Ma display mobile knickpoints whereas those crossing faults with slip rates unchanged for several million years have concave-up profiles.

Such transient features may take several forms (Lague, 2014) reflecting different deformation events. In this respect, beyond extended knickzones that often express spatial variations in uplift rate or, alternatively, an uplift acceleration slow enough to create only a smooth convexity, one distinguishes vertical step knickpoints separating segments of similar concavity and steepness, i.e., segments aligned in S-A plots, from slope-break knickpoints opposing a downstream segment of high steepness and a less steep upstream segment (**Fig. 7**). It is easily seen that, while the latter result from a change in uplift regime toward a permanently increased uplift rate, the former are produced by an uplift pulse temporarily superimposed on a background uplift rate or, in the shortest term, by a coseismic scarp across the river profile. Direct evidence has been provided for knickpoint formation and propagation in response to, e.g., increase in fault slip rate (Whittaker et al., 2007a, 2008), coseismic surface rupture (Yanites et al., 2010; Huang et al., 2013), and postglacial rebound (Bishop et al., 2005; Castillo et al., 2013). In addition, a great many studies have mapped sets of tectonic knickpoints sweeping through drainage systems of uplifting regions all over the world (e.g., Zaprowski et al., 2001; Schoenbohm et al., 2004; Crosby and Whipple, 2006; Berlin and Anderson, 2007; Anthony and Granger, 2007; Harkins et al., 2007; Cook et al., 2009; Loget and Van den Driessche, 2009; Schildgen et al., 2010, 2012; Whittaker and Boulton, 2012; Beckers et al., 2015).

Concurrently, the theory of knickpoint migration has been examined in the frame of various incision models that show knickpoint behaviour ranging from purely advective to essentially diffusive propagation, depending on the major constraint on incision (Crosby et al., 2007). Rearrangement of equation (5) yields the migration rate, or celerity, *c* of the erosion wave in the detachment-limited setting of bedrock rivers

$$c = \mathrm{K}A^{\mathrm{m}}S^{\mathrm{n-1}} \tag{18}$$

which many studies have simplified to

$$c = \mathrm{K}A^{\mathrm{m}} \tag{19}$$

(dimension of K: $\mathrm{L}^{1\text{-}2\mathrm{m}}\mathrm{T}^{-1}$) by assuming n to be close to unity (e.g., Crosby and Whipple, 2006; Berlin and Anderson, 2007; Beckers et al., 2015). While the effective value n may in fact be larger than 1, this assumption nevertheless allowed these authors to perform successful first-order modelling of knickpoint propagation. Advected knickpoints retain their shape while migrating upstream at speeds decreasing in function of a power of A. Therefore, at any moment, knickpoints have travelled variable distances in the diverse branches of a system, depending on the rapidity with which they approach their sources. However, Niemann et al. (2001) showed that the vertical velocity of knickpoints is constant, provided the two river reaches down- and upstream of the knickpoint satisfy the equilibrium equation (7) relative to the new and former conditions, respectively, and K and U are spatially uniform. Consequently beyond the lithology-independent geographic distribution of knickpoints, their altitudinal constancy is thus a testable characteristic of their belonging to a tectonically-driven erosion wave (e.g., Wobus et al., 2006; Cook et al., 2009). By contrast, under transport-limited conditions or with a predominant role of the sediment load, with dual tool and cover effects in bedrock streams, incision models suggest a diffusive or more complex migration of knickpoints, which may make knickzones undetectable (Crosby et al., 2007). Moreover, the shape of migrating knickpoints may be altered even in simple detachment-limited conditions in the case where incision shows a non-linear dependence on channel slope (Tucker and Whipple, 2002; Finnegan, 2013). Supported by field evidence of channel narrowing at knickpoints (Whipple et al., 2000; Amos and Burbank, 2007; Whittaker et al., 2007b), a recent advance in the understanding of the transient response of river profiles has been the replacement in the stream power approach of the static relation between channel width and A, via Q, by an expression that also links it dynamically with slope (Finnegan et al., 2005; Whittaker et al., 2007b; Attal et al., 2008; Turowski et al., 2009; Yanites and Tucker, 2010). Integrating several additional variables, Lague (2014) came to the conclusion that, while following a general rule with n > 1, notably owing to the existence of a threshold shear stress for erosion and the stochastic occurrence of effective discharge, incision could locally follow a simpler n = 1 rule at the height of the migrating knickpoint because of the dynamic relationship between channel narrowing and steepening that prevails there.

There are many studies that have used knickpoint data sets with twofold aims: (1) investigating their origin and controlling factors of propagation, and (2) testing how much SPIMs are able to explain their distribution, and calibrating the stream power law (e.g., Crosby and Whipple, 2006; Berlin and Anderson, 2007; Anthony and Granger, 2007; Cook et al., 2009; Loget and Van den Driessche, 2009; Beckers et al., 2015). As detachment-limited conditions frequently prevail (or are assumed to prevail) in uplifting areas, the simple SPIM form of equation (5) has been generally used, and the overall results confirm that the most simple n = 1 assumption is often acceptable as a first-order approximation (Van der Beek and Bishop, 2003; Berlin and Anderson, 2007; Whittaker and Boulton, 2012; Beckers et al., 2015). Within this frame, m estimates range from 1.13 for incision through highly erodible rocks in New Zealand (Crosby and Whipple, 2006) through 0.68 in the Ardenne (Beckers et al., 2015) to 0.54 for ~8-Ma-old knickpoints in the Colorado (W USA) catchment (Berlin and Anderson, 2007). Other authors have considered empirical relations between distance travelled by the knickpoints and catchment size and found a similar power law, whose drainage area exponent is identical to m if n = 1. Again, values of the exponent range from 1.26 (Bishop et al., 2005) to 0.50 (Loget and Van den Driessche, 2009) and 0.34 (Harkins et al., 2007). Measured or modelled rates of knickpoint displacement, local or averaged over longer distances, have also been published, supported in some cases by independent incision rate estimates (e.g., Anthony and Granger, 2007; Cook et al., 2009; Schildgen et al., 2012; Cyr et al., 2014; DiBiase et al., 2015). Though depending on catchment size, they are often in the order of a few millimetres to decimetres per year, with values up to a few m/yr only for major rivers (see a compilation in Loget and Van den Driessche, 2009; Whittaker and Boulton, 2012; Demoulin et al., 2012). Exceptionally high discharges are capable of causing much faster but highly episodic knickpoint recession. For example, Baynes et al (2015) demonstrated that three extreme flood events (glacial outburst floods with peak discharge of several $10^5$ $m^3/s$) caused cumulative knickpoint retreat of more than 2 km in hard columnar basalts during the Holocene in Iceland. Not surprisingly, snapshot observation of river response to perturbation tends to record retreat rates higher than those averaged over ky to My periods. Extreme rates of up to several hundred metres per year have occasionally been recorded over short time scales (~$10^1$ years) where bedload material is considerably more resistant than the very erodible channel bedrock, as exemplified by the knickpoint created in the Da'an River (Taiwan) by the surface rupture of the Chi Chi 1999 earthquake (Cook et al., 2013). Direct observation has also shown that individual scour events may cause rapid knickpoint retreat even in strong rocks if they are structurally preconditioned. For instance, Anton et al. (2015) measured 270 m headward erosion over 6 years from moderate floods (< 1500 $m^3$ $s^{-1}$) in fractured granite in NW Spain. However, no clear effect of lithology has been noted in general on the propagation rate of knickpoints (Roberts and White, 2010; Whittaker and Boulton, 2012; Beckers et al., 2015).

Profile segments upstream of knickpoints may often reflect a pre-uplift steady state, from which characteristic incision amounts since the uplift event may then be estimated. Using the relict profile concavity and steepness, equation (12) allows extrapolating channel gradients for its continuation down to the point of interest, in general the confluence with the trunk stream, and integration of these slope data yields the ancient profile elevation and the magnitude of incision since it has been abandoned (e.g., Schoenbohm et al., 2004; Harkins et al., 2007; Cook et al., 2009). Incision amounts may also be expressed as incision rates if the timing of knickpoint formation is known and the erosion wave has not yet reached erosion thresholds causing the stagnation of knickpoints (Crosby and Whipple, 206; Beckers et al., 2015).

**2.4 Profile inversion and uplift history**

Pritchard et al. (2009) and Roberts and White (2010) have suggested combining simple forward modelling of river incision with an inversion algorithm in order to reconstruct long-term regional uplift histories *U(t)*. Such studies have been performed at the continental (Roberts and White, 2010; Czarnota et al., 2014) and regional scales (e.g., Roberts et al., 2012; Barnett-Moore et al., 2014). They have used a simple general incision rule combining an advective term that describes the propagation of the erosion wave under detachment-limited conditions and a diffusive term accounting for the transport-limited component of erosion (Roberts and White, 2010; Roberts et al., 2012; Czarnota et al. 2014)

$$E(x,t) = -KA^m(x)\left(\frac{\partial z}{\partial x}\right)^n + \kappa \frac{\partial^2 z}{\partial x^2} \tag{20}$$

where $\kappa$ is a diffusivity coefficient. They make profiles evolve following

$$\frac{\partial z}{\partial t} = U(x,t) + E(x,t) \tag{21}$$

As river profiles contain only indirect uplift timescale information determined by *K*, m, n, and $\kappa$, these parameter values must be chosen with great care. Based on independent data such as, e.g., dated paleoprofiles (Czarnota et al., 2014), local incision rate estimates (Wilson et al., 2014) or the present-day elevations of dated shallow marine deposits (Barnett-Moore et al., 2014), and on the observation that uplift history reconstruction is barely sensitive to a large range of $\kappa$ variations (Roberts and White, 2010), the parameterization of equation (20) may be achieved by systematic search through the (n,m,K) space with a fixed $\kappa$ value. Best fits generally confirm that the most appropriate value of n is unity, while a trade-off is required between K and m along the best fit line in the (m,K) plane. Alternatively, Goren et al. (2014), taking n = 1 and including no diffusive term in the erosion equation, define m and K from chi plots of present profiles. Once parameters are fixed, the inverse approach consists in the estimation of a misfit function that both minimizes the difference between computed and observed profiles and smooths the U(t) curve, by systematically varying U(t) in a Monte Carlo process (Roberts and White, 2010). Owing to recent improvements of the method, which now deals with non-zero initial topography (Czarnota et al., 2014), variable reference level (Barnett-Moore et al., 2014), and non-uniform uplift rates (Goren et al., 2014), remaining major assumptions chiefly relate to constant K through space and time, the role of variable discharges, and absence of temporal changes in drainage planform.

Inverse modelling of river profiles has been successfully applied at the continental scale to the reconstruction of the long-term evolution of dynamic topography in Africa (Roberts and White, 2010) and Australia (Czarnota et al., 2014), although the regional study of Barnett-Moore et al. (2014) reconstructs somewhat variable uplift histories in adjacent basins of SW Australia. It has also allowed a long-term uplift history to be predicted for the Colorado Plateau (Roberts et al., 2012) and the Inyo Mountains, California (Goren et al., 2014). Strikingly, all profile inversion studies point to weak or non-existent lithological control on long-term incision and knickpoint migration rates. However some of the assumptions made by these models, which include the long term erosional dynamics and the need for drainage network stability over time, mean that these inversion techniques are not necessarily appropriate in every transient landscape. More widely, the outcomes of such large-scale analysis of river profiles are probably best seen as producing first-order results on the broad scale, but do provide one tool to analyse the evolution of continental drainage in time and space in response to long-wavelength mantle processes.

Another important point raised by profile inversion studies concerns the very long (up to 120 Ma) uplift histories produced, which correspond to long response times. Roberts and White (2010) noted however that modifying the trade-off between m and K induces no change in the reconstructed number and magnitude of uplift events, but larger m produce younger events. Integrating equation (19) and using Hack's law, response time $\tau$ is expressed as

$$\tau = (L^{1-hm} - x^{1-hm})/(K\,(1 - hm)) \quad (22)$$

with L = river length. Equation (22) shows that response time increases logically with river length but also with smaller K. Yet, at equal m, say m = 0.25, K values may differ by up to two orders of magnitude between various areas, ranging from lowest values around 5-15 $m^{0.5}Myr^{-1}$ (and longest response times) in Australia (Czarnota et al., 2014; Barnett-Moore et al., 2014) to intermediate values in Africa (Roberts and White, 2010) and the Colorado Plateau (Berlin and Anderson, 2007; Roberts et al., 2012), and largest values in the order of 100-500 $m^{0.5}Myr^{-1}$ in western Europe and the Apennines (Whittaker and Boulton, 2012; Beckers et al., 2015). These differences in K may explain the highly contrasted response times published, of a few million years in the Apennines and Turkey (Whittaker and Boulton, 2012) and other active areas worldwide (Baldwin et al., 2003; Demoulin, 2012) compared with up to 120 Myr in Australia. While lithology has been observed to have a limited effect in several studies (e.g., Whittaker and Boulton, 2012; Beckers et al., 2015), climate (through precipitation amount, ratio of precipitation to infiltration, availability of abrasive tools in the bed load) and uplift rate might be the main controls on such differences. In line with Whittaker and Boulton (2012), who have shown that, in the Apennines and SE Turkey, knickpoint migration rates scale with fault slip (and associated uplift) rates, K variations shown above also scale with uplift rates that vary from a few 0.01 mm/yr in Australia through 0.1-0.2 mm/yr in Colorado to 0.2-2 mm/yr in the cited European and Mediterranean case studies.

## 3 Integrative catchment morphometry: the R/$S_R$ approach

Building on the idea that not only individual river profiles but also the fluvial landscape as a whole keeps track of uplift events, Demoulin (2011) proposed a new approach to uplift age estimation based on a composite landscape metric that integrates information relating to a range of time scales. This metric relies on the statistics of incision at nested levels, from individual profiles through tributary networks to catchment data at the regional scale. Calculable for every catchment with a more than embryonic network of tributaries, the metric *R* is the ratio of two-by-two differences between the normalized hypsometric integrals of the catchment $H_b$, its drainage network $H_n$ and trunk stream $H_r$, referring to the long-, middle-, and short-term components of uplift-triggered incision, respectively

$$R = \frac{\int_0^1 (H_n - H_r)\,dl^*}{\int_0^1 (H_b - H_n)\,dl^*} \quad (23)$$

where $l^*$ is the dimensionless expression of length (for $H_r$ and $H_n$) or area (for $H_b$) (**Fig. 8A**). It provides a quantitative description of the relative progress stages of trunk stream and tributary incision and interfluve denudation, which, based on the concept of headward erosion, translates into an estimate of the time elapsed since the fluvial landscape started responding to the latest perturbation that induced a relative base-level lowering. However, the intuition that catchment size also determines the contrast in response rate between trunk stream and tributary network, thus also *R*, is clearly evidenced by the generally strong correlation observed between *A* and *R* within any region of homogeneous uplift timing (**Fig. 8B**). Consequently, uplift age estimates are instead derived from the slope $S_R$ of the linear fit on a semi-logarithmic plot of *R* against ln(*A*) (Demoulin, 2011). Indeed, the theoretical expectation that, following a base-level fall, *R* and $S_R$ first rapidly increase due to swift propagation of incision in the trunk stream, then gradually diminish in the middle term ($10^4$-$10^6$ years), in parallel with the migration of the erosion front in an increasing number of tributaries and sub-tributaries, is fully confirmed by real data from several regions worldwide where uplift age is independently constrained, allowing Demoulin (2012) to propose a quantified power relation between $S_R$ and uplift time (**Fig. 8C**). The very existence of such a relationship underlines the fact that the *R* metric not only is mostly insensitive to lithology but is also usable across a large range of climatic settings. The main limitation to meaningful calculation of *R* lies in the catchment planform and the related stream network development, whose elongation or systematic irregularity (for example an imbalance between tributary network of the lower and upper catchment halves) bias $R$ toward extreme values. Practically, after correction for catchment elongation (Demoulin, 2012; Demoulin et al., 2013), only few catchments, which are in general discarded as outliers of the $R$ – ln($A$) correlation, cannot be used because of persisting shape-related problems. Another practical constraint of the method is the extent of the uplifted region, which should be large enough to encompass a few catchments ≥ 1000 km$^2$ in order to stabilize the $R$ – ln($A$) relation. However, Demoulin et al. (2015) showed that a substitute approach based on producing $R$ long profiles of the longest available rivers may work for smaller areas, with the further potential for identifying river segments with different $S_R$ if the river flows across differently uplifted blocks.

## 4 Crustal deformation and terrace staircases

River terraces appearing as stepped morphologies along valley flanks, which can be essentially aggradational or degradational in nature, have long been used to infer rates of fluvial incision (Burbank and Anderson 2012). A degradational, or 'strath' terrace generally results from lateral erosion into bedrock and displays bevelled bare rock more or less veneered with gravels corresponding to the former transiting bedload. By contrast, an aggradational, or 'fill', terrace is characterized by a thicker alluvial cover bearing witness to a longer stage or a higher rate of sediment accumulation and, often, concomitant larger floodplain widening. In mountainous terrain, local fill terraces are also frequently found as a result of valley damming by landslides (e.g. Korup et al., 2006). Terrace formation basically requires that a widened valley floor be formed by lateral erosion during a stage of vertical (quasi-) stability of the channel before incision resumes, leaving remnants of the former floodplain above the newly formed valley bottom. Although they are described in a general context of uplift-driven valley incision, the climatic character of many such terraces has long been recognized (e.g Bull 1990). In the frame of the stream power model, the climate control occurs essentially through variations in effective precipitation, which impact directly effective river discharge and indirectly sediment load (Hancock and Anderson, 2002). Variations in water discharge and sediment supply in turn may cause high changes in the ratio of lateral to vertical erosion. We expect in principle that lateral erosion is favoured either by decreased discharge (though some channel geometries may induce the displacement of peak shear stresses from the axis to the walls of the channel and increase bank erosion for higher flows; Knight and Sterling, 2000) or by increased sediment load, leading to aggradation, covering of the channel bottom, and strongly reduced or stopped channel bedrock incision (Hancock and Anderson, 2002; Finnegan et al., 2007; Turowski et al., 2008; Johnson and Whipple, 2010; Yanites and Tucker, 2010). Field observation, for instance in the Liwu River, Taiwan (Hartshorn et al., 2002), suggests that the coupled impact of changes in discharge and sediment supply is dominated by the latter, promoting lateral erosion during large floods. This is confirmed by Stark et al. (2010), who note that maximum average sinuosity of incising rivers is recorded in the typhoon-dominated subtropical area of the western Pacific where extreme rainfall and flood events are more common, and decreases with the variability of precipitation on both sides of this latitudinal belt. All this is in line with the common observation in temperate areas that aggradation and valley widening take place mainly during Quaternary cold periods, when large snowmelt-driven spring floods occur yearly but still larger sediment fluxes are delivered by hillslopes and clutter braided floodplains (Bridgland, 2000; Maddy et al., 2001; Vandenberghe, 2008; Lewin and Gibbard, 2010). A return to lower sediment fluxes may then lead to incision and terrace formation, especially if high discharges are maintained during the warming and/or cooling transitions (Bridgland, 2000; Cordier et al., 2006).

Field evidence of Quaternary terrace staircases shows that, considering the interplay of uplift and climate, it is the uplift that determines the amplitude of the vertical spacing between consecutive terraces while the intensity of climatic oscillations controls the more or less aggradational or degradational character of the terraces. As a general rule, information about the timing of incision is more easily extracted from strath than fill terraces because, in the latter case, duration of aggradation is an additional unknown to resolve before estimating incision rates (Rixhon et al., 2011;

Burbank and Anderson, 2012). Lagged or complex responses to perturbation may also blur rate estimates even in dominantly degradational settings (Bull, 1990; Hancock and Anderson, 2002).

While there is now a consensus that the development of terrace flights requires, and their presence thus attests to, regional uplift (e.g., Maddy, 1997; Bridgland, 2000; Bridgland and Westaway, 2008), equating the incision rates revealed by such flights with the causative uplift rates is not always straightforward. Indeed, this assumes that lateral erosion and floodplain development necessary for later terrace preservation occurred after the incising river had (re)established a steady state profile indicative of dynamic equilibrium between incision and uplift. However, this might not be true in many cases where the drainage system response time to a tectonic perturbation is in the order of a few million years (Whipple, 2001; Whittaker et al., 2007a), much longer than the glacial-interglacial cycles that control the pace of Quaternary terrace formation. A main requirement for incision rates being a safe proxy for uplift rates is thus short response time, which is verified chiefly in large rivers and highly active areas (e.g., Leland et al., 1998; Whittaker and Boulton, 2012; Blöthe et al., 2014). In the case of climatic perturbation of the incision/uplift dynamic equilibrium, rivers have often been considered to return rapidly to steady state as soon as the climatic conditions become favourable to bedrock incision because river profiles may rapidly recover from the small perturbations cold-period aggradation imposes on them (Bogaart and Van Balen, 2000; Carretier et al., 2006). Based on this assumption, related to that of parallel terrace profiles, incision rates calculated from terrace age-elevation data have been thought to be a reliable proxy of uplift rates (e.g., Maddy et al., 2000)

### 4.1 Estimating incision/uplift rates from terrace studies

Estimating regional incision rates from dated remnants of fluvial terraces requires terrace long profiles to be reliably reconstructed. In this respect, detailed vertical terrace sequences preserved in valley reaches constitute important anchor points for along-stream correlation (e.g., Juvigné and Renard, 1992; Van den Berg, 1996; Bridgland, 2010; Viveen et al., 2012; Harmand and Cordier, 2012). Terrace levels with distinctive characteristics, such as an anomalously large lateral development (e.g., the main terraces of the middle Rhine: Boenigk and Frechen, 2006; Peters and Van Balen, 2007), thicker than average alluvium, sudden change in the petrological or mineralogical assemblage of the sediments (e.g., in the Meuse terrace following the capture of the upper Moselle: Pissart et al., 1997), biostratigraphic markers (e.g., Schreve et al., 2007; Antoine et al., 2007), provide additional useful constraints, as do soil or duricrust formation and the degree of weathering of pebbles (e.g., Pazzaglia and Brandon, 2001; Stange et al., 2013). However, profile reconstruction, which should allow evaluation of the relative elevation of a terrace with respect to the modern floodplain, i.e., incision amounts, is strongly dependent on the quality and density of terrace data, making it often more or less speculative (Merritts et al., 1994). This is especially true when additional local terraces complicate the overall picture. In the case of discontinuous terrace treads, geometric criteria of correlation may be frequently misleading if employed alone because slope relations between the terrace and modern river profiles are unknown and the geometrically reconstructed profile may even be largely independent of the paleo-channel gradient if terrace formation is linked to the propagation of a wave of incision (Finnegan, 2013).

When effective dating methods of river sediment was not available beyond the last few ten thousand years, inferences about terrace chronology strongly depended on local circumstances such as the presence of Palaeolithic artefacts (e.g., Bridgland et al., 2006; Mishra et al., 2007) or dated tephra in the terrace deposits (e.g., Izett et al., 1992; Berryman et al., 2000; Dethier, 2001; Pastre, 2004; Suzuki, 2008), interfingering with dated lava flows (e.g., Westaway et al., 2009; Van Gorp et al., 2016), direct relationships with glacial features in the European Alps (e.g., Mandier, 1984), or often hard-to-handle palaeomagnetic data (e.g., Van den Berg, 1996). Subsequently, growing field evidence that Quaternary terrace sequences have formed in synchrony with the glacial-interglacial cycles (e.g., Antoine, 1994) led to the still common habit of complementing often sparse numerical terrace dating with their systematic reference to marine isotopic stages (MIS) (e.g., Bridgland, 2000; Cordier et al., 2006), even though this approach could be regarded as overly simplistic in many cases, as attested by varying MIS assignments of the Meuse terraces (Van den Berg, 1996; Van Balen et al., 2000; Westaway, 2002; Bridgland and Westaway, 2014). Since the 1990s, continuous developments in the luminescence dating techniques and the explosion of cosmogenic (radio)nuclide (CRN) studies have fostered the establishment of numerical chronologies of terrace sequences up to ~1 Ma (e.g., Brocard et al., 2003; Cordier et al., 2006, 2010, 2014; Rixhon et al., 2011; Viveen et al., 2012; Geach et al., 2015b; Ruszkiczay-Rüdiger et al., 2016). Additionally, the various ways of obtaining CRN ages of terrace deposits (CRN concentration depth profiles: Braucher et al., 2009; isochron method: Balco and Rovey II, 2008) has renewed our approach to the exact meaning of the obtained ages, namely offering opportunities for separating exposure ages (time of terrace abandonment) and aggradation ages (starting time of terrace sediment accumulation) (Rixhon et al., 2011).

Moreover, while primarily needed for rate calculation, reliable age data has also proved extremely useful in constraining the correlation of terrace treads and revealed that the usual extrapolation of local ages to whole profiles under the assumption that incision occurs synchronously along the entire river course may not always be true (Anthony and Granger, 2007; Rixhon et al., 2011; Baynes et al., 2015). Combined with the study of knickpoints propagating at the expense of the system's main terrace (Beckers et al., 2015), CRN ages obtained by Rixhon et al. (2011) along the lower Meuse – tributary lower Ourthe – sub-tributary Amblève drainage line in the Ardenne demonstrate the time-transgressive formation of this terrace (**Fig. 9**). This diachronous character of terraces formed through knickpoint propagation had been previously assumed from the very nature of this erosion process where tectonic knickpoints had been unequivocally identified (e.g., Zaprowski et al., 2001; Crosby and Whipple, 2006). Investigating the theoretical implications of this mechanism of terrace formation for the slope of a profile that has to be restored from discontinuous terrace fragments, Finnegan (2013) showed that this slope is essentially a function of the ratio between the knickpoint migration rate and the rate of incision of the river upstream of the knickpoint and, as such, is mostly different from the slope of the paleo-channel. Using the stream power law of river erosion and based only on geometric considerations in which the elevation of the retreating knickpoint crest defines the nascent terrace, he derived an expression of the expected terrace slope $S_t$

$$S_t/S_r = 1 - (S_r/S_k)^{n-1} \tag{24}$$

with $S_r$ = channel slope upstream of the knickpoint and $S_k$ = knickpoint slope, which highlights the dependence of the terrace slope on n. In the frequently assumed case where n=1, the time-transgressive terrace formed by knickpoint retreat should display zero slope. While the terrace slopes downstream for n > 1, n < 1 theoretically implies that it has a counterslope gradient (absolute elevations of the terrace increase downstream). Based on an analysis of waterfalls and knickzones along rivers of the San Gabriel Mountains, California, DiBiase et al. (2015) further stressed the need for careful sampling of time-transgressive strath terraces if knickpoint retreat rates are to be estimated.

**4.2 Terrace profile geometry**

The many case studies where sound terrace profiles could be reconstructed from relatively continuous field evidence have shown that terrace flights display three basic patterns: (1) parallel profiles, (2) upstream diverging profiles, and (3) downstream diverging profiles (e.g, Pazzaglia et al., 1998; Colombo, 2005) (**Fig. 10**). In any case, the relative profile attitude concurrently depends on changes in equilibrium slope of the successive channel profiles on the one hand and change with time of the original terrace slope on the other. Supposed to reflect equilibrium conditions (Bull, 1990; Pazzaglia and Brandon, 2001), parallel terrace profiles (e.g., Westaway, 2002; Stange et al., 2013) are generally considered to indicate regions of spatially uniform uplift rate (Pazzaglia et al., 1998) but a further condition for parallelism is that uplift rate also remains constant through time, so that the successive channel equilibrium profiles have similar gradients. As for upstream diverging profiles (e.g., Pierce and Morgan, 1992; Colombo, 2005; Hetzel et al., 2006; Boenigk and Frechen, 2006; Gabris and Nador, 2007), they are usually interpreted as an indication of higher uplift rates near the headwaters than in the lower catchment part (Pazzaglia et al., 1998), i.e., downstream directed tilt (e.g., Pierce and Morgan, 1992).

Conversely, downstream diverging profiles are often thought to reflect higher uplift rates in the lower course of the river, or upstream directed tilt (Pierce and Morgan, 1992). The more vague association of such a profile pattern with simple base-level fall (Pazzaglia et al., 1998; Colombo, 2005) is unlikely as long as no uplift acceleration imposing steeper gradients to the new equilibrium profile can be established. Only if episodic uplift pulses were superposed on a constant background rate might a set of parallel terrace profiles converge upstream with a modern transient profile, the lowest terrace(s) still merging with the present channel profile at the height of knickpoints migrating up the latter (e.g., Seidl and Dietrich, 1992; Howard et al., 1994; Zaprowski et al., 2001). However, observing that all middle-sized rivers flowing down the epeirogenetically uplifted Ardenne display downstream divergent terrace profiles, whatever their orientation, Macar (1957) pointed to an alternative cause of divergence. According to him, the progressive deepening of valleys through river incision entails a proportional increase in sediment delivery from lengthened steep valley sides to the channel, which, for unchanged water discharge, imposes gradually steeper equilibrium channel gradients.

Two other aspects of terrace flights, characterized by warped or vertically offset profiles, are also encountered and bear witness to more local deformation (**Fig. 10**). Warped profiles are produced by the growth of a fold oriented orthogonally or obliquely with respect to the river course. If the river's power is high enough for it to cope with the rate of fold growth, a situation of antecedence develops, where the pre-existing river incises across the growing fold. If for any (e.g., climatic) reason, incision is episodically interrupted by terrace formation, every terrace will display a degree of warping directly proportional to its age, which evidences the geometry of the surface deformation associated with the fold growth, thus to some extent the type of folding (Scharer et al., 2006; Hubert-Ferrari et al., 2007), and allows growth rate estimation. The archetypal example of such an evolution was described for rivers flowing down the Himalaya and crossing the rising anticline that forms the Siwaliks Hills above the Main Frontal thrust in central Nepal (Lavé and Avouac, 2001) but similar case studies have also been published from other regions of active folding worldwide (e.g., Molnar et al., 1994; Haghipour et al., 2012; Veloza et al., 2015). As for vertically offset terrace profiles, though often obscuring the general profile reconstruction, they may be used for the estimation of displacement rates on active dip-slip faults crossing a river if tread continuity, age data or other unambiguous terrace markers allow a reliable terrace correlation (e.g., Rockwell et al., 1984; Peters and Van Balen, 2007; Abou Romieh et al., 2009; Walker et al., 2010).

### 4.3 An integrated tectono-climatic model of Quaternary valley incision

Much progress has been achieved in the understanding of Quaternary river incision during the last two decades. However, distinct research lines were followed within two poorly connected communities. On the one hand, 'fluvial archive geomorphologists' have performed extensive field work, analysing and dating predominantly fill terraces from terrace sequences of many alluvial rivers worldwide (see a recent synthesis in Bridgland and Westaway, 2014). Within the FLAG (Fluvial Archives Group) framework, river terrace sequences have been mapped, described and, in many cases, dated in the most varied tectonic settings, from very active mountains (e.g., Tibet: Vandenberghe et al., 2011; Zhu et al., 2014), through regions of moderate tectonic activity (e.g., Syria: Demir et al., 2007; Westaway et al., 2009; Turkey: Bridgland et al., 2012; Maddy et al., 2012; Iberia: Stokes and Mather, 2003; Cunha et al., 2005; Santisteban and Schulte, 2007; Harvey et al., 2014), epeirogenetically uplifted (Rhenish shield: Van den Berg, 1996; Pissart et al., 1997; Boenigk and Frechen, 2006; Cordier et al., 2009; French Central Massif: Pastre, 2004) and tectonically stable (Britain: Bridgland, 2010; Bridgland et al., 2015; Paris Basin: Cordier et al., 2006; Antoine et al., 2007; Despriée et al., 2007) areas of NW Europe, Russian Arctic (Alekseev and Drouchits, 2004; Patyk-Kara and Postolenko, 2004), to cratonic areas (South Africa: Helgren, 1978; Ukrainian shield: Matoshko et al., 2004; Australia: Nott, 1992; Nott et al., 2002). Some of this research has highlighted that many rivers worldwide show a similar temporal pattern of increased incision rate since the early Middle

Pleistocene, and attributed this to the mid-Pleistocene climatic degradation enhancing erosion and, thus, erosional isostatic rebound of the crust (Westaway et al., 2003; Bridgland and Westaway, 2008, 2014). This would suggest that the part of the total uplift/incision that responds to this climate-driven mechanism in tectonically active areas is more or less systematically superposed on the true tectonic component of uplift. This may be true in epeirogeneically deformed continental interiors, where both components are of the same order of magnitude (e.g., Demoulin and Hallot, 2009) but is also a subject of debate in more active mountains (see, for example., the aneurysm vs fold growth controversy about the dominant cause of extreme uplift rate in the eastern Himalayan syntaxis; Zeitler et al., 2001; Seward and Burg, 2008).

On the other hand, process geomorphologists have developed a parallel approach more centred on numerical modelling of river erosion in uplifting areas and mainly interested in quantifying controls on incision. A distinctive trait of their research, which has been reviewed mainly in section 2, is the special interest paid to the transient response of bedrock rivers to tectonic perturbations in active orogens (recent syntheses in Whipple et al., 2013; Lague, 2014). While modellers have so far made limited attempts to model terrace formation (e.g., Veldkamp, 1992; Hancock and Anderson, 2002; Finnegan, 2013; Stange et al., 2014; Norton et al., 2015, Geach et al., 2015a), many fluvial archive geomorphologists tend to be reluctant to incorporate transient features and their implications, i.e., knickpoints and time-transgressive terraces, in their reconstructions of terrace sequences (e.g., Bridgland and Westaway, 2012). Equally, it is also highly debatable whether the systematic global application of the model proposed by Westaway (e.g., 2002, 2012) to terrace sequences is meaningful in the many regions where loading gradients of erosional origin are much too small to cause lower crustal flow. Progress in the understanding of the complex interplay between tectonic activity and surface processes clearly requires the rapprochement of the two communities (Briant et al., 2016), both of whom essentially work on the same fundamentals.

Based on detailed terrace studies in the Ardenne where the climatic and tectonic controls narrowly intermingle, Demoulin et al. (2012) recently proposed a conceptual hybrid model of valley downcutting that acknowledges the alternation of climatic terrace succession and knickpoint propagation. The main ingredients of drainage system incision in the Ardenne during the Quaternary are a pulse of accelerated uplift (~0.3 mm/yr) around 0.7 Ma superposed on a background uplift rate close to zero prior to 0.7 Ma and very slightly higher (~0.05 mm/yr) after the pulse (Demoulin and Hallot, 2009; Beckers et al., 2015) interacting with the glacial-interglacial cycles. Demoulin et al. (2012) oppose a steady state evolution under constant background uplift, which leads to the formation of climatic terraces evolving simultaneously in the whole drainage system, in agreement with the classical cyclic model (e.g., Bridgland, 2000; Vandenberghe, 2008), and a transient episode responding to the uplift pulse by the creation and propagation in the system of knickpoints, whose displacements caused from 0.7 Ma onwards the formation of one time-transgressive terrace level in the Ardennian valleys. Evidenced by CRN dating (Rixhon et al., 2011), the diachronic character of this particular level is easily measured in the Meuse tributaries ($A < 4000$ km$^2$) but is not resolvable in the Meuse itself ($A \approx 20,000$ km$^2$) where the erosion wave migrated much faster. Currently located in the system's headwaters and reactivated during each climate-dependent episode of incision, the knickpoints constitute a mobile line of separation between an upstream area where the pre-pulse steady state still induces very limited incision and a downstream region where younger terraces more or less parallel to the modern profile illustrate the interplay between climate oscillations and the current steady state uplift/incision rate (**Fig. 9B**). In this case study, climate oscillations may have helped in developing a sharp profile discontinuity from a rather small change in U because high sediment delivery from hillslopes prevented incision during cold periods, temporarily freezing the system's response and allowing the accumulation of a large finite base level fall at the edge of the uplifting area before incision resumed at the next climatic transition (~20-m-high knickpoints required 65 ky to form from a ~0.3 mm/yr increase in uplift rate).

## 5 Planform changes in fluvial systems

### 5.1 Changes in channel form

Active vertical crustal deformation is recorded not only in the vertical evolution of rivers but also in changes of the planform patterns of alluvial channels. Based on experiments and field evidence, Ouchi (1985) showed that a meandering river crossing a growing anticline tends to respond first by increasing its sinuosity on the oversteepened downstream limb of the fold and, conversely, straightening its course across the fold's upstream half where the valley profile flattens (**Fig. 11**). However, in the latter zone, the ponding of the river and the associated aggradation often induce also the development of reticulate or anabranching channel patterns. In the case of braided rivers, transverse folding leads to an up-fold transition from braided to meandering-braided pattern. Downstream the resulting sedimentation and flow concentration forms a straight single channel incising the fold core before returning to braided channels downstream of the fold. Further examples of such short-term responses of alluvial rivers have been given by, e.g., Jain and Sinha (2005), Petrovszki and Timar (2010), Burbank and Anderson (2012). Moreover, Harbor (1998) and Amos and Burbank (2007) note that the first response of small alluvial rivers to fold growth is by channel narrowing. Only if the amount of differential uplift increases must channel narrowing be complemented by gradient steepening, first through channel straightening then knickpoint formation, in order to maintain antecedence. However, in a study of low-gradient alluvial rivers in SE Louisiana (USA), Gasparini et al. (2015) are not able to see a clear lead and lag between channel narrowing and changes in sinuosity in response to small differential uplift rates, nor do they identify the factors that determine an incisional versus planform response.

Based on observation of the response of the braided Da'an River to 10 m uplift of the Dongshi anticline during the 1999 Chi-Chi earthquake in Taiwan, Cook et al. (2014) recently introduced the concept of downstream sweep erosion, responsible for gorge eradication. They note that, after a gorge had rapidly formed through knickpoint retreat across the uplifted valley reach and had transiently widened through channel wall undercutting, propagation of the knickzone in the sediment wedge upstream of the anticline largely removed them over a width of 250 m, causing aggradation in the gorge and exposing the upstream-facing edge of the anticline. Owing to the abrupt narrowing of a ~800-m-wide braidplain into a 25-m-wide gorge, channel shifts through avulsions in the plain drove rapid erosion of parts of the exposed anticline scarp, resulting in its parallel downstream retreat, consumption of the uplifted topography, bevelling of the valley floor, and shortening of the gorge length (**Fig. 12**). Observing that the rate of this process is one order of magnitude higher than that of gorge widening and that previous coseismic uplifts of the anticline have left no trace in the topography, Cook et al. (2014) propose that, at least in the case of episodic uplift, downstream sweep erosion is an efficient mechanism for the erasure of a gorge created downstream of a broad floodplain.

### 5.2 Capture and drainage reorganisation

If the uplift rate is too high for river erosion to keep pace with it (depending on the balance between sediment flux, upstream ponding and river power, see Humphrey and Konrad, 2000) and antecedence cannot be maintained, stream diversion (sensu Bishop 1995), generated by, e.g., lake spillover (Hood et al., 2014) or stream piracy, can lead to drainage reorganisation at a range of scales. Van der Beek et al. (2002) also show that, in the case of drainage transverse to active fault-propagation folding, the axial slope developing at the back of the growing fold for a non-zero dip of the underlying detachment favours stream deflection toward the propagating fold tip, so that the spacing of transverse rivers is controlled much more by the characteristic fault segment length than the ratio between uplift and incision rates. Beyond the drainage system planform geometry, traces of this process in the landscape are mainly windgaps (Burbank et al., 1996) and the incision response to redistribution of discharge (e.g., Yanites et al., 2013). River captures determined by differential uplift occur at all spatial scales, from local to subcontinental. To take one example of the latter, in their compilation of the drainage history in E and SE Tibet, Clark et al. (2004) document a number of captures and drainage reversal events by which the lower Yangtze successively diverted to the east streams that originally gathered in a single major SE-flowing stream from which the modern Red River represents the subsisting lower course, while other rivers of the ancient Red River catchment, including the upper Mekong, Salween and, possibly, Tsangpo-Brahmaputra, would have been diverted to the S and SW (**Fig. 13A**). Despite lacking age constraints, they argue this large-scale drainage reorganisation, and especially reversal of the middle Yangtze and capture of the upper Yangtze, occurred possibly in Oligocene to mid-Miocene times, prior to regional uplift of E Tibet, which imposed ~2000 m incision since reversal of the flow direction of the middle Yangtze. Based on mass balancing between eroded and deposited rock volumes and isotopic analysis of sediments from the Hanoi Basin, Vietnam, Clift et al. (2006) confirm this view of large-scale beheading of the Red River catchment, possibly including loss of the middle Yangtze, before ~24 Ma. Recently, Kong et al. (2012) challenged the old age of these events, using detrital zircon U-Pb and cosmogenic $^{10}$Be/$^{26}$Al burial ages of fluvial sands to conclude that rerouting of the upper Yangtze would instead have been realised within the last 1.7 Ma, although these conclusions are disputed by other researchers (Bridgland and Westaway, 2012).

In continental Iberia, river capture has operated on a variety of scales, connecting previously endorheic continental basins with the Atlantic (e.g., Anton et al., 2012; Martins et al., 2017) and Mediterranean (e.g., Harvey et al., 2014). These captures, whose drivers have principally been attributed to differential uplift rates, are associated with rapid and dramatic base-level changes which stimulate accelerated bedrock erosion in rejuvenated catchments and the development of transient knickpoints that migrate headward (e.g., Stokes et al., 2002; Mather et al., 2002). One of the best documented events occurred on a small sedimentary basin scale (capture of 300 km$^2$ of adjoining drainage) in the Sorbas Basin (SE Spain). The river capture was first reported by Harvey and Wells (1987). Later work by Mather (2000a, b), Mather et al. (2003), and Stokes et al. (2002) together with advances in dating techniques applied to the regional fluvial terrace sequence (e.g., Candy et al., 2005; Geach et al., 2015b) enable constraints to be placed on rates and nature of landscape change relating to the 90 m drop in base-level effected by the capture, and migration of the ensuing wave of incision (Mather et al., 2002). The main response was a dominance of vertical incision following headward knickpoint migration and a change to lower post-capture width/depth ratio of valley sections, landsliding of the oversteepened slopes being a secondary valley-side response. The capture event occurred after a terrace was abandoned at ~70 ka and significantly before aggradation of the next terrace (~30-40 ka). Based on these dates, a minimum sevenfold increase in incision rate (>1.4m/ka) has been estimated in the diverted stream after the capture event. The head of the knickzone has now reached some 20 km upstream since the capture, and is still actively migrating through the system (e.g., Mather and Stokes, 2016). In contrast, the beheaded drainage has limited incision and localised aggradation. Similar responses have been recorded in other capture events (e.g., Azañón et al., 2005).

However, stream piracy can also result from a range of non-tectonic causes and the link between capture and tectonic surface uplift or tilt is often more difficult to isolate and/or to prove. An instance of this is provided by the Plio-Quaternary captures that made the Aare River successively belong to the Danube basin, then the Rhône basin (through the paleo-Doubs), and finally to the modern Rhine basin flowing to the North Sea (Giamboni et al., 2004; Ziegler and Fraefel, 2009; Schlunegger and Mosar, 2011) (**Fig. 13B**). There, the main driver of captures was base level falls in different active grabens much more than moderate uplift in the intervening areas. The first westward diversion of the Aare from the Danube to the Rhône catchment at ~4.2 Ma was caused by headward incision of the proto-Doubs, whose base level was constituted by the subsiding Bresse graben, toward the Aare-Danube, which flowed along the SE margin of the Vosges-Black Forest crustal arching. Likewise, the diversion of the Aare toward the proto-Rhine basin in the north at 2.9 Ma also resulted from a large gradient in vertical motion between main resuming subsidence in the southern part of the graben and subordinate uplift of the Sundgau area.

Whilst quantitative estimates of the impact of captures (of any origin) on incision rates and patterns and of the corresponding response times have recently been provided for several case studies (e.g., Mather et al., 2002., Stokes et al., 2002; Prince et al., 2011; Schlunegger and Mosar, 2011; Andrews et al., 2012; Brocard et al., 2012; Yanites et al., 2013; Aslan et al., 2014, Anton et al., 2014), numerical modelling of the mechanisms governing divide migration and drainage reorganisation has yielded insights into other aspects of the dynamics of landscape evolution. Willett et al. (2014) devised a new way to estimate drainage divide disequilibrium, i.e., the degree of competition between streams eroding the opposite sides of mountain ridges. They note that, by definition linearly related to steady-state channel elevation, the values of Perron and Royden's (2013) $\chi$ variable defined in equation (17) should be equal across water divides that have reached geometric equilibrium between steady-state catchments. Therefore, $\chi$ maps (at constant m/n) of drainage networks and comparison of the headwater values across divides highlight the zones out of equilibrium, with drainage divide migration expected in the direction of higher $\chi$ values. Though employing several simplifying assumptions (stream power erosion, uniform U, K, precipitation rates) that are also typically used in formal inversion techniques (section 2.4), this approach identifies the NW migration of the Blue Ridge in SW United States and suggests unstable second-order divides on the eastern flank of the Central Range, Taiwan (Willett et al., 2014).

Studying how drainage networks react to a combination of uplift and horizontal shear strain on both flanks of the Southern Alps of New Zealand, Castelltort et al. (2012) also illustrate how drainage divide migration conditions different records of the horizontal shear in the river courses on both sides of the range. Taking into account a transverse gradient in uplift rate (decreasing SE-ward) and the orographic effect on precipitation, which favours erosion on the western flank, in their modelling of oblique convergence along the Alpine fault, they show that actively eroding rivers of the NW side extend their catchment at the expense of those of the other side of the range by gradually pushing the divide to the SE. Therefore, the NW rivers maintain their course roughly orthogonal to the main divide through a succession of small drainage reversal and capture events, thus removing the effect of shear strain from their planform pattern, whereas the less competitive rivers of the SE flank tend to rotate passively, keeping record of the shear history. Goren et al. (2015) further confirm these findings in their analysis of rivers draining the western flank of Mount Lebanon, where rotated basins record distributed horizontal deformation and $\chi$ differences across secondary divides transverse to the mount axis image the resulting disequilibrium in divide position. In brief, despite potential interferences with other controls on drainage network evolution, these studies highlight that crustal deformation is a primary control on drainage system evolution in active mountains and underline how powerful numerical modelling is in retrieving the tectonic history from the landscape response characteristics. However, as shown by laboratory modelling experiments and observations in the Aconquija Range of NW Argentina (Bonnet and Crave, 2003; Bonnet, 2009), while regional erosion is prompted by uplift, differential incision and drainage divide shifts may equally result from either tectonic (uplift gradient) or non-tectonic (e.g., rainfall gradient, lithological contrast) causes. Finally, we do not consider here the primary organisation and general characteristics of drainage networks in relation to relief creation (e.g., Hovius, 1996; Talling et al., 1997; Castelltort and Simpson, 2006; Perron et al., 2009).

## 6 Depositional environments: stratigraphy produced by fluvial system deformation

It is fundamental to appreciate that if fluvial landscapes can respond transiently to tectonic perturbations over timescales of millions of years (e.g. Whittaker et al., 2007b; Roberts and White, 2010), then fluvial stratigraphies, whether preserved in terraces or neighbouring depo-centres, can record and preserve the erosional response of landscapes to tectonic forcing over similar periods (Allen, 2008; Whittaker et al., 2010; Duller et al., 2012; Michael et al., 2013). In principle, the terrestrial sedimentary record therefore provides a “mirror” view of river response to tectonic forcing. Such archives are of particular value if their corresponding erosional landscape is no longer preserved (Michael et al., 2014), and thus where stratigraphy serves as the only record of mass transfer across the surface of the Earth in response to past boundary conditions. While the sensitivity and response timescales of erosional-depositional systems to high-frequency, high magnitude climate changes remain highly contentious (e.g. Jerolmack and Paola, 2010; Simpson and Castelltort, 2012; Armitage et al., 2013), field studies provide growing evidence that the response of fluvial systems to active faulting and, more generally, crustal deformation is indeed reflected in changes to the characteristics of sediment both generated in upland catchments and subsequently preserved in down-system archives (e.g Milliman and Sivitksi, 1992; Allen 2008; Whittaker et al., 2010; Parsons et al., 2012).

For instance, Whittaker et al. (2010) showed that for modern catchments crossing active normal faults in central Italy, and responding transiently to an increase in slip rate within the last million years, the majority of sediment export came from the migrating knickzone upstream of the faults, driven by the associated hillslope response to rapid fluvial incision. The upstream propagation of these knickzones was likened to the firing of a "sediment gun" which led to the production of greater sediment volumes and the export of coarser grain sizes resulting from landsliding into the channel. Similar results have been observed for the Feather River catchment, California, in response to a rapid drop in base level (Attal et al., 2015), and together these types of study emphasise the close and dynamic coupling of hillslope and river processes in generating fluvial sediment fluxes in tectonically active areas (cf Allen, 2008). Numerical models also demonstrate clearly the linkages between tectonic forcing, river response and sediment supply (e.g., Cowie et al., 2006; Armitage et al., 2011; Van de Wiel and Coulthard, 2010; Simpson and Castelltort, 2012, Allen et al., 2013; Forzoni et al., 2014). Cowie et al. (2006) coupled a fault growth and interaction model to the landscape evolution model CASCADE and demonstrated that the volumes and locus of sediment export were controlled, with a noticeable time lag, by the growth and linkage of fault segments, and this dynamic evolution significantly influenced river long profiles, drainage networks and the points at which sediment was fluxed to hanging-wall depo-centres as through-going faults increased their slip rates. Recent work by Allen et al. (2015) quantified this grain size supply effect and demonstrated that it exerted a fundamental control on depositional stratigraphy.

Stratigraphic models explicitly linking catchments to their fluvial stratigraphies have also made plain the quantitative links between sediment supply characteristics, driven by landscape response to active tectonics, and proximal terrestrial sediment archives. Forzoni et al. (2014) show clearly how sediment supply and grain size trends in their 1D model are influenced by tectonic forcing using catchments in the Italian Apennines as a template, while Armitage et al. (2011, 2013), using a non-linear diffusion approach, show that changes in tectonic uplift rate produce diagnostic patterns in fluvial stratigraphy. Their results indicated that grain size trends in sedimentary basins are predictable functions of accommodation space creation and of the degree of tectonic perturbation affecting the footwall/hangingwall system (cf Fedele and Paola, 2007; Duller et al., 2010). Moreover, an increase in fault slip rate resulted in differing vertical grain size trends through the resulting stratigraphy, depending on the distance from the depositional fan apex. This response was fundamentally caused by the lag-time between the instantaneous generation of tectonic subsidence following an increase in fault slip rate, compared to the slower sediment supply response driven by the landscape system. Rohais et al. (2012), using an analogue modelling approach, arrived at similar conclusions. In particular, their results suggested that trends in sediment calibre in terrestrial stratigraphy recorded a non-linear response of their coupled catchment-depositional systems to changes in both tectonic and climatic boundary conditions. The result of these changes included a time-dependent disequilibrium between sediment supply and sediment transport capacity in the modelled catchment. Overall, these studies all indicate that the transient stratigraphy produced by river response to tectonic perturbation, such as a change in fault uplift rate, might initially be seen as a contemporaneous fining in proximal deposits, as accommodation space is generated initially, followed by a prograding wedge of coarse fluvial gravels, as sediment supply and median grain sizes exported from upland catchments increase during the transient landscape response phase (cf Whittaker et al., 2010). Rates of stratigraphic grain size fining are documented to increase for a decrease in sediment supply and an increase in accommodation generation, respectively (e.g., Parsons et al., 2012).

It is evident that if fluvial stratigraphy records river response to tectonic forcing, then in principle we can exploit, e.g., the nature of a fluvial terrace fill to say something about past tectonic (or environmental) forcing. One strategy here is to concentrate on the implied depositional long profile gradient of the river channel that deposited the terrace sediments, exploiting grain size analysis of the terrace fill. Using a dimensionless shear stress (Shields stress) approximation, where river long profile gradients, depths and widths trade off against each other predictably, a number of authors have reconstructed palaeo-slopes from fluvial deposits (e.g., Paola and Mohrig, 1996) and thus obtained palaeo-long profiles from fluvial stratigraphy. In northern Colorado and Western Nebraska, for instance, based on contrasting the apparently differing transport or depositional slopes of Late Miocene river sediments with present day long-profile estimates, this approach has led to a lively debate as to whether these sediments have been tilted post-depositionally by regional uplift processes (McMillan et al., 2002; Duller et al., 2012). Other authors have concentrated on constraining stratigraphic grain size fining rates and using this to invert fluvial stratigraphy for both sediment fluxes and distribution of tectonic subsidence in areas of active faulting and uplift (Whittaker et al., 2011; Paola and Martin, 2012; D'Arcy et al., 2016). Moreover, if the entire down-system sediment routing system can be constrained, ideally including non-tectonic controls (e.g., particle abrasion; Attal and Lavé, 2006, 2009), then the stratigraphy can be used to determine the volumes, rates and characteristics of sediment eroded from the uplifting area as a whole (Michael et al., 2013, 2014). Such an approach is particularly powerful when combined with techniques such as detrital thermochronometry (e.g., Kuhlemann, 2007; Whitchurch et al., 2011). These results therefore underline that information about river response to tectonic forcing can and should be extracted not just from the morphology of, e.g., a terrace fill or fluvial deposit, but also from the sedimentary characteristics themselves, and exploiting this record remains an attractive target for future research.

## 7 Conclusion: challenges and prospects

In this review, we illustrate the wealth of information fluvial archives and present-day characteristics of rivers and drainage systems contain about vertical crustal deformation and associated landscape evolution. However, developments in the study of the fluvial system response to tectonic forcing are currently so fast and involve so many different approaches that a review such as this can only touch on the wide range of literature addressing these important topics. While this review shows that a great deal of progress has been made in understanding how uplift influences both the erosional landforms generated by fluvial processes, and their depositional stratigraphy, a number of key challenges remain. To conclude, we highlight some of major issues that will have to be addressed in future research about the links between crustal deformation and river evolution. In particular we need to:

(1) Reduce uncertainties linked to how the effects of non-tectonic controls on river erosion (lithology, hillslope sediment delivery, sediment flux, channel hydraulic geometry, stochasticity of effective discharge) affect the river response to tectonic perturbations

(2) Increase the quantity and quality of integrated data sets that combine field evidence (e.g., fluvial terraces, sediment load), erosion and incision rates (CRN, low-T thermochronology), river profile analysis, and drainage system morphometry. This would provide a strong support to model benchmarking and an improved understanding of the spatio-temporal characteristics of tectonic forcing

(3) Exploit the tectonic information contained in the sediment component of fluvial systems (material characteristics and depositional environments)

(4) Explore all prospects offered by new high-resolution remote sensing products (Lidar DSMs and DTMs, three-dimensional scanning, global high-resolution DTMs)

(5) Bridge the gaps between research communities (e.g., modellers vs field geomorphologists, specialists of surface versus deep crustal processes) to increase the consistency of the global picture.

**Acknowledgments.** We warmly thank reviewer M. Attal and guest editor D. Bridgland for their constructive comments, which helped improve the balance between viewpoints on some controversial issues.

## References

Abou Romieh M., Westaway R., Daoud M., Radwan Y., Yassminh R., Khalil A., al-Ashkar A., Loughlin S., Arrell K., Bridgland D., 2009. Active crustal shortening in NE Syria revealed by deformed terraces of the River Euphrates. *Terra Nova* 21, 427-437.

Alekseev M., Drouchits V., 2004. Quaternary fluvial sediments in the Russian Arctic and Subarctic: Late Cenozoic development of the Lena River system, northeastern Siberia. *Proc. Geol. Assoc.* 115, 339-346.

Allen P., 2008. Time scales of tectonic landscapes and their sediment routing systems. *Geological Society, London, Special Publications* 296, 7-28.

Allen P., Armitage J., Carter A., 2013. The Qs problem: Sediment volumetric balance of proximal foreland basin systems. *Sedimentology* 60, 102-130.

Allen P., Armitage J., Whittaker A., Michael N., Roda-Boluda D., D'Arcy M., 2015. Fragmentation model of the grain size mix of sediment supplied to basins. *Journal of Geology*124, 405-427.

Amos C., Burbank D., 2007. Channel width response to differential uplift. *J. Geophys. Res.* 112F, F02010, doi:10.1029/2006JF000672.

Anderson R., Anderson S., 2010. Geomorphology. The mechanics and chemistry of landscapes. Cambridge Univ. Press, 637 p.

Andrews G., Russell J., Brown S., Enkin R., 2012. Pleistocene reversal of the Fraser River, British Columbia. *Geol.* 40, 111-114.

Anthony D., Granger D., 2007. An empirical stream power formulation for knickpoint retreat in Appalachian Plateau fluviokarst. *J. Hydrol.* 343, 117-126.

Antoine P., 1994. The Somme Valley terrace system (Northern France); a model of river response to Quaternary climatic variations since 800 000 BP. *Terra Nova* 6, 453-464.

Antoine P., Limondin-Lozouet N., Chaussé C., Lautridou J.-P., Pastre J.-F., Auguste P., Bahain J.-J., Falguères C., Galehb B., 2007. Pleistocene fluvial terraces from northern France (Seine, Yonne, Somme): synthesis, and new results from interglacial deposits. *Quat. Sci. Rev.* 26, 2701-2723.

Antón, L., Rodés, A., De Vicente, G., Pallàs, R., Garcia-Castellanos, D., Stuart, F.M., Braucher, R., Bourlès, D., 2012. Quantification of fluvial incision in the Duero Basin (NWIberia) from longitudinal profile analysis and terrestrial cosmogenic nuclide concentrations. Geomorphology 165–166, 50–61.

Antón, L., De Vicente G., Muñoz-Martin A., Stokes M., 2014. Using river long profiles and geomorphic indices to evaluate the geomorphological signature of continental scale drainage capture,Duero basin (NW Iberia). Geomorphology 206, 250-261

Antón L., Mather A., Stokes M., Muñoz-Martin A., De Vicente G., 2015. Exceptional river gorge formation from unexceptional floods. *Nature Communications* 6, 7963. DOI: 10.1038ncomms8963

Armitage J., Duller R., Whittaker A., Allen P., 2011. Transformation of tectonic and climatic signals from source to sedimentary archive. *Nature Geoscience* 4, 231-235.

Armitage J., Dunkley Jones T., Duller R., Whittaker A., Allen P., 2013. Temporal buffering of climate-driven sediment flux cycles by transient catchment response. *Earth and Planetary Science Letters* 369-370, 200-210.

Aslan A., Hood W., Karlstrom K., Kirby E., Granger D., Kelley S., Asmerom Y., 2014. Abandonment of Unaweep Canyon (1.4-0.8 Ma), western Colorado: Effects of stream capture and anomalously rapid Pleistocene river incision. *Geosph.* 10, 428-446.

Attal M., Lavé J., 2006. Changes of bedload characteristics along the Marsyandi River (central Nepal): Implications for understanding hillslope sediment supply, sediment load evolution along fluvial networks, and denudation in active orogenic belts. In Willett S., Hovius N., Brandon M., Fisher D. (Eds), *Tectonics, climate, and landscape evolution*, Geol. Soc. Am. Special Paper 398, pp. 143-171.

Attal M., Lavé J., 2009. Pebble abrasion during fluvial transport: Experimental results and implications for the evolution of the sediment load along rivers. *J. Geophys. Res.* 114F, F04023, doi: 10.1029/2009JF001328.

Attal M., Mudd S., Hurst M., Weinman B., Yoo K., Naylor M., 2015. Impact of change in erosion rate and landscape steepness on hillslope and fluvial sediments grain size in the Feather River basin (Sierra Nevada, California). *Earth Surf. Dynam.* 3, 201–222.

Attal M., Tucker G., Whittaker A., Cowie P., Roberts G., 2008. Modeling fluvial incision and transient landscape evolution: Influence of dynamic channel adjustment. *J. Geophys. Res.* 113F, F03013, doi:10.1029/2007JF000893.

Azañón, J. Azor, A., Pérez-Peña, J., Carrillo, J. 2005. Late Quaternary large-scale rotational slides induced by river incision: The Arroyo de Gor area (Guadix basin, SE Spain). Geomorphology 69, 152-168

Azañón J., Pérez-Peña J., Giaconia F., Booth-Rea G., Martinez-Martinez J., Rodriguez-Peces M., 2012. Active tectonics in the central and eastern Betic Cordillera through morphotectonic analysis: the case of Sierra Nevada and Sierra Alhamilla. *J. Iber. Geol.* 38, 225-238.

Balco G., Rovey II C., 2008. An isochron method for cosmogenic-nuclide dating of buried soils and sediments. *Am. J. Sci.* 308, 1083-1114.

Baldwin J., Whipple K., Tucker G., 2003. Implications of the shear stress river incision model for the timescale of postorogenic decay of topography. *J. Geophys. Res.* 108B, 2158, doi:10.1029/2001JB000550.

Barnett-Moore N., Flament N., Heine C., Butterworth N., Müller R., 2014. Cenozoic uplift of south Western Australia as constrained by river profiles. *Tectonophys.* 622, 186-197.

Baynes E., Attal M., Niedermann S., Kirstein L., Dugmore A., Naylor M., 2015. Erosion during extreme flood events dominates Holocene canyon evolution in northeast Iceland. *PNAS* 112, 2355-2360.

Beckers A., Bovy B., Hallot E., Demoulin A., 2015. Controls on knickpoint migration in a drainage network of the moderately uplifted Ardennes Plateau, Western Europe. *Earth Surf. Proc. Landf.* 40, 357-374.

Berlin M., Anderson R., 2007. Modeling of knickpoint retreat on the Roan Plateau, western Colorado. *J. Geophys. Res.* 112F, F03S06. DOI:10.1029/2006JF000553.

Berryman K., Marden M., Eden D., Mazengarb C., Ota Y., Moriya I., 2000. Tectonic and paleoclimatic significance of Quaternary river terraces of the Waipaoa River, east coast, North Island, New Zealand. *N. Zeal. J. Geol. Geophys.* 43, 229-245.

Bianchi V., Salles T., Ghinassi M., Billi P., Dallanave E., Duclaux G., 2015. Numerical modeling of tectonically driven river dynamics and deposition in an upland incised valley. *Geomorph.* 241, 353-370.

Bishop P. 1995. Drainage rearrangement by river capture, beheading and diversion. *Prog. Phys. Geogr.* 19, 449-473.

Bishop P., Hoey T., Jansen J., Lexartza Artza I., 2005. Knickpoint recession rate and catchment area: the case of uplifted rivers in Eastern Scotland. *Earth Surf. Proc. Landf.* 30, 767-778.

Blöthe J., Munack H., Korup O., Fülling A., Garzanti E., Resentini A., Kubuk P., 2014. Late Quaternary valley infill and dissection in the Indus River, western Tibetan Plateau margin. *Quat. Sci. Rev.* 94, 102-119.

Boenigk W., Frechen M., 2006. The Pliocene and Quaternary fluvial archives of the Rhine system. *Quat. Sci. Rev.* 25, 550-574.

Bogaart P., Van Balen R., 2000. Numerical modeling of the response of alluvial rivers to Quaternary climate change. *Global Planet. Change* 27, 147-163.

Bonnet S., 2009. Shrinking and splitting of drainage basins in orogenic landscapes from the migration of the main drainage divide. *Nat. Geosci.* 2, 766-771.

Bonnet S., Crave A., 2003. Landscape response to climate change: Insights from experimental modeling and implications for tectonic versus climatic uplift of topography. *Geology* 31, 123-126.

Boulton S., Stokes M., Mather A., 2014. Transient fluvial incision as an indicator of active faulting and Plio-Quaternary uplift of the Moroccan High Atlas. *Tectonophys.* 633, 16-33.

Bourgeois O., Ford M., Diraison M., Le Carlier de Veslud C., Gerbault M., Pik R., Ruby N., Bonnet S., 2007. Separation of rifting and lithospheric folding signatures in the NW-Alpine foreland. *Int. J. Earth Sci.* 96, 1003-1031.

Braucher R., Del Castillo P., Siame L., Hidy A., Bourlès D., 2009. Determination of both exposure time and denudation rate from an in situ-produced $^{10}$Be depth profile: A mathematical proof of uniqueness. Model sensitivity and applications to natural cases. *Quat. Geochron.* 4, 56-67.

Braun J., Voisin C., Gourlan A., Chauvel C., 2015. Erosional response of an actively uplifting mountain belt to cyclic rainfall variations. *Earth Surf. Dynam.* 3, 1-14.

Bravard J.P., Petit F., 1997. Les cours d'eau. Dynamique du système fluvial. *A. Colin*, Paris, 222 p.

Briant R., Cohen K., Cordier S., Demoulin A., Macklin M., Mather A., Rixhon G., Veldkamp A., Wainwright J., Whittaker A., Wittmann H., 2016. State of Science: Does current fieldwork practice enable effective field-model comparison of fluvial landscape evolution? *Earth Surf. Proc. Landf.* (in revision).

Bridgland D., 2000. River terrace systems in north-west Europe: an archive of environmental change, uplift, and early human occupation. *Quat. Sci. Rev.* 19, 1293-1303.

Bridgland D., 2010. The record from British Quaternary river systems within the context of global fluvial archives. *J. Quat. Sci.* 25, 433-446.

Bridgland D., Westaway R., 2008. Climatically controlled river terrace staircases: a worldwide Quaternary phenomenon. *Geomorph.* 98, 285-315.

Bridgland D., Westaway R., 2012. The use of fluvial archives in reconstructing landscape evolution: the value of sedimentary and morphostratigraphical evidence. *Netherl. J. Geosci.* 91, 5-24.

Bridgland D., Westaway R., 2014. Quaternary fluvial archives and landscape evolution: a global synthesis. *Proc. Geol. Assoc.* 125, 600-629.

Bridgland D., Antoine P., Limondin-Lozouet N., Santisteban J., Westaway R., White M., 2006. The Palaeolithic occupation of Europe as revealed by evidence from the rivers: data from IGCP 449. *J. Quat. Sci.* 21, 437-455.

Bridgland D., Westaway R., Abou Romieh M., Candy I., Daoud M., Demir T., Galiatsatos M., Schreve D., Seyrek A., Shaw A., White T., Whittaker J., 2012. The River Orontes in Syria and Turkey: downstream variation of fluvial archives in different crustal blocks. *Geomorph.* 165-166, 25-49.

Bridgland D., Howard A., White M., White T., Westaway R., 2015. New insight into the Quaternary evolution of the River Trent, UK. *Proc. Geol. Assoc.* 126, 466-479.

Brocard G., Van der Beek P., 2006. Influence of incision rate, rock strength, and bedload supply on bedrock river gradients and valley-flat widths: Field-based evidence and calibrations from western Alpine rivers (southeast France). In Willett S., Hovius N., Brandon M., Fisher D. (Eds), *Tectonics, climate, and landscape evolution*, Geol. Soc. Am. Special Paper 398, pp. 101-126.

Brocard G., Van der Beek P., Bourlès D., Siame L., Mugnier J.-L., 2003. Long-term fluvial incision rates and postglacial river relaxation time in the French Western Alps from $^{10}$Be dating of alluvial terraces with assessment of inheritance, soil development and wind ablation effects. *Earth Planet. Sci. Lett.* 209, 197-214.

Brocard G., Willenbring J., Suski B., Audra P., Authemayou C., Cosenza-Muralles B., Moran-Ical S., Demory F., Rochette P., Vennemann T., Holliger K., Teyssier C., 2012. Rate and processes of river network rearrangement during incipient faulting: the case of the Cahabon River, Guatemala. *Am. J. Sci.* 312, 449-507.

Brookfield M., 1998. The evolution of the great river systems of southern Asia during the Cenozoic India-Asia collision: rivers draining southwards. *Geomorph.* 22, 285-312.

Bull W., 1990. Stream-terrace genesis: implications for soil development. *Geomorph.* 3, 351-367.

Burbank D., Anderson R., 2012. Tectonic geomorphology. Wiley-Blackwell, 454 p.

Burbank D., Meigs A., Brozović N., 1996. Interactions of growing folds and coeval depositional systems. *Basin Res.* 8, 199-223.

Candy I., Black S., Sellwood B., 2005. U-series isochron dating of immature and mature calcretes as a basis for constructing Quaternary landform chronologies. *Quatern. Res.* 64, 100–111.

Carretier S., Nivière B., Giamboni M., Winter T., 2006. Do river profiles record along-stream variations of low uplift rate? *J. Geophys. Res.* 111F, F02024, doi:10.1029/2005JF000419.

Castelltort S., Simpson G., 2006. River spacing and drainage network growth in widening mountain ranges. *Basin Res.* 18, 267-276.

Castelltort S., Goren L., Willett S., Champagnac J.-D., Herman F., Braun J., 2012. River drainage patterns in the New Zealand Alps primarily controlled by plate tectonic strain. *Nat. Geosci.* 5, 744-748.

Castillo M., Bishop P., Jansen J., 2013. Knickpoint retreat and transient bedrock channel morphology triggered by base-level fall in small bedrock river catchments: The case of the Isle of Jura, Scotland. *Geomorph.* 180-181, 1-9.

Chen Y., Sung Q., Cheng K., 2003. Along-strike variations of morphotectonic features in the Western Foothills of Taiwan: tectonic implications based on stream-gradient and hypsometric analysis. *Geomorph.* 56, 109-137.

Church M., Biron P., Roy A. (Eds), 2012. Gravel bed rivers: Processes, tools, environments. *Wiley-Blackwell*, 580 p.

Clark M., Schoenbohm L., Royden L., Whipple K., Burchfiel B., Zhang X., Tang W., Chen L., 2004. Surface uplift, tectonics, and erosion of eastern Tibet from large-scale drainage patterns. *Tectonics* 23, TC1006, doi:10.1029/2002TC001402.

Clift P., Blusztajn J., Nguyen A.D., 2006. Large-scale drainage capture and surface uplift in eastern Tibet-SW China before 24 Ma inferred from sediments of the Hanoi Basin, Vietnam. *Geophys. Res. Lett.* 33, L19403, doi: 10.1029/2006GL027772.

Cloetingh S., Burov E., Beekman F., Andeweg B., Andriessen P., Garcia-Castellanos D., de Vicente V., Vegas R., 2002. Lithospheric folding in Iberia. *Tectonics* 21, 1041, doi: 10.1029/2001TC901031.

Cloetingh S., Ziegler P., Beekman F., Andriessen P., Matenco L., Bada G., Garcia-Castellanos D., Hardebol N., Dèzes P., Sokoutis D., 2005. Lithspheric memory, state of stress and rheology: neotectonic controls on Europe's intraplate continental topography. *Quat. Sci. Rev.* 24, 241-304.

Colombo F., 2005. Quaternary telescopic-like alluvial fans, Andean Ranges, Argentina. In Harvey A., Mather A., Stokes M. (Eds), *Alluvial fans. Geomorphology, sedimentology, dynamics*, Geol. Soc., London, Special Publ. 251, pp. 69-84.

Cook K., Whipple K., Heimsath A., Hanks T., 2009. Rapid incision of the Colorado River in Glen Canyon – insights from channel profiles, local incision rates, and modelling of lithologic controls. *Earth Surf. Proc. Landf.* 34, 994-1010.

Cook K., Turowski J., Hovius N., 2013. A demonstration of the importance of bedload transport for fluvial bedrock erosion and knickpoint propagation. *Earth Surf. Proc. Landf.* 38, 683-695.

Cook K., Turowski J., Hovius N., 2014. River gorge eradication by downstream swep erosion. *Nat. Geosci.* 7, 682-686.

Cordier S., Harmand D., Frechen M., Beiner M., 2006. Fluvial system response to Middle and Upper Pleistocene climate change in the Meurthe and Moselle valleys (Paris basin and Rhenish Massif). *Quat. Sci. Rev.* 25, 1460-1474.

Cordier S., Frechen M., Harmand D., 2009. The Pleistocene fluvial deposits of the Moselle and middle Rhine valleys: new correlations and compared evolutions. *Quat.* 20, 35-47.

Cordier S., Frechen M., Tsukamoto S., 2010. Methodological aspects on luminescence dating of fluvial sands from the Moselle basin, Luxembourg. *Geochronometria* 35, 67-74.

Cordier S., Frechen M., Harmand D., 2014. Dating fluvial erosion: fluvial response to climate change in the Moselle catchment (France, Germany) since the Late Saalian. *Boreas* 43, 450-468.

Cordier S. et al., in review. The Fluvial Archives Group: 20 years of research connecting fluvial geomorphology and (palaeo)environments. *Quat. Sci. Rev.*, this issue.

Cowie P., Attal M., Tucker G., Whittaker A., Naylor M., Ganas A., Robert, G., 2006. Investigating the Surface Process Response to Fault Interaction and Linkage Using a Numerical Modelling Approach, *Basin Research* 18, 231-266.

Crosby B., Whipple K., 2006. Knickpoint initiation and distribution within fluvial networks: 236 waterfalls in the Waipaoa River, North Island, New Zealand. *Geomorph.* 82, 16-38.

Crosby B., Whipple K., Gasparini N., Wobus C., 2007. Formation of fluvial hanging valleys: Theory and simulation. *J. Geophys. Res.* 112F, F03S10. DOI:10.1029/2006JF000566.

Cunha P., Martins A., Daveau S., Friend P., 2005. Tectonic control of the Tejo river fluvial incision during the late Cenozoic, in Ródão – central Portugal (Atlantic Iberian border). *Geomorph.* 64, 271-298.

Cyr A., Granger D., Olivetti V., Molin P., 2014. Distinguishing between tectonic and lithologic controls on bedrock channel longitudinal profiles using $^{10}$Be erosion rates and channel steepness index. *Geomorph.* 209, 27-38.

Czarnota K. Roberts G., White N., Fishwick S., 2014. Spatial and temporal patterns of Australian dynamic topography from river profile modelling. *J. Geophys. Res.* 119F, 1384-1424, doi:10.1002/2013JB010436.

Davis W.M., 1899. The geographical cycle. Geographical Journal 14, 481-504.

D'Arcy M., Whittaker A., Roda-Boluda D., 2016. Measuring alluvial fan sensitivity to glacial-interglacial climate change using a self-similarity approach to grain size fining, Death Valley, California. *Sedimentology*, in press.

Demir T., Westaway R., Seyrek A., Bridgland D., 2007. Terrace staircases of the River Euphrates in southeast Turkey, northern Syria and western Iraq: evidence for regional surface uplift. *Quat. Sci. Rev.* 26, 2844-2863.

Demoulin A., 1998. Testing the tectonic significance of some parameters of longitudinal river profiles: the case of the Ardenne (Belgium, NW Europe). *Geomorph.* 24, 189-208.

Demoulin A., 2011. Basin and river profile morphometry: A new index with a high potential for relative dating of tectonic uplift. *Geomorph.* 126, 97-107.

Demoulin A., 2012. Morphometric dating of the fluvial landscape response to a tectonic perturbation. *Geophys. Res. Lett.* 39, L15402, doi:10.1029/2012GL052201.

Demoulin A., Hallot E., 2009. Shape and amount of the Quaternary uplift of the western Rhenish shield and the Ardennes (western Europe). *Tectonophys.* 474, 696-708.

Demoulin A., Beckers A., Rixhon G., Braucher R., Bourlès D., Siame L., 2012. Valley downcutting in the Ardennes (W Europe): Interplay between tectonically triggered regressive erosion and climatic cyclicity. *Netherl. J. Geosci.* 91, 79-90.

Demoulin A., Bayer Altin T., Beckers A., 2013. Morphometric age estimate of the last phase of accelerated uplift in the Kazdag area (Biga Peninsula, NW Turkey). *Tectonophys.* 608, 1380-1393.

Demoulin A., Beckers A., Hubert-Ferrari A., 2015. Patterns of Quaternary uplift of the Corinth rift southern border (N Peloponnese, Greece) revealed by fluvial landscape morphometry. *Geomorph.* 246, 188-204.

Despriée J., Voinchet P., Bahain J.-J., Tissoux H., Flaguères C., Dépont J., Dolo J.-M., 2007. Les nappes alluviales pléistocènes de la vallée moyenne du Cher (région Centre, France): contexte morphosédimentaire, chronologie ESR et préhistoire. Premiers résultats. *Quat.* 18, 349-368.

Dethier D., 2001. Pleistocene incision rates in the western United States calibrated using Lava Creek B tephra. *Geology* 29, 783-786.

DiBiase R., Whipple K., Heimsath A., Ouimet W., 2010. Landscape form and millennial erosion rates in the San Gabriel Mountains, Ca. *Earth Planet. Sci. Lett.* 289, 134-144.

DiBiase R., Whipple K., Lamb M., Heimsath A., 2015. The role of waterfalls and knickzones in controlling the style and pace of landscape adjustment in the western San Gabriel Mountains, California. *Bull. Geol. Soc. Am.* 127, 539-559.

Duller R., Whittaker A., Fedele J., Whitchurch A., Springett J., Smithells R., Fordyce S., Allen, P., 2010. From grain size to tectonics. *J. Geophys. Res.* 115, F03022.

Duller R., Whittaker A., Swinehart J., Armitage J., Sinclair H., Bair, A., Allen P., 2012. Abrupt landscape change post-6 Ma on the central Great Plains, USA. *Geology* 40, 871-874.
Duvall A., Kirby E., Burbank D., 2004. Tectonic and lithologic controls on bedrock channel profiles and processes in coastal California. *J. Geophys. Res.* 109F, F03002, doi:10.1029/2003JF000086.
Fedele J., Paola C., 2007. Similarity solutions for fluvial sediment fining by selective deposition, *J. Geophys. Res.* 112, F02038, doi:10.1029/2005JF000409.
Finnegan N., 2013. Interpretation and downstream correlation of bedrock river terrace treads created from propagating knickpoints. *J. Geophys. Res.* 118F, 54-64, doi:10.1029/2012JF002534.
Finnegan N., Roe G., Montgomery D., Hallet B., 2005. Controls on the channel width of rivers: Implications for modeling fluvial incision of bedrock. *Geol.* 33, 229-232.
Finnegan N., Sklar L., Fuller T., 2007. Interplay of sediment supply, river incision, and channel morphology revealed by the transient evolution of an experimental bedrock channel. *J. Geophys. Res.* 112F, F03S11, doi: 10.1029/2006JF000569.
Flint J., 1974. Stream gradient as a function of order, magnitude, and discharge. *Water Resour. Res.* 10, 969-973.
Forzoni A., Storms J., Whittaker A., de Jager G., 2014. Delayed delivery from the sediment factory: a model to simulate the impact of catchment response time on sediment flux and fluvio-deltaic stratigraphy. *Earth Surface Processes and Landforms* 39, 689-704.
Fuchs M., Gloaguen R., Krbetschek M., Szulc A., 2014. Rates of river incision across the main tectonic units of the Pamir identified using optically stimulated luminescence dating of fluvial terraces. *Geomorph.* 216, 79-92.
Gabris G., Nador A., 2007. Long-term fluvial archives in Hungary: response of the Danuba and Tisza rivers to tectonic movements and climatic changes during the Quaternary: a review and new synthesis. *Quat. Sci. Rev.* 26, 2758-2782.
Gasparini N., Fischer G., Adams J., Dawers N., Janoff A., 2015. Morphological signatures of normal faulting in low-gradient alluvial rivers in south-eastern Louisiana, USA. *Earth Surf. Proc. Landf.*, DOI: 10.1002/esp.3852.
Geach M., Viveen W., Mather A., Telfer M., Fletcher W., Stokes M., Peyron, O., 2015a. An integrated field and numerical modelling study of controls on Late Quaternary fluvial landscape development (Tabernas, SE Spain). *Earth Surface Processes and Landforms* 40, 1907-1926. DOI 10.1002/esp.3768
Geach M., Thomsen K., Buylaert J., Murray A., Mather A., Telfer M., Stokes M., 2015b. Single-grain and multi-grain OSL dating of river terrace sediments in the Tabernas Basin, SE Spain. *Quaternary Geochronology* 30, 213-218. DOI: 10.1016/j.quageo.2015.05.021
Giaconia F., Booth-Rea G., Martinez-Martinez J., Azañon J., Pérez-Peña J., 2012. Geomorphic analysis of the Sierra Cabrera, an active pop-up in the constrictional domain of conjugate strike-slip faults: The Palomares and Polops fault zones (eastrn Betics, SE Spain). *Tectonophys.* 580, 27-42.
Giamboni M., Wetzel A., Nivière B., 2004. Plio-Pleistocene folding in the southern Rhinegraben recorded by the evolution of the drainage network (Sundgau area; northwestern Switzerland and France). *Eclogae Geol. Helv.* 97, 17-31.
Gioia D., Gallicchio S., Moretti M., Schiattarella M., 2014. Landscape response to tectonic and climatic forcing in the foredeep of the southern Apennines, Italy: insights from Quaternary stratigraphy, quantitative geomorphic analysis, and denudation rate proxies. *Earth Surf. Proc. Landf.* 39, 814-835.
Goldrick G., Bishop P., 2007. Regional analysis of bedrock stream long profiles: evaluation of Hack's SL form, and formulation and assessment of an alternative (the DS form). . *Earth Surf. Proc. Landf.* 32, 649-671.
Goren L., Fox M., Willett S., 2014. Tectonics from fluvial topography using formal linear inversion: Theory and applications to the Inyo Mountains, California. *J. Geophys. Res.* 119F, 1651-1681, doi:10.1002/2014JF003079.
Goren L., Castelltort S., Klinger Y., 2015. Modes and rates of horizontal deformation from rotated river basins: Application to the Dead Sea fault system in Lebanon. *Geol.* 43, 843-846.

Hack J., 1957. Studies of longitudinal stream profiles in Virginia and Maryland. *US Geol. Surv. Profess. Paper* 294-B, 45-97.

Hack J., 1973. Stream profile analysis and stream-gradient index. *J. Res. US Geol. Surv.* 1, 421-429.

Haghipour N., Burg J.-P., Kober F., Zeilinger G., Ivy-Ochs S., Kubik P., Faridi M., 2012. Rate of crustal shortening and non-Coulomb behaviour of an active accretionary wedge: The folded fluvial terraces in Makran (SE Iran). *Earth Planet. Sci. Lett.* 355-356, 187-198.

Hancock G., Anderson R., 2002. Numerical modelling of fluvial strath-terrace formation in response to oscillating climate. *Geol. Soc. Am. Bull.* 114, 1131-1142.

Harbor D., 1998. Dynamic equilibrium between an active uplift and the Sevier River, Utah. *J. Geol.* 106, 181-194.

Harel M.-A., Mudd S., Attal M., 2016. Global analysis of the stream power law parameters based on worldwide $^{10}$Be denudation rates. *Geomorph.* 268, 184-196.

Harkins N., Kirby E., Heimsath A., Robinson R., Reiser U., 2007. Transient fluvial incision in the headwaters of the Yellow River, northeastern Tibet, China. *J. Geophys. Res.* 112F, F03S04, doi:10.1029/2006JF000570.

Harmand D., Cordier S., 2012. The Pleistocene terrace staircases of the present and past rivers downstream from the Vosges Massif (Meuse and Moselle catchments). *Netherl. J. Geosci.* 91, 91-109.

Hartshorn K., Hovius N., Dade W., Slingerland R., 2002. Climate-driven bedrock incision in an active mountain belt. *Science* 297, 2036-2038.

Harvey A., Wells S., 1987. Response of Quaternary Fluvial Systems to differential epeirogenic uplift: Aguas and Feos river systems, southeast Spain. *Geology* 15, 689-693.

Harvey A., Whitfield E., Stokes M., Mather A., 2014. The Late Neogene to Quaternary drainage evolution of the uplifted Neogene sedimentary basins of Almeria, Betic Chain. In Guttiérez F., Guttiérez M. (Eds), *Landscapes and landforms of Spain*, Springer, pp. 37-61.

Helgren D., 1978. Acheulian settlement along the lower Vaal River, South Africa. *J. Archaeol. Sci.* 5, 39-60.

Hetzel R., Niedermann S., Tao M., Kubik P., Strecker M., 2006. Climatic versus tectonic control on river incision at the margin of NE Tibet: $^{10}$Be exposure dating of river terraces at the mountain front of the Qilian Shan. *J. Geophys. Res.* 111F, F03012, doi:10.1029/2005JF000352.

Holbrook J., Schumm S., 1999. Geomorphic and sedimentary response of rivers to tectonic deformation: a brief review and critique of a tool for recognizing subtle epeirogenic deformation in modern and ancient settings. *Tectonophys.* 305, 287-306.

Hood W., Aslan A., Betton C., 2014. Aftermath of a steam capture: Cactus Park lake spillover and the origin of East Creek, Uncompahgre Plateau, western Colorado. *Geosph.* 10, 447-461.

Hovius N., 1996. Regular spacing of drainage outlets from linear mountain belts. *Basin Res.* 8, 29-44.Howard A., Dietrich W., Seidl M., 1994. Modeling fluvial erosion on regional to continental scale. *J. Geophys. Res.* 99B, 13,971-13,986.

Huang M., Pan Y., Liao J., 2013. A case of rapid rock riverbed incision in a coseismic uplift reach and its implications. *Geomorph.* 184, 98-110.

Hubert-Ferrari A., Suppe J., Gonzalez-Mieres R., Wang X., 2007. Mechanisms of active folding of the landscape (southern Tian Shan, China). *J. Geophys. Res.* 112B, B03S09, doi: 10.1029/2006JB004362.

Humphrey N., Konrad S., 2000. River incision or diversion in response to bedrock uplift. *Geol.* 28, 43-46.

Izett G., Pierce K., Naeser N., Jaworowski C., 1992. Isotopic dating of Lava Creek B tephra in terrace deposits along the Wind River, Wyoming – Implications for post-0.6 Ma uplift of the Yellowstone hotspot. *Geol. Soc. Am. Abstracts with Programs* 24, 7, annual meeting of the GSA, Cincinnati .

Jain V., Sinha R., 2005. Response of active tectonics on the alluvial Baghmati River, Himalayan foreland basin, eastern India. *Geomorph.* 70, 339-356.

Jerolmack D., Paola C., 2010. Shredding of environmental signals by sediment transport. *Geophysical Research Letters* 37, 1-5.

Johnson J., Whipple K., 2010. Evaluating the controls of shear stress, sediment supply, alluvial cover, and channel morphology on experimental bedrock incision rate. *J. Geophys. Res.* 115F, F02018, doi: 10.1029/2009JF001335.

Juvigné E., Renard F., 1992. Les terrasses de la Meuse de Liège à Maastricht. *Ann. Soc. Géol. Belg.* 115, 167-186.

Keller E., 1986. Investigation of active tectonics: Use of surficial earth processes. In *Active tectonics*, Studies in Geophysics, NRC, Washington, D.C., pp. 136-147.

Kirby E., Ouimet W., 2011. Tectonic geomorphology along the eastern margin of Tibet: insights into the pattern and processes of active deformation adjacent to the Sichuan Basin. In Gloaguen R., Ratschbacher L. (Eds), *Growth and collapse of the Tibetan Plateau*, Geol. Soc., London, Spec. Publ. 353, pp. 165-188.

Kirby E., Whipple K., 2001. Quantifying differential rock-uplift rates via stream profile analysis. *Geol.* 29, 415-418.

Kirby E., Whipple K., 2012. Expression of active tectonics in erosional landscapes. *J. Struct. Geol.* 44, 54-75.

Knight D., Sterling M., 2000. Boundary shear in circular pipes running partially full. *J. Hydraul. Engin.* 126, 263-275.

Kong P., Zheng Y., Caffee M., 2012. Provenance and time constraints on the formation of the first bend of the Yangtze River. *Geochem., Geophys., Geosyst.* 13, Q06017, doi: 10.1029/2012GC004140.

Korup O., 2006. Rock-slope failure and the river long profile. *Geol.* 34, 45-48.

Korup O., Strom A., Weidinger J., 2006. Fluvial response to large rock-slope failures: Examples from the Himalayas, the Tien Shan, and the Southern Alps in New Zealand. *Geomorph.* 78, 3-21.

Krzyszkowski D., Przybylski B., Badura J., 2000. The role of neotectonics and glaciations along the Nysa-Kłodzka River in the Sudeten Mountains (southwestern Poland). *Geomorph.* 33, 149-166.

Kuhlemann J., 2007. Paleogeographic and paleotopographic evolution of the Swiss and Eastern Alps since the Oligocene. *Glob. Planet. Change* 58, 224-236.

Lague D., 2010. Reduction of long-term bedrock incision efficiency by short-term alluvial cover intermittency. *J. Geophys. Res.* 115F, F02011, doi:10.1029/2008JF001210.

Lague D., 2014. The stream power river incision model: evidence, theory and beyond. *Earth Surf. Proc. Landf.* 39, 38-61.

Lague D., Hovius N., Davy P., 2005. Discharge, discharge variability, and the bedrock channel profile. *J. Geophys. Res.* 110F, F04006, doi:10.1029/2004JF000259.

Lane S., Westaway R., Hicks D., 2003. Estimation of erosion and deposition volumes in a large, gravel-bed, braided river using synoptic remote sensing. *Earth Surf. Proc. Landf.* 28, 249-271.

Larue J.-P., 2011. Longitudinal profiles and knickzones: the example of the rivers of the Cher basin in the northern French Massif Central. *Proc. Geol. Assoc.* 122, 125-142.

Lavé J., Avouac J.-P., 2000. Active folding of fluvial terraces across the Siwalik Hills, Himalayas of central Nepal. *J. Geophys. Res.* 105B, 5735-5770.

Lavé J., Avouac J.-P., 2001. Fluvial incision and tectonic uplift across the Himalayas of central Nepal. *J. Geophys. Res.* 106B, 26,561-26,591.

Leland J., Reid M., Burbank D., Finkel R., Caffee M., 1998. Incision and differential bedrock uplift along the Indus River near Nanga Parbat, Pakistan Himalaya, from $^{10}$Be and $^{26}$Al exposure age dating of bedrock straths. *Earth Planet. Sci. Lett.* 154, 93-107.

Lewin J., Gibbard P., 2010. Quaternary river terraces in England: Forms, sediments and processes. *Geomorph.* 120, 293-311.

Litchfield N., Wilson K., Berryman K., Wallace L., 2010. Coastal uplift mechanisms at Pakarae River mouth: Constraints from a combined Holocene fluvial and marine terrace dataset. *Mar. Geol.* 270, 72-83.

Loget N., Van den Driessche J., 2009. Wave train model for knickpoint migration. *Geomorph.* 106, 376-382.

Macar P., 1957. Résultats d'ensemble d'études récentes sur les terrasses fluviales et les formes d'érosion associées en Haute Belgique. *Ann. Soc. Géol. Belg.* 80, B395-412.

Mackin J., 1948. Concept of the graded river. *Geol. Soc. Am. Bull.* 59, 463-512.

McMillan M., Angevine C., Heller P., 2002. Post-depositional tilt of the Miocene-Pliocene Ogallala Group on the western Great Plains: Evidence of late Cenozoic uplift of the Rocky Mountains. *Geology* 30, 63–66, doi:10.1130/0091-7613(2002)030<0063:PTOTMP>2.0.CO;2.

Maddy D., 1997. Uplift driven valley incision and River Terrace formation in Southern England. *J. Quat. Sci.* 12, 539-545.

Maddy D., Bridgland D., Green C., 2000. Crustal uplift in southern England: evidence from the river terrace records. *Geomorph.* 33, 167-181.

Maddy D., Bridgland D., Westaway R., 2001. Uplift-driven valley incision and climate-controlled river terrace development in the Thames Valley, UK. *Quat. Int.* 79, 23-36.

Maddy D., Demir T., Veldkamp A., Bridgland D., Stemerdink C., van der Schriek T., Schreve D., 2012. The obliquity-controlled early Pleistocene terrace sequence of the Gediz River, western Turkey: a revised correlation and chronology. *J. Geol. Soc.* 169, 67-82.

Mandier P., 1984. Signification dynamique et climatique des formations et terrasses fluviatiles Quaternaires dans les Alpes et leur périphérie. *Bull. Assoc. Fr. Etudes Quat.* 1984, 113-118.

Mather A., 2000a. Adjustment of a drainage network to capture induced base-level change. *Geomorphology* 34, 271-289.

Mather A.; 2000b. Impact of headwater river capture on alluvial system development. *J. Geol. Soc. London* 157, 957-966.

Mather A., Hartley A., 2006. The application of drainage system analysis in constraining spatial patterns of uplift in the Coastal Cordillera of northern Chile. In Willett S., Hovius N., Brandon M., Fisher D. (Eds) *Tectonics, Climate, and Landscape Evolution*, Geol. Soc. Am. Spec. Pap., 398, pp. 87–99.

Mather, A.E. & Stokes, M. 2016. Extracting palaeoflood data from coarse-grained Pleistocene river terrace archives: an example from SE Spain. Earth Surface Processes and Landforms 41, 1991-2004.

Mather, A.E., Stokes, M., Griffiths, J.S., 2002. Quaternary landscape evolution: A framework for understanding contemporary erosion, southeast Spain. Land Degradation and Development 13, 89-109.

Mather A., Griffiths J., Stokes M., 2003. Anatomy of a 'fossil' landslide from the Pleistocene of SE Spain. *Geomorphology* 50, 135-149.

Martins, A., Cabral, J., Cunha, P., Stokes, M., Borges, J., Caldeira, B., Martins, A.C. 2017. Tectonic and lithological controls on fluvial landscape development in central-eastern Portugal: Insights from long profile tributary stream analyses. Geomorphology 276, 144-163

Matoshko A., Gozhik P., Danukalova G., 2004. Key Late Cenozoic fluvial archives of eastern Europe: the Dniester, Dnieper, Don and Volga. *Proc. Geol. Assoc.* 115, 141-173.

Merritt D., Vincent K., 1989. Geomorphic response of coastal streams to low, intermediate, and high rates of uplift, Mendocino triple junction region, northern California. *Geol. Soc. Am. Bull.* 101, 1373-1388.

Merritts D., Vincent K., Wohl E., 1994. Long river profiles, tectonism, and eustasy: A guide to interpreting fluvial terraces. *J. Geophys. Res.* 99B, 14,031-14,050.

Michael N., Whittaker A., Allen P., 2013. The functioning of sediment routing systems using a mass balance approach: Example from the Eocene of the southern Pyrenees. *J. Geol.* 121, 581-606.

Michael N., Whittaker A., Carter A., Allen P., 2014. Volumetric budget and grain-size fractionation of a geological sediment routing system: Eocene Escanilla Formation, south-central Pyrenees. *Geol. Soc. Am. Bull* 126, 585-599.

Miller S., Slingerland R., Kirby E., 2007. Characteristics of steady state fluvial topography above fault-bend folds. *J. Geophys. Res.* 112F, F04004, doi: 10.1029/2007JF000772.

Milliman J., Syvitski J., 1992. Geomorphic/Tectonic Control of Sediment Discharge to the Ocean: The Importance of Small Mountainous Rivers. *J. Geol.* 100**,** 525–544.

Mishra S., White M., Beaumont P., Antoine P., Bridgland D., Howard A., Limondin-Lozouet N., Santisteban J., Schreve D., Shaw A., Wenban-Smith F., Westaway R., White T., 2007. Fluvial deposits as an archive of early human activity. *Quat. Sci. Rev.* 26, 2996-3016.

Molin P., Fubelli G., Nocentini M., Sperini S., Ignat P., Grecu F., Dramis F., 2012. Interaction of mantle dynamics, crustal tectonics, and surface processes in the topography of the Romanian Carpathians: A geomorphologial approach. *Global Planet. Change* 90-91, 58-72.

Molnar P., Brown E., Burchfiel B., Qidong D., Xianyue F., Jun L., Raisbeck G., Jianbang S., Zhangming W., Yiou F., Huichuan Y., 1994. Quaternary climate change and the formation of river terraces across growing anticlines on the north flank of the Tien Shan, China. *J. Geol.* 102, 583-602.

Morris P., Williams D., 1997. Exponential longitudinal profiles of streams. *Earth Surf. Proc. Landf.* 22, 143-163.

Mudd S., Attal M., Milodowski D., Grieve S., Valters D., 2014. A statistical framework to quantify spatial variation in channel gradients using the integral method of channel profile analysis. *J. Geophys. Res.* 119F, 138-152, doi:10.1002/2013JF002981.

Niemann J., Gasparini N., Tucker G., Bras R., 2001. A quantitative evaluation of Playfair's law and its use in testing long-term stream erosion models. *Earth Surf. Proc. Landf.* 26, 1317-1332.

Norton K., Schlunegger F., Litty C., 2015. On the potential for regolith control of fluvial terrace formation in semi-arid escarpments. *Earth Surf. Dynam. Discuss.* 3, 715-738.

Nott J., 1992. Long-term drainage evolution in the Shoalhaven catchment, southeast highlands, Australia. *Earth Surf. Proc. Landf.* 17, 361-374.

Nott J., Price D., Nanson G., 2002. Stream response to Quaternary climate change: evidence from the Shoalhaven River catchment, southeastern highlands, temperate Australia. *Quat. Sci. Rev.* 21, 965-974.

Ouchi S., 1985. Response of alluvial river to slow active tectonic movement. *Geol. Soc. Am. Bull.* 96, 504-515.

Ouimet W., Whipple K., Granger D., 2009. Beyond threshold hillslopes: Channel adjustment to base-level fall in tectonically active mountain ranges. *Geol.* 37, 579-582.

Paola C., Martin J., 2012. Mass-balance effects in depositional systems. *Journal of Sedimentary Research* 82, 435-450.

Paola C., Mohrig D., 1996. Palaeohydraulics revisited: Palaeoslope estimation in coarse-grained braided rivers. *Basin Research* 8, 243–254, doi:10.1046/j.1365-2117.1996.00253.x.

Parsons A., Michael N., Whittaker A., Duller R., Allen P., 2012. Grain-size trends reveal the late orogenic tectonic and erosional history of the south-central Pyrenees, Spain. *J. Geol. Soc.* 169, 111-114.

Pastre J.F., 2004. The Perrier Plateau: A Plio-Pleistocene long fluvial record in the River Allier basin, Massif Central, France. *Quat.* 15, 87-101.

Patyk-Kara N., Postolenko G., 2004. Structure and Cenozoic evolution of the Kolyma river valley, eastern Siberia, from its upper reaches to the continental shelf. *Proc. Geol. Assoc.* 115, 325-338.

Pazzaglia F., Brandon M., 2001. A fluvial record of long-term steady-state uplift and erosion across the Cascadia forearc high, western Washington State. *Am. J. Sci.* 301, 385-431.

Pazzaglia F., Gardner T., Merritts D., 1998. Bedrock fluvial incision and longitudinal profile development over geologic time scales determined by fluvial terraces. In Tinkler K, Wohl E. (Eds) *Rivers over rock. Fluvial processes in bedrock channels*, AGU Geophysical Monograph 107, pp. 207-235.

Pérez-Peña J., Azañon J., Delgado J., 2004. Metodología para el análisis de redes de drenaje mediante índices geomorfológicos y su relación con la tectónica activa. *Geo-Temas* 6, 259-262.

Pérez-Peña J., Azañon J., Azor A., Delgado J., Gonzalez-Lodeiro F., 2009. Spatial analysis of stream power using GIS: SLk anomaly maps. *Earth Surf. Proc. Landf.* 34, 16-25.

Pérez-Peña J., Azor A., Azañon J., Keller E., 2010. Active tectonics in the Sierra Nevada (Betic Cordillera, SE Spain): Insights from geomorphic indexes and drainage pattern analysis. *Geomorph.* 119, 74-87.

Perron T., Royden L., 2013. An integral approach to bedrock river profile analysis. *Earth Surf. Proc. Landf.* 38, 570-576.

Perron J., Kirchner J., Dietrich W., 2009. Formation of evenly spaced ridges and valleys. *Nature* 460, 502-505.

Peters G., Van Balen R., 2007. Pleistocene tectonics inferred from fluvial terraces of the northern Upper Rhine Graben, Germany. *Tectonophys.* 430, 41-65.

Petrovszki J., Timar G., 2010. Channel sinuosity of the Körös River system, Hungary/Romania, as possible indicator of the neotectonic activity. *Geomorph.* 122, 223-230.

Phillips J., 2011. Emergence and pseudo-equilibrium in geomorphology. *Geomorph.* 132, 319-326.

Pierce K., Morgan L., 1992. The track of the Yellowstone hot spot: Volcanism, faulting, and uplift. In Link K., Kuntz M., Platt L. (Eds), *Regional geology of Eastern Idaho and Western Wyoming*, Geol. Soc. Am. Memoir 179, pp. 1-54.

Pissart A., Harmand D., Krook L., 1997. L'évolution de la Meuse de Toul à Maastricht depuis le Miocène: corrélations chronologiques et traces des captures de la Meuse Lorraine d'après les minéraux denses. *Géogr. Phys. Quat.* 51, 267-284.

Prince P., Spotila J., Henika W., 2011. Stream capture as driver of transient landscape evolution in a tectonically quiescent setting. *Geol.* 39, 823-826.

Pritchard D., Roberts G., White N., Richardson C., 2009. Uplift histories from river profiles. *Geophys. Res. Lett.* 36, L24301, doi:10.1029/2009GL040928.

Rice S., Church M., 2001. Longitudinal profiles in simple alluvial systems. *Water Resour. Res.* 37, 417-426.

Ritter J., Jordan M., Christensen U., Achauer U., 2001. A mantle plume below the Eifel volcanic fields, Germany. *Earth Planet. Sci. Lett.* 186, 7-14.

Rixhon G., Braucher R., Bourlès D., Siame L., Bovy B., Demoulin A., 2011. Quaternary river incision in NE Ardennes (Belgium) – Insights from $^{10}$Be/$^{26}$Al dating of river terraces. *Quat. Geochronol.* 6, 273-284.

Rixhon G., Briant R., Cordier S., Duval M., Jones A., Scholz D., 2016. Revealing the pace of river landscape evolution during the Quaternary: recent developments in numerical dating methods. *Quat. Sci. Rev.*, this issue.

Roberts G., White N., 2010. Estimating uplift rate histories from river profiles using African examples. *J. Geophys. Res.* 115B, B02406, doi:10.1029/2009JB006692.

Roberts G., White N., Martin-Brandis G., Crosby A., 2012. An uplift history of the Colorado Plateau and its surroundings from inverse modelling of longitudinal river profiles. *Tectonics* 31, TC4022, doi:10.1029/2012TC003107.

Rockwell T., Keller E., Clark M., Johnson D., 1984. Chronology and rates of faulting of Ventura River terraces, California. *Geol. Soc. Am. Bull.* 95, 1466-1474.

Roe G., Montgomery D., Hallet B., 2002. Effects of orographic precipitation variations on the concavity of steady-state river profiles. *Geol.* 30, 143-146.

Rohais S., Bonnet S., Eschard R.. 2012. Sedimentary record of tectonic and climatic erosional perturbations in an experimental coupled catchment-fan system. *Basin Research* 24, 198–212.

Ruszkiczay-Rüdiger Z., Braucher R., Novothny A., Csillag G., Fodor L., Molnar G., Madarasz B., ASTER Team, 2016. Tectonic and climatic control on terrace formation: Coupling in situ produced $^{10}$Be depth profiles and luminescence approach, Danube River, Hungay, Central Europe. *Quat. Sci. Rev.* 131, 127-147.

Santisteban J., Schulte L., 2007. Fluvial networks of the Iberian Peninsula: a chronological framework. *Quat. Sci. Rev.* 26, 2738-2757.

Scharer K., Burbank D., Chen J., Weldon II R., 2006. Kinematic models of fluvial terraces over active detachment folds: Constraints on the growth mechanism of the Kashi-Atushi fold system, Chinese Tian Shan. *Geol. Soc. Am. Bull.* 118, 1006-1021.

Schildgen T., Ehlers T., Whipp D., van Soest M., Whipple K., Hodges K., 2009. Quantifying canyon incision and Andean Plateau surface uplift, southwest Peru: A thermochronometer and numerical modelling approach. *J. Geophys. Res.* 114F, F04014, doi:10.1029/2009JF001305.

Schildgen T., Balco G., Shuster D., 2010. Canyon incision and knickpoint propagation recorded by apatite $^{4}$He/$^{3}$He thermochronometry. *Earth Planet. Sci. Lett.* 293, 377-387.

Schildgen T., Cosentino D., Bookhagen B., Niedermann S., Yildirim C., Echtler H., Wittmann H., Strecker M., 2012. Multi-phased uplift of the southern margin of the Central Anatolian plateau, Turkey: A record of tectonic and upper mantle processes. *Earth Planet. Sci. Lett.* 317-318, 85-95.

Schlunegger F., Mosar J., 2011. The last erosional stage of the Molasse Basin and the Alps. *Int. J. Earth Sci.* 100, 1147-1162.

Schoenbohm L., Whipple K., Burchfiel B., Chen L., 2004. Geomorphic constraints on surface uplift, exhumation, and plateau growth in the Red River region, Yunnan Province, China. *Geol. Soc. Am. Bull.* 116, 895-909.

Schreve D., Keen D., Limondin-Lozouet N., Auguste P., Santisteban J., Ubilla M., Matoshko A., Bridgland D., Westaway R., 2007. Progress in faunal correlation of Late Cenozoic fluvial sequences 2000-4: the report of the IGCP 449 biostratigraphy subgroup. *Quat. Sci. Rev.* 26, 2970-2995.

Schumm S., Dumont J., Holbrook J., 2000. Active tectonics and alluvial rivers. Cambridge Univ. Press, 276 p.

Seeber L., Gornitz V., 1983. River profiles along the Himalayan arc as indicators of active tectonics. *Tectonophys.* 92, 335-367.

Seidl M., Dietrich W., 1992. The problem of channel erosion into bedrock. *Catena Suppl.* 23, 101-124.

Seward D., Burg J.-P., 2008. Growth of the Namche Barwa Syntaxis and associated evolution of the Tsangpo Gorge: Constraints from structural and thermochronological data. *Tectonophys.* 451, 282-289.

Simpson G., Castelltort S., 2012. Model shows that rivers transmit high-frequency climate cycles to the sedimentary record. *Geol.* 40, 1131-1134.

Sklar L., Dietrich W., 1998. River longitudinal profiles and bedrock incision models: Stream power and the influence of sediment supply. In Tinkler K., Wohl E. (Eds), *Rivers over rock: Fluvial processes in bedrock channels*, Geophys. Monogr. Series 107, AGU, Washington, D.C., pp. 237-260.

Sklar L., Dietrich W., 2001. Sediment and rock strength controls on river incision into bedrock. *Geol.* 29, 1087-1090.

Sklar L., Dietrich W., 2004. A mechanistic model for river incision into bedrock by saltating bed load. *Water Resour. Res.* 40, W06301. DOI:10.1029/2003WR002496.

Sklar L., Dietrich W., 2006. The role of sediment in controlling steady-state bedrock channel slope: Implications of the saltation-abrasion incision model. *Geomorph.* 82, 58-83.

Snow R., Slingerland R., 1987. Mathematical modeling of graded river profiles. *J. Geol.* 95, 15-33.

Snyder N., Whipple K., Tucker G., Merritts D., 2000. Landscape response to tectonic forcing: Digital elevation model analysis of stream profiles in the Mendocino triple junction region, northern California. *Geol. Soc. Am. Bull.* 112, 1250-1263.

Snyder N., Whipple K., Tucker G., Merritts D., 2003. Importance of a stochastic distribution of floods and erosion thresholds in the bedrock river incision problem. *J. Geophys. Res.* 108B, 2117, doi:10.1029/2001JB001655.

Stange K., Van Balen R., Vandenberghe J., Peña J., Sancho C., 2013. External controls on Quaternary fluvial incision and terrace formation at the Segre River, Southern Pyrenees. *Tectonophys.* 602, 316-331.

Stange K., Van Balen R., Garcia-Castellanos D., Cloetingh S., 2014. Numerical modelling of Quaternary terrace staircase formation in the Ebro foreland basin, southern Pyrenees, NE Iberia. *Basin Res.* 28, 124-146.

Stark C., 2006. A self-regulating model of bedrock river channel geometry. *Geophys. Res. Lett.* 33, L04402. DOI:10.1029/2005GL023193.

Stark C., Foufoula-Georgiou E., Ganti V., 2009. A nonlocal theory of sediment buffering and bedrock channel evolution. *J. Geophys. Res.* 114F, F01029, doi:10.1029/2008JF000981.

Stark C., Barbour J., Hayakawa Y., Hattanji T., Hovius N., Chen H., Lin C.-W., Horng M., Xu K.-Q., Fukahata Y., 2010. The climatic signature of incised river meanders. *Science* 327, 1497-1501.

Stokes, M., Mather, A. 2003. Tectonic origin and evolution of a transverse drainage: the Rio Almanzora, Betic Cordillera, Southeast Spain. Geomorphology 50, 59-81

Stokes M., Mather A.. Harvey A., 2002. Quantification of river capture induced base-level changes and landscape development, Sorbas Basin, SE Spain. In Jones S., Frostick L. (Eds), *Sediment Flux to Basins: Causes, Controls and Consequences*. Geol. Soc., London Spec. Publ. 191, pp. 23-35.

Suzuki T., 2008. Analysis of titanomagnetite within weathered middle Pleistocene KMT tephra and its application for fluvial terrace chronology, Kanto Plain, central Japan. *Quat. Int.* 178, 119-127.

Talling P., Stewart M., Stark C., Gupta S., Vincent S., 1997. Regular spacing of drainage outlets from linear fault blocks. *Basin Res.* 9, 275-302.

Troiani F., Della Seta M., 2008. The use of the Stream Length-Gradient index in morphotectonic analysis of small catchments: A case study from Central Italy. *Geomorph.* 102, 159-168.

Troiani F., Della Seta M., 2011. Geomorphological response of fluvial and coastal terraces to Quaternary tectonics and climate as revealed by geostatistical topographic analysis. *Earth Surf. Proc. Landf.* 36, 1193-1208.

Troiani F., Galve J., PiacentiniD., Della Seta M., Guerrero J., 2014. Spatial analysis of stream length-gradient (SL) index for detecting hillslope processes: A case of the Gallego River headwaters (Central Pyrenees, Spain). *Geomorph.* 214, 183-197.

Tucker G., Bras R., 2000. A stochastic approach to modeling the role of rainfall variability in drainage basin evolution. *Water Resour. Res.* 36, 1953-1964.

Tucker G., Whipple K., 2002. Topographic outcomes predicted by stream erosion models: Sensitivity analysis and intermodel comparison. *J. Geophys. Res.* 107B, 2179, doi:10.1029/2001JB000162.

Turowski J., Lague D., Hovius N., 2007. Cover effect in bedrock abrasion: A new derivation and its implications for the modeling of bedrock channel morphology. *J. Geophys. Res.* 112F, F04006, doi:10.1029/2006JF000697.

Turowski J., Hovius N., Meng-Long H., Lague D., Men-Chiang C., 2008. Distribution of erosion across bedrock channels. *Earth Surf. Proc. Landf.* 33, 353-363.

Turowski J., Lague D., Hovius N., 2009. Response of bedrock channel width to tectonic forcing: Insights from a numerical model, theoretical considerations, and comparison with field data. *J. Geophys. Res.* 114F, F03016, doi:10.1029/2008JF001133.

Van Balen R., Houtgast R., Van der Wateren F., Vandenberghe J., Bogaart P., 2000. Sediment budget and tectonic evolution of the Meuse catchment in the Ardennes and the Roer Valley Rift System. *Global Planet. Change* 27, 113-129.

Van den Berg M., 1996. Fluvial sequences of the Maas. A 10 Ma record of neotectonics and climate change at various time-scales. PhD Thesis, Landbouwuniversiteit, Wageningen, 181 p.

Vandenberghe J., 2008. The fluvial cycle at cold-warm-cold transitions in lowland regions: A refinement of theory. *Geomorph.* 98, 275-284.

Vandenberghe J., Wang X., Lu H., 2011. Differential impact of small-scaled tectonic movements on fluvial morphology and sedimentology (the Huang Shui catchment, NE Tibet Plateau). *Geomorph.* 134, 171-185.

Van der Beek P., Bishop P., 2003. Cenozoic river profile development in the Upper Lachlan catchment (SE Australia) as a test of quantitative fluvial incision models. *J. Geophys. Res.* 108B, 2309, doi:10.1029/2002JB002125.

Van der Beek P., Champel B., Mugnier J.-L., 2002. Control of detachment dip on drainage development in regions of active fault-propagation folding. *Geol.* 30, 471-474.

Van de Wiel M., Coulthard T., 2010. Self-organized criticality in river basins: challenging sedimentary records of environmental change. *Geology* 38, 87–90.

Van Gorp W., Schoorl J., Temme A., Reimann T., Wijbrans J., Maddy D., Demir T., Veldkamp T., 2016. Catchment response to lava damming: integrating field observation, geochronology and landscape evolution modelling. *Earth Surf. Proc. Landf.* 41, 1629-1644.

Veldkamp A., 1992. A 3-D model of Quaternary terrace development, simulations of terrace stratigraphy and valley asymmetry: A case study for the Allier terraces (Limagne France). *Earth Surf. Proc. Landf.* 17, 487-500.

Veldkamp A., Baartman J., Coulthard T., Maddy D., Schoorl J., Storms J., Temme A., van Balen R., van de Wiel M., van Gorp W., Viveen W., Westaway R., Whittaker A., 2016. Two decades of numerical modelling to understand long term fluvial archives: Advances and future perspectives. *Quat. Sci. Rev.*, this issue.

Veloza G., Taylor M., Mora A., Gose J., 2015. Active mountain building along the eastern Colombian Subandes: A folding history from deformed terraces across the Tame anticline, Llanos Basin. *Geol. Soc. Am. Bull.* 127, 1155-1173.

Viveen W., Braucher R., Bourlès D., Schoorl J., Veldkamp A., Van Balen R., Wallinga J., Fernandez-Mosquera D., Vidal-Romani J., Sanjurjo-Sanchez J., 2012. A 0.65 Ma chronology and incision rate assessment of the NW Iberian Miño River terraces based on $^{10}$Be and luminescence dating. *Global Planet. Change* 94-95, 82-100.

Viveen W., Schoorl J., Veldkamp A., Van Balen R., 2014. Modelling the impact of regional uplift and local tectonics on fluvial terrace preservation. *Geomorph.* 210, 119-135.

Walker R., Claisse S., Telfer M., Nissen E., England P., Bryant C., Bailey R., 2010. Preliminary estimate of Holocene slip rate on active normal faults bounding the southern coast of the Gulf of Evia, central Greece. *Geosph.* 6, 583-593.

Westaway R., 2001. Flow in the lower continental crust as a mechanism for the Quaternary uplift of the Rhenish Massif, northwest Europe. In Maddy D., Macklin M., Woodward J. (Eds), *River basin sediment systems: Archives of environmental change*, Balkema, pp. 87-167.

Westaway R., 2002. Long-term river terrace sequences: Evidence for global increases in surface uplift rates in the Late Pliocene and early Middle Pleistocene caused by flow in the lower continental crust induced by surface processes. *Netherl. J. Geosci.* 81, 305-328.

Westaway R., 2007. Late Cenozoic uplift of the eastern United States revealed by fluvial sequences of the Susquehanna and Ohio systems: coupling between surface processes and lower-crustal flow. *Quat. Sci. Rev.* 26, 2823-2843.

Westaway R., 2012. A numerical modelling technique that can account for alternations of uplift and subsidence revealed by Late Cenozoic fluvial sequences. *Geomorph.* 165-166, 124-143.

Westaway R., Maddy D., Bridgland D., 2002. Flow in the lower continental crust as a mechanism for the Quaternary uplift of south-east England: constraints from the Thames terrace record. *Quat. Sci. Rev.* 21, 559-603.

Westaway R., Bridgland D., Mishra S., 2003. Rheological differences between Archaean and younger crust can determine rates of Quaternary vertical motions revealed by fluvial geomorphology. *Terra Nova* 15, 287-298.

Westaway R., Guillou H., Seyrek A., Demir T., Bridgland D., Scaillet S., Beck A., 2009a. Late Cenozoic surface uplift, basaltic volcanism, and incision by the River Tigris around Diyarbakir, SE Turkey. *Int. J. Earth Sci.* 98, 601-625.

Whipple K., 2001. Fluvial landscape response time: How plausible is steady-state denudation? *Am. J. Sci.* 301, 313-325.

Whipple K., 2004. Bedrock rivers and the geomorphology of active orogens. *Ann. Rev. Earth Planet. Sci.* 32, 151-185.

Whipple K., Tucker G., 1999. Dynamics of the stream-power river incision model: Implications for height limits of mountain ranges, landscape response timescales, and research needs. *J. Geophys. Res.* 104B, 17,661-17,674.

Whipple K., Tucker G., 2002. Implications of sediment-flux-dependent river incision models for landscape evolution. *J. Geophys. Res.* 107B, 10.1029/2000JB000044.

Whipple K., Hancock G., Anderson R., 2000. River incision into bedrock: Mechanics and relative efficacy of plucking, abrasion and cavitation. *Geol. Soc. Am. Bull.* 112, 490-503.

Whipple K., DiBiase R., Crosby B., 2013. Bedrock rivers. In Shroder J. (Ed in Chief), Wohl (Ed), *Treatise on Geomorphology*, Acad. Press, San Diego, CA, vol. 9, Fluvial Geomorphology, pp. 550-573.

Whitchurch A., Carter A., Sinclair H., Duller R., Whittaker A., Allen P., 2011. Sediment routing systems and the lag-time concept: A case study from the southern Pyrenees. *Am. J. Sci.* 311, 442–482, doi: 10.2475 /04 .2011 .00.

Whittaker A., Boulton S., 2012. Tectonic and climatic controls on knickpoint retreat rates and landscape response times. *J. Geophys. Res.* 117F, F02024, doi:10.1029/2011JF002157.

Whittaker A., Cowie P., Attal M., Tucker G., Roberts G., 2007a. Contrasting transient and steady-state rivers crossing active normal faults: new field observations from the Central Apennines, Italy. *Basin Res.* 19, 529-556.

Whittaker A., Cowie P., Attal M., Tucker G., Roberts G., 2007b. Bedrock channel adjustment to tectonic forcing: Implications for predicting river incision rates. *Geol.* 35, 103-106.

Whittaker A., Attal M., Cowie P., Tucker G., Roberts G., 2008. Decoding temporal and spatial patterns of fault uplift using transient river long profiles. *Geomorph.* 100, 506-526.

Whittaker A., Attal M., Allen P., 2010. Characterising the origin, nature and fate of sediment exported from catchments perturbed by active tectonics. *Basin Research* 22, 809–828.

Whittaker A., Duller R., Springett J., Smithells R., Whitchurch A., Allen P., 2011. Decoding downstream trends in stratigraphic grain size as a function of tectonic subsidence and sediment supply. *Geol. Soc. Am. Bull.* 123, 1363–1382, doi:10.1130/B30351.1.

Willett S., Brandon M., 2002. On steady states in mountain belts. *Geol.* 30, 175-178.

Willett S., Slingerland R., Hovius N., 2001. Uplift, shortening, and steady state topography in active mountain belts. *Am. J. Sci.* 301, 455-485.

Willett S., McCoy S., Perron T., Goren L., Chen C., 2014. Dynamic reorganization of river basins. *Science* 343, 1248765, DOI: 10.1126/science.1248765.

Wilson J., Roberts G., Hoggard M., White N., 2014. Cenozoic epeirogeny of the Arabian Peninsula from drainage modelling. *$G^3$/Geochem., Geophys., Geosyst.* 15, 3723-3761.

Wobus C., Whipple K., Kirby E., Snyder N., Johnson J., Spyropolou K., Crosby B., Sheehan D., 2006. Tectonics from topography: Procedures, promise, and pitfalls. In Willett S., Hovius N., Brandon M., Fisher D. (Eds) *Tectonics, Climate, and Landscape Evolution*, Geol. Soc. Am. Spec. Pap., 398, pp. 55-74.

Wohl E., 2010. Mountain rivers revisited. *AGU Water Resources Monograph Series* 19, 573 p.

Wohl E., 2014. Time and the rivers flowing: Fluvial geomorphology since 1960. *Geomorph.* 216, 263-282.

Yager E., Turowski J., Rickenmann D., McArdell B., 2012. Sediment supply, grain protrusion, and bedload transport in mountain streams. *Geophys. Res. Lett.* 39, L10402, doi:10.1029/2012GL051654.

Yanites B., Tucker G., 2010. Controls and limits on bedrock channel geometry. *J. Geophys. Res.* 115F, F04019, doi: 10.1029/2009JF001601.

Yanites B., Tucker G., Mueller K., Chen Y., 2010. How rivers react to large earthquakes: Evidence from central Taiwan. *Geol.* 38, 639-642.

Yanites B., Ehlers T., Becker J., Schnellmann M., Heuberger S., 2013. High magnitude and rapid incision from river capture: Rhine River, Switzerland. *J. Geophys. Res.* 118F, 1060-1084, doi:10.1002/jgrf.20056.

Zaprowski B., Evenson E., Pazzaglia F., Epstein J., 2001. Knickzone propagation in the Black Hills and northern High Plains: A different perspective on the late Cenozoic exhumation of the Laramide Rocky Mountains. *Geol.* 29, 547-550.

Zeitler P., Meltzer A., Koons P., Craw D., Hallet B., Chamberlain C., Kidd W., Park S., Seeber L., Bishop M., Shroder J., 2001. Erosion, Himalayan geodynamics, and the geomorphology of metamorphism. *GSA Today* 11, 4-9.

Zhu S., Wu Z., Zhao X., Li J., Xiao K., 2014. Ages and genesis of terrace flights in the middle reaches of the Yarlung Zangbo River, Tibetan Plateau, China. *Boreas* 43, 485-504.

Ziegler P., Fraefel M., 2009. Response of drainage systems to Neogene evolution of the Jura fold-thrust belt and Upper Rhine Graben. *Swiss J. Geosci.* 102, 57-75.

**Figure captions**

1. Graded (Aisne) versus transient (Hoëgne) river long profiles and their analysis by S-A plots, as exemplified by two Ardennian rivers. Note that an abrupt change in bedrock lithology could impose the same kind of discontinuity to a steady state profile as that displayed by the transient Hoëgne profile. However, the S-A plot would not display this type of $k_s$ change.

2. A. Hack's *SL* index definition and measurement for three 2-km-long reaches of the Aisne (Ardenne): *SL* variations are small along a graded stream. B. Example of *SL* mapping: Gallego upper catchment (Spanish Pyrenees, UTM zone 30T) (from Troiani et al., 2014, fig. 9).

3. Metrics of the geometric concavity of a river profile (after Demoulin, 1998). The combination of two metrics, namely $E_q$ (normalized distance to source of $H_{max}$) and either $E_r$ (light yellow area) or $H_{max}$ (maximum normalized difference in elevation) completely describes the profile concavity.

4. SL (A) and ksn (B) maps featuring river profile steepness in the same area of the San Gabriel Mountains, California, and showing the overall consistency between both types of measurements (A. modified after Keller 1986; B. from DiBiase et al., 2010).

5. Long profile metrics of the Kerynitis River (northern Peloponnese, Greece). The profile is extracted from a 20-m-resolution DEM. A. S-A plot displaying such noisy slope data that concavity and steepness estimates are erratic and hardly meaningful and segment separation rather subjective (the featured separation is imported from the chi plot in B). B. Segmented chi plot of the same profile. Segment separation is performed by visual inspection of the chi plot of the entire stream. Best fit m/n represent concavity values; slope of best fits (in brackets) indicates segment steepness. These $k_s$ steepness values are related to different concavities and thus not directly comparable. Normalized steepness values $k_{sn}$ of 0.32 and 0.25 ($\theta_{ref}$ = 0.5) are obtained for example for segments S1 and S2, respectively, i.e., in inverse relation with respect to the corresponding $k_s$ values. Note that the scale of chi axis changes with best fit m/n, resulting in altered relative lengths of the successive segment plots. WP. Whole profile.

6. Relation between steepness index and uplift rate. A. Modelled for streams in the low and high uplift zones (LUZ and HUZ, respectively) of the Mendocino triple junction area, northern California (from Snyder et al., 2003). Fitting a curve to both points requires either taking into account a threshold shear stress (model of Tucker and Bras, 2000) or taking n = 3.8. B. Compilation of published data, assuming that the investigated fluvial landscapes are close to or at steady state and, thus, denudation, incision, and uplift rates are equal (from Lague, 2014, with references therein).

7. Types of knickpoint in synthetic stream profiles (left) and their appearance on S-A plots (right). A. Vertical step knickpoint separating segments of same $\theta$ and $k_{sn}$ (e.g., transient knickpoint produced by a pulse of uplift; permanent lithologic knickpoint). B. Slope-break knickpoint trailing a new higher-$k_{sn}$ downstream profile in equilibrium with increased uplift rate; steady-state concavity is unchanged after passage of the knickpoint. C. Knickzone pointing to either disequilibrium downstream profile ($k_s$ meaningless) or steady-state spatial gradient in uplift. S1 and S2: segments upstream and downstream of the profile discontinuity, respectively; $k_{s(n)}$ and $\theta$ are numbered accordingly in the right-hand graphs.

8. A. Description of the *R* metric components for the Selinous River (northern Peloponnese): $l^* = l/l_0$, with $l_0$ = length of the river, cumulative length of its drainage network, and basin area respectively for $H_r$, $H_n$, and $H_b$; $h^* = h/h_0$, with $h_0$ = basin relief. $H_b$, $H_n$ and $H_r$: hypsometric curves of the basin, the drainage network, and the trunk stream ($H_r$ is therefore simply the trunk stream long profile). *E* describes the basin's elongation. For the definition of *R*, see equation (22) in the main text. B. Control of drainage area *A* on *R*, illustrated in the northern (N), central ('Centre'), and southern (S) parts of the Rhenish shield (W Europe). The slope $S_R$ of the relation is characteristic of each subregion with a distinct age of the tectonic perturbation ($t_U$ = age of last uplift pulse) (modified after Demoulin, 2011). C. Empirical power law dependence of $S_R$ on time since the last tectonic perturbation,

obtained from $S_R$ estimates in regions with uplift of known age. RS. Rhenish shield (from Demoulin, 2012).

9. A. $^{10}Be/^{26}Al$ terrace ages (yellow stars, in ka – after Rixhon et al., 2011) of abandonment of the time-transgressive "Younger Main Terrace" along the Lower Meuse – lower Ourthe – Amblève drainage line (Ardenne, UTM zone 31U). Additional age data come from a buried knickpoint in a beheaded valley (red star) and the corresponding knickpoints in modern channels (circled green stars). B. Sketch of river incision and terrace pattern associated with the propagation of an erosion wave caused by rapid base level fall, showing that, in this case, geometrically reconstructed terraces parallel to the modern profile would not catch the actual incision history of the river (after Demoulin et al., 2012).

10. Examples of terrace profile patterns (variable distance and elevation scales). A. Parallel: Segre River, Spanish Pyrenees (modified after Stange et al., 2013). B. Upstream diverging: Shiyou He River, NE Tibet (modified after Hetzel et al., 2006). C. Downstream diverging: Pakarae River, North Island, New Zealand (modified after Litchfield et al., 2010). D. Parallel, diverging from the modern channel profile: Rappahannock River, Virginia, USA (modified after Howard et al., 1994). E. Warped: Bagmati River, central Nepal (modified after Lavé and Avouac, 2000). MFT Main Frontal Thrust.

11. Form change as first response of a meandering alluvial channel to a nascent anticlinal fold orthogonal to the river (modified after Ouchi, 1985). Sinuosity increases in order to compensate for the increased channel gradient on the downstream-dipping limb of the fold. Reduced gradients upstream of the fold induce straightening and reticulating of the channel.

12. Downstream sweep erosion upstream of the Da'an river gorge incised in the anticline which was reactivated during the 1999 Chi-Chi earthquake (Taiwan). a. Channel width versus distance along the gorge (the gorge reach described in **a** is located between white arrows in **b**). Dated vertical lines show knickpoint location during gorge growth. b. Evolution with time of gorge edges, downstream retreat of the upstream-facing slope scarp of the anticline, and sweeping channel in the broad floodplain upstream of the anticline (from Cook et al., 2014).

13. Examples of captures and drainage reorganisation. A. Margin of E and SE Tibet: progressive capture of a large part of the paleo-Red River drainage network (highlighted in yellow) by the lower Yangtze (highlighted in white). This evolution probably took place in Miocene times as a consequence of the first uplift stages in eastern Tibet. Tentatively numbered red stars locate the successive capture events that beheaded the Red River catchment, in parallel with progressive drainage reversal along the middle Yangtze. Green stars and arrows suggest that similar events occurred possibly also on the other side of the uplifted region, at the benefit of the present Mekong, Salween and, possibly, Brahmaputra rivers (modified after Clark et al., 2004 and Clift et al., 2006). B. Aare River, northern margin of the Central Alps: timing, in Ma, of the successive captures (red stars, with arrows indicating the change in flow direction) that diverted the Aare successively from the Danube to the Rhone (via the Doubs) catchment, then from the Rhone to the upper Rhine catchment. A more recent event diverted also the Alpine Rhine at the benefit of the upper Rhine catchment. The successive courses of the Aare are denoted by wide turquoise, medium-width middle blue, and thin dark blue vectors (modified after Ziegler and Fraefel, 2009).

Figure 1
Click here to download high resolution image

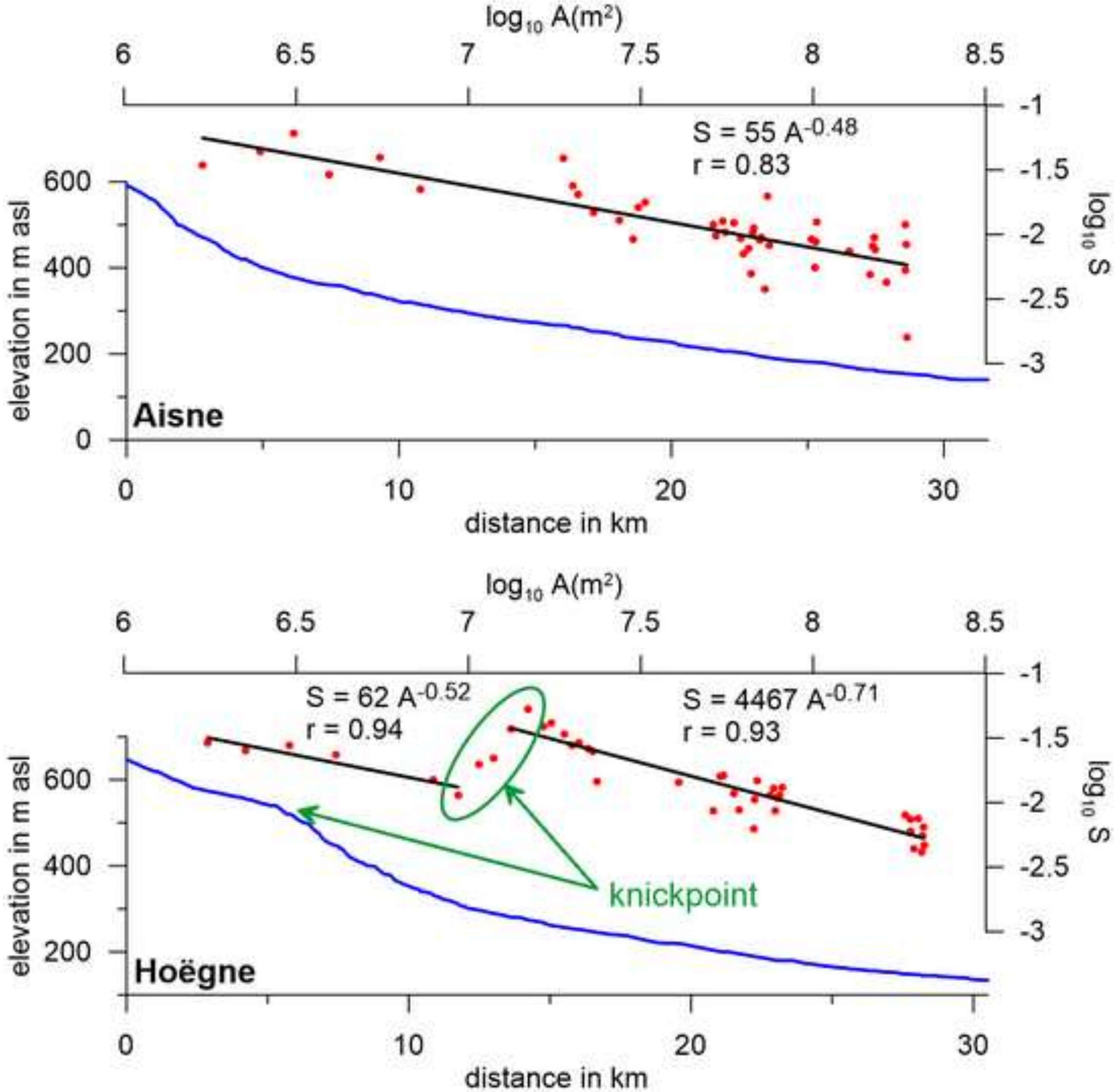

**Figure 2**
**Click here to download high resolution image**

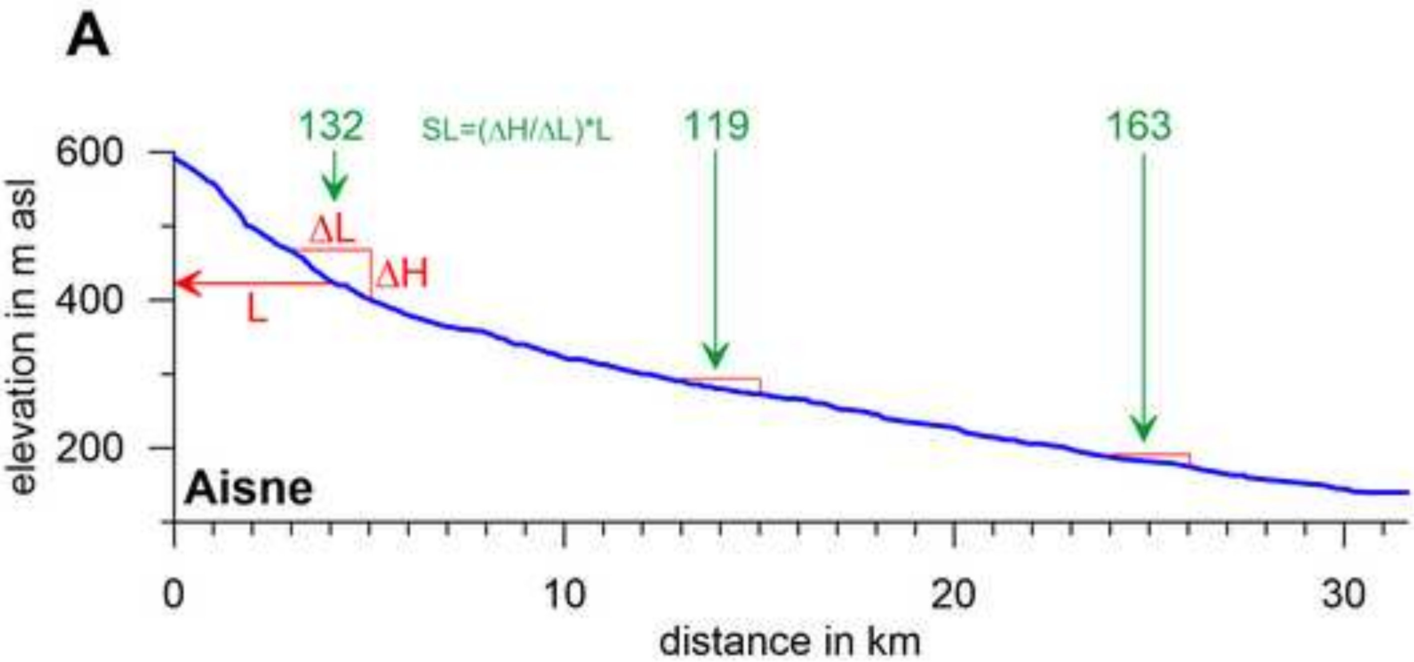


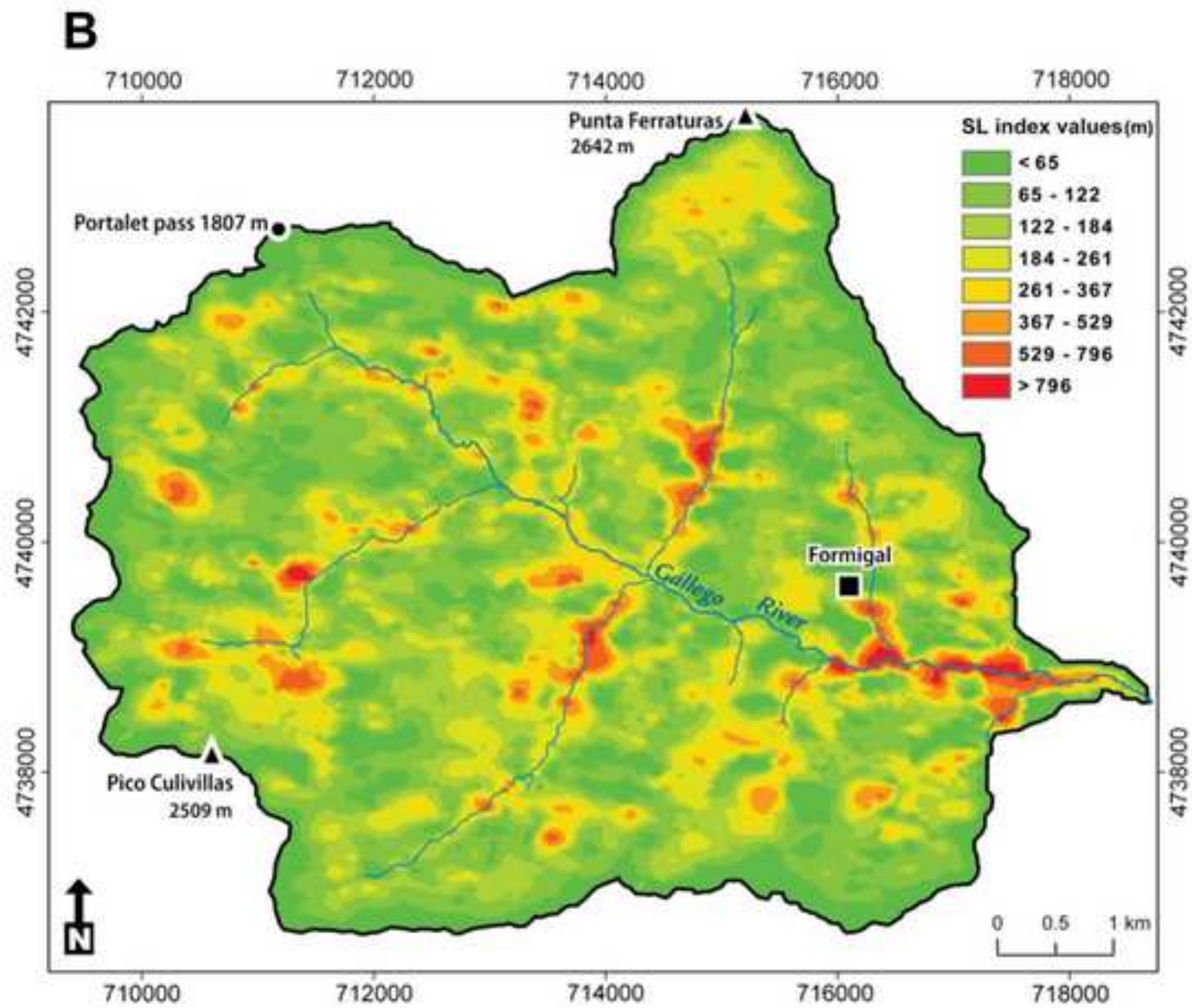

Figure 3
Click here to download high resolution image

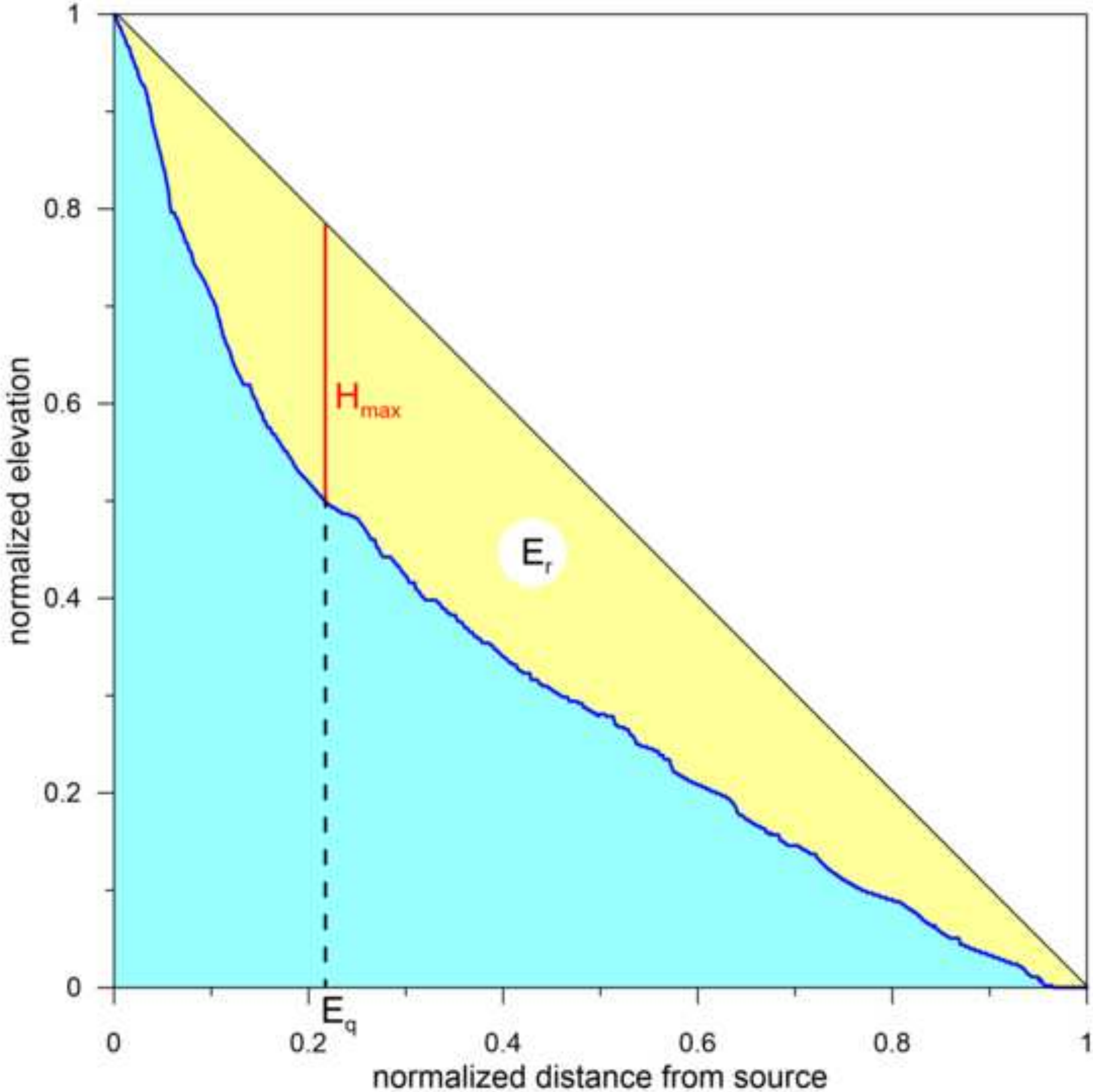

Figure 4
Click here to download high resolution image

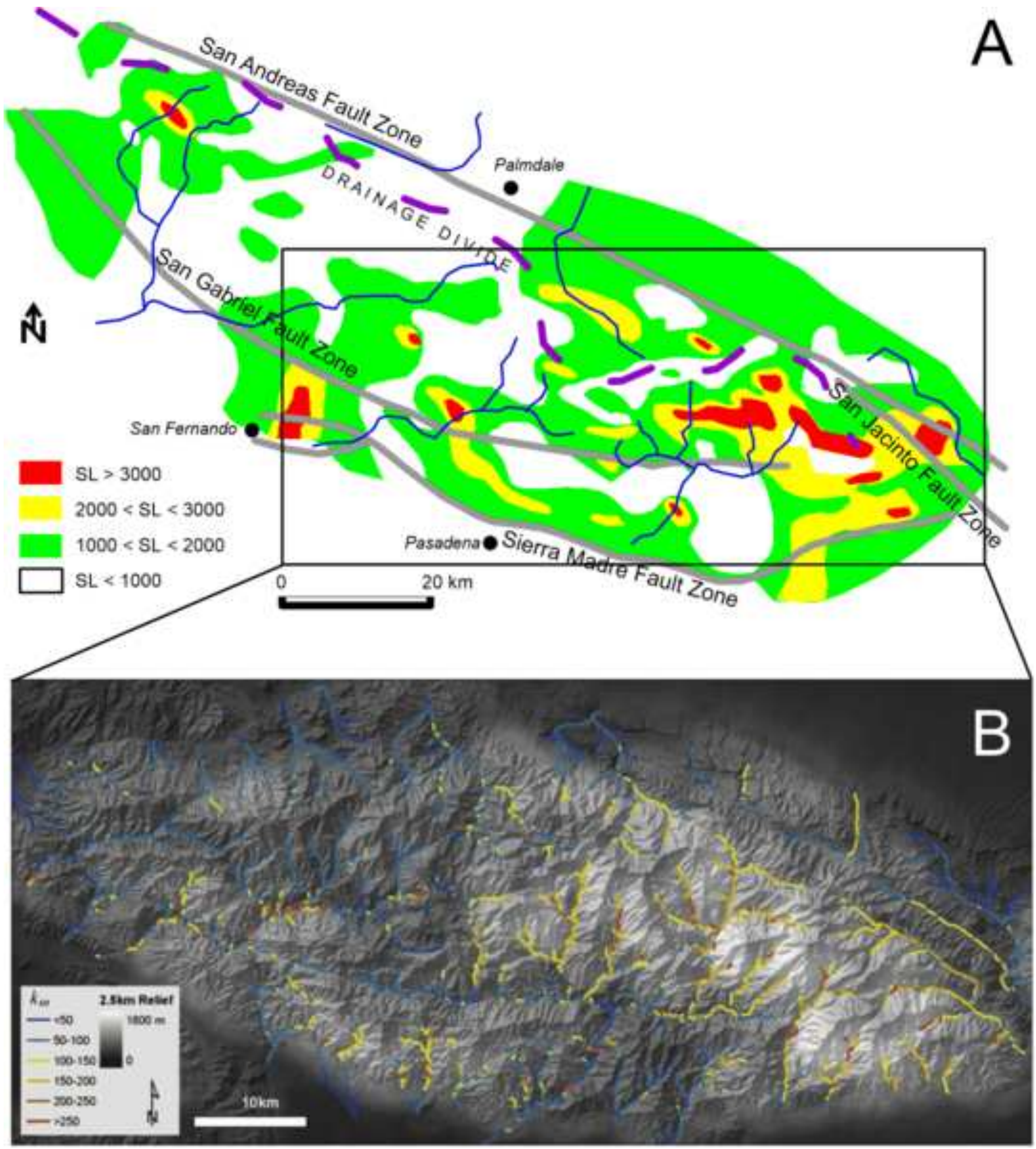

**Figure 5**
Click here to download high resolution image

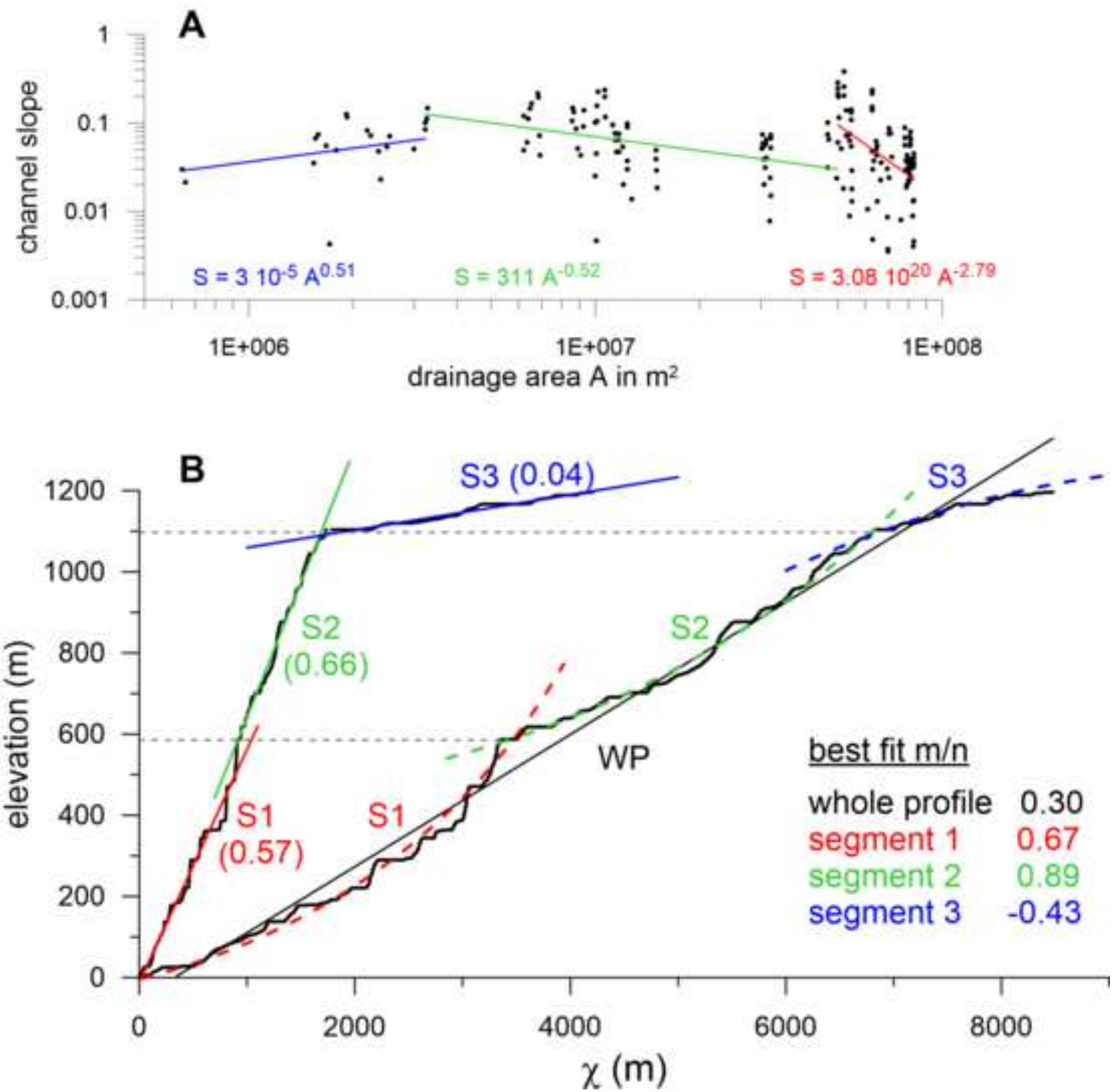

Figure 6
Click here to download high resolution image

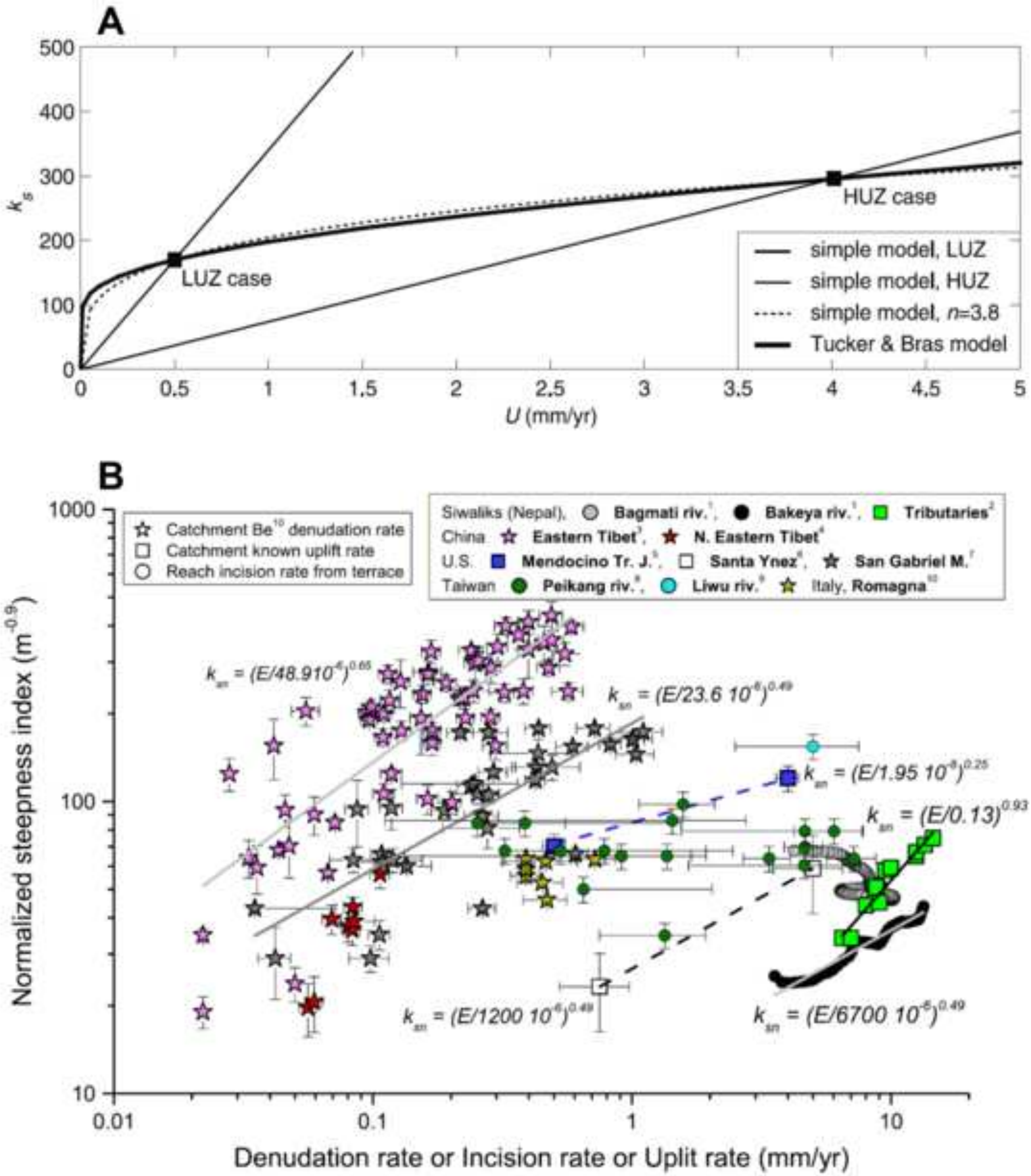

Figure 7
Click here to download high resolution image

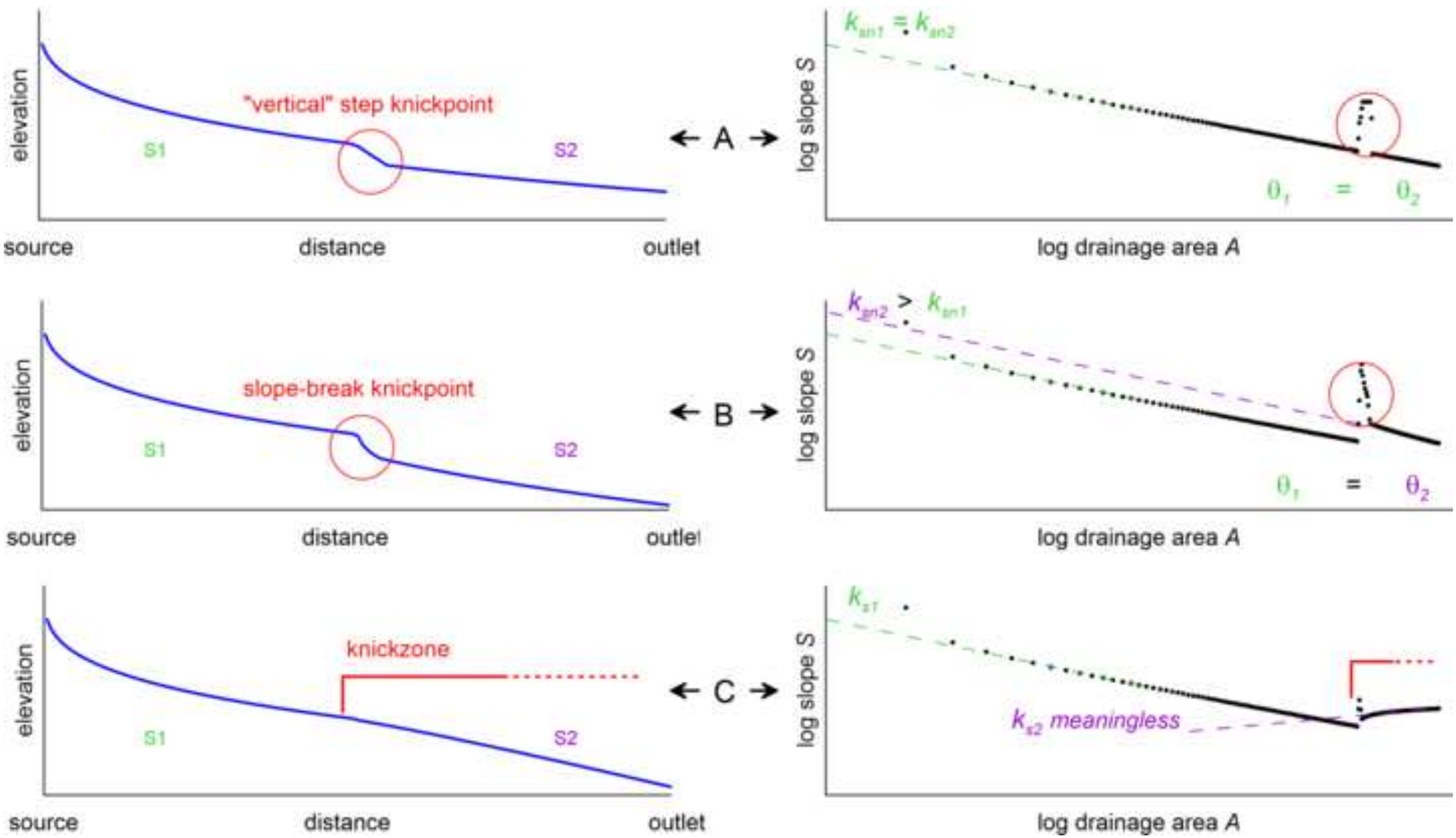

Figure 8
Click here to download high resolution image

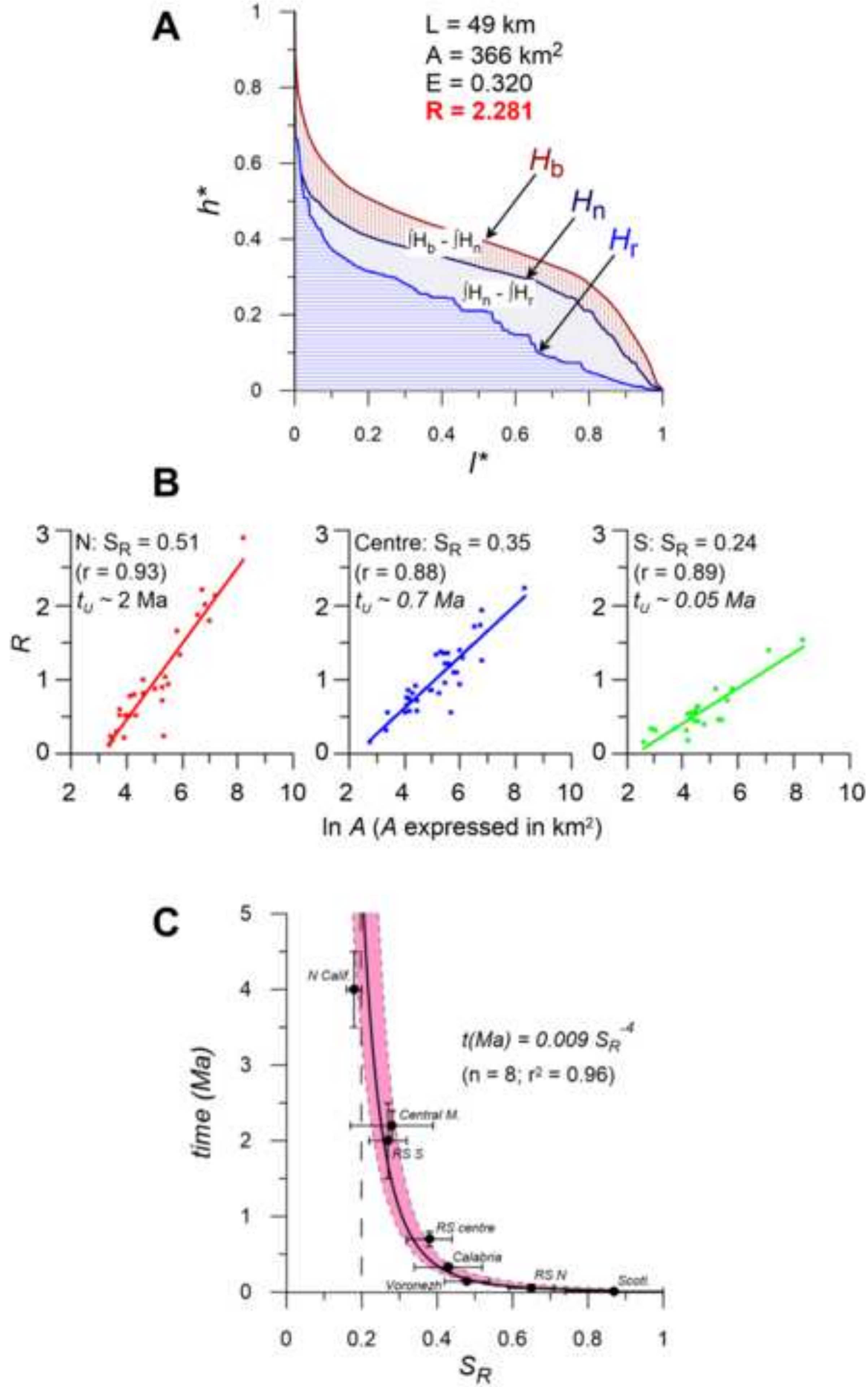

Figure 9
Click here to download high resolution image

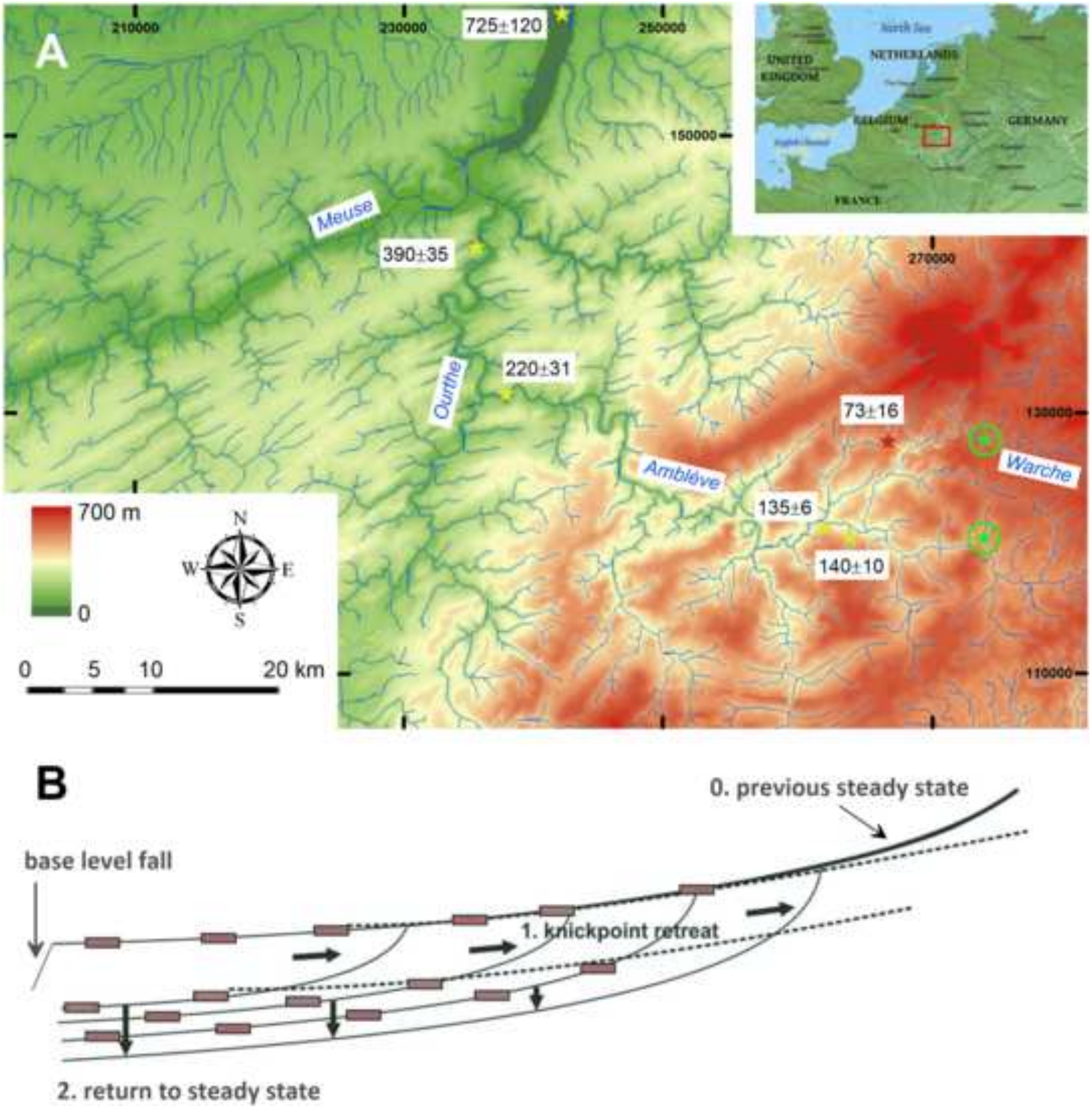

**Figure 10**
**Click here to download high resolution image**

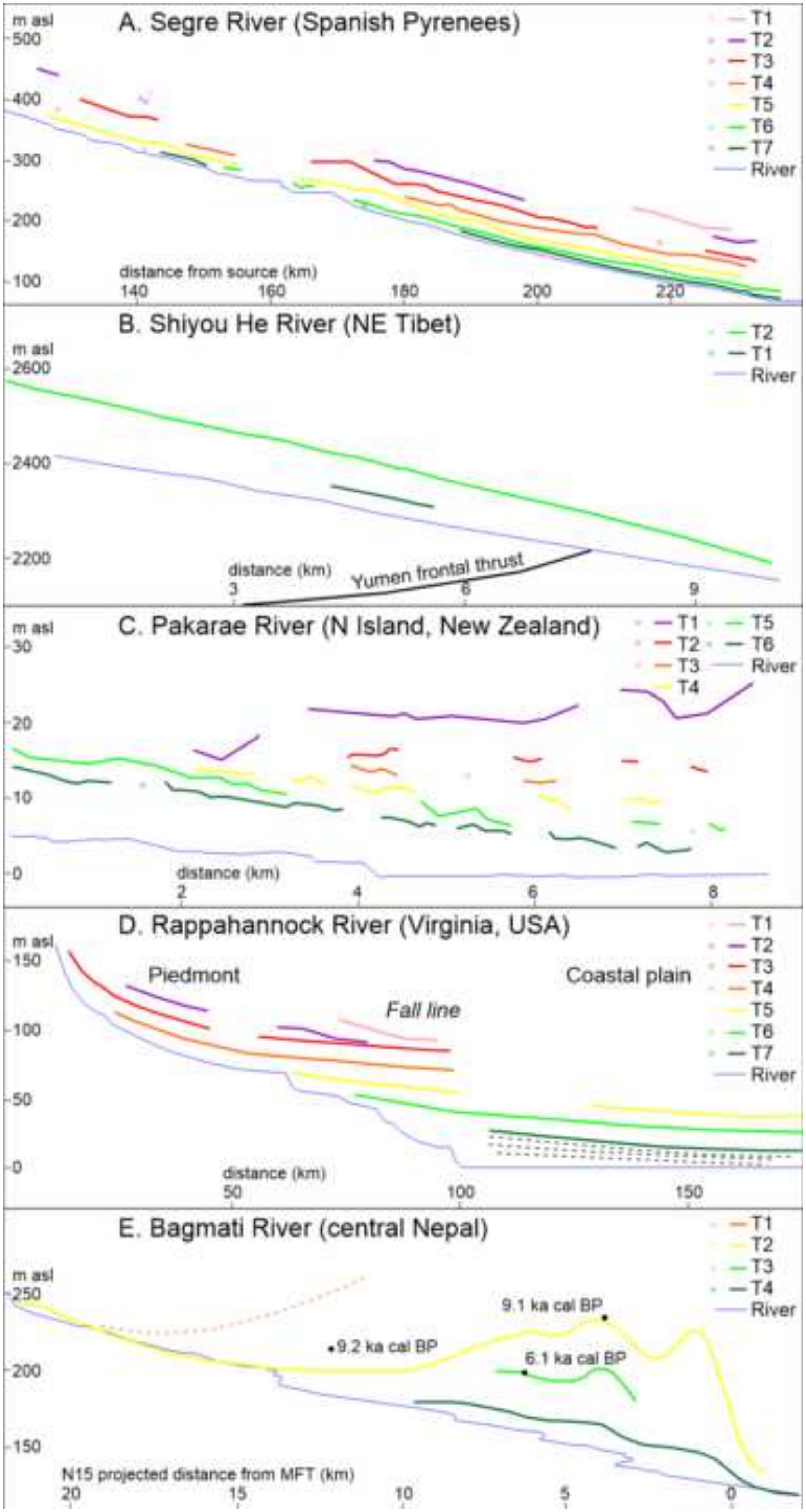

Figure 11
Click here to download high resolution image

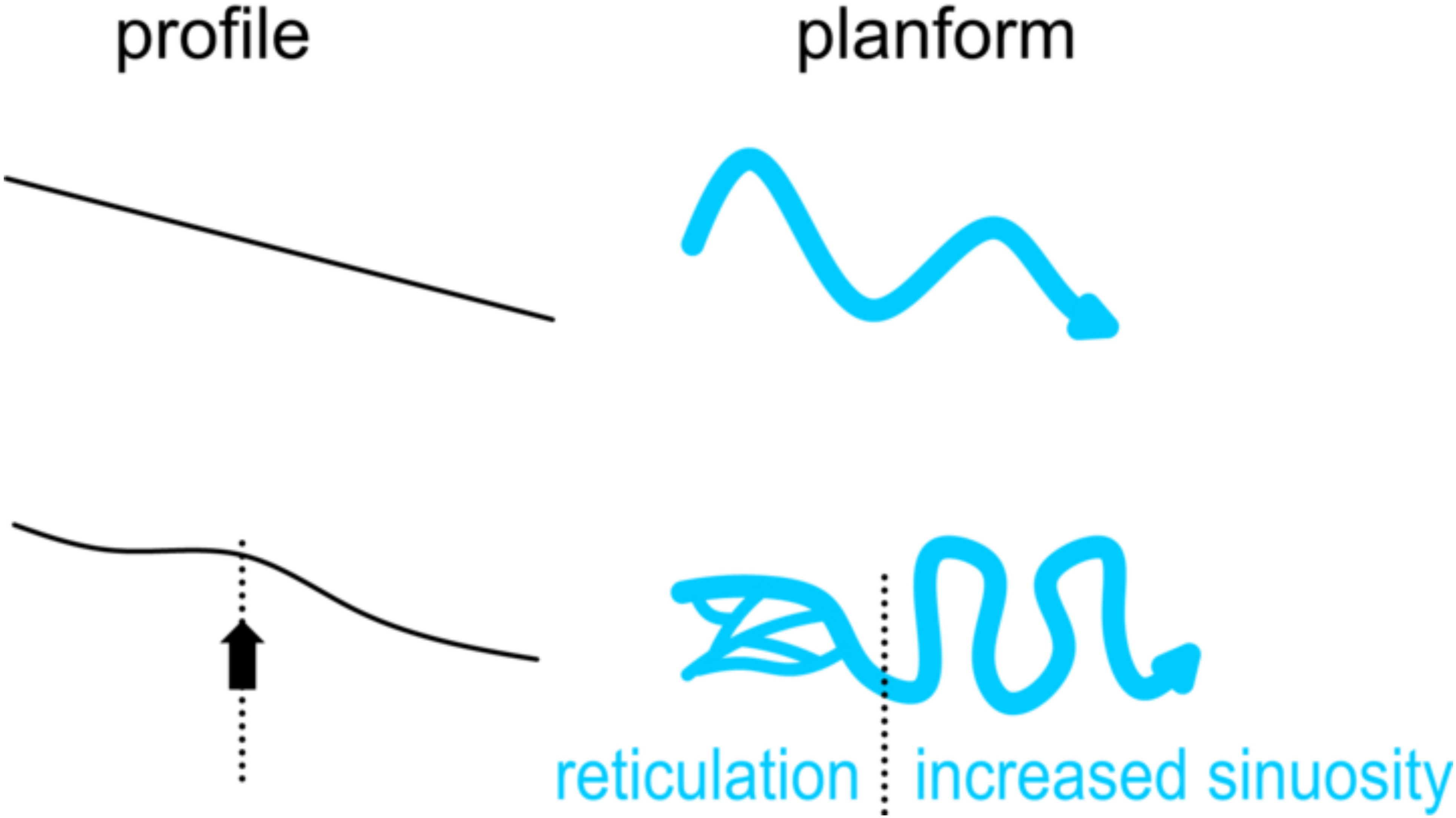

Figure 12
Click here to download high resolution image

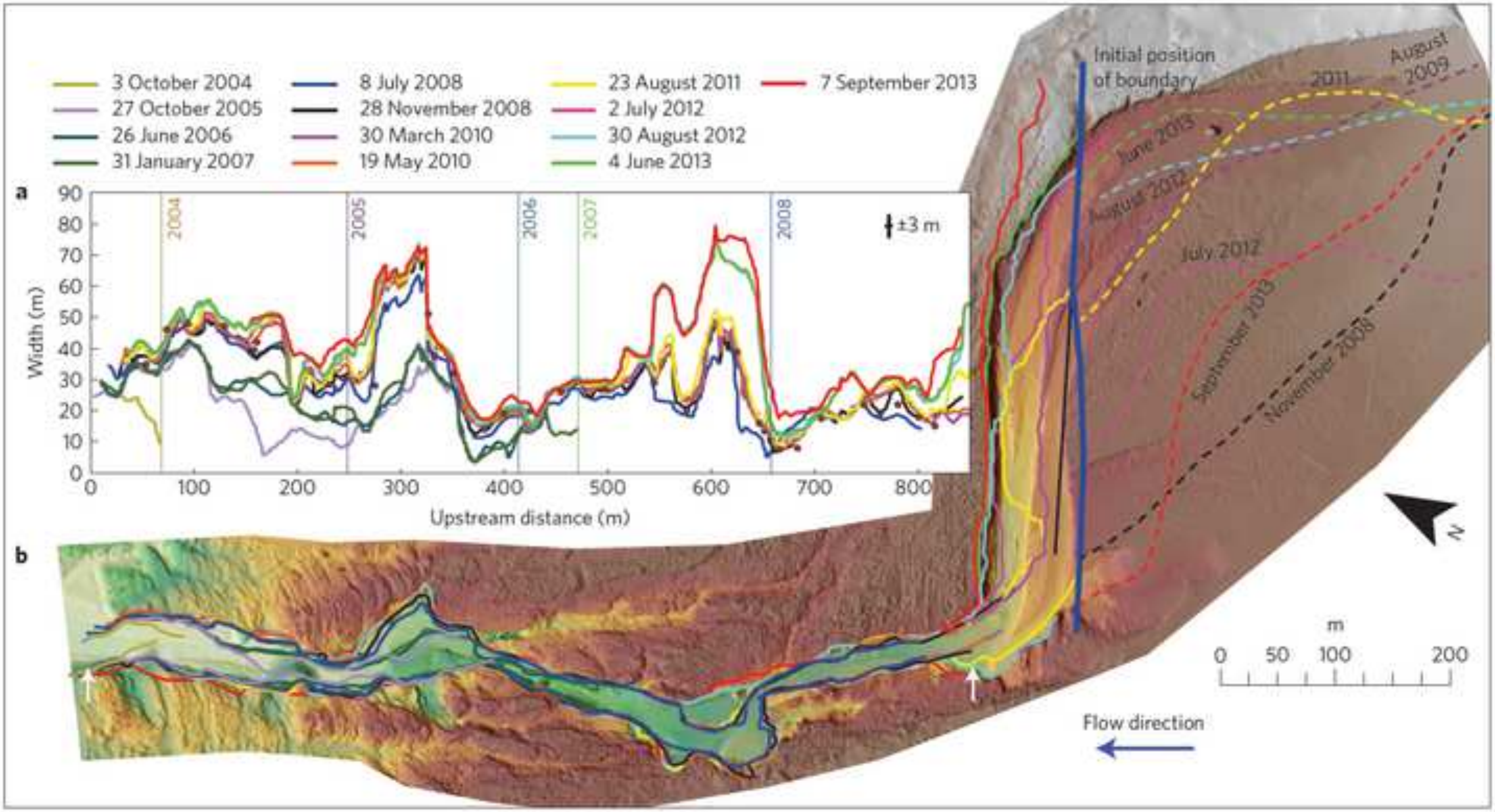

Figure 13
Click here to download high resolution image